

Introduction to Mössbauer spectroscopy

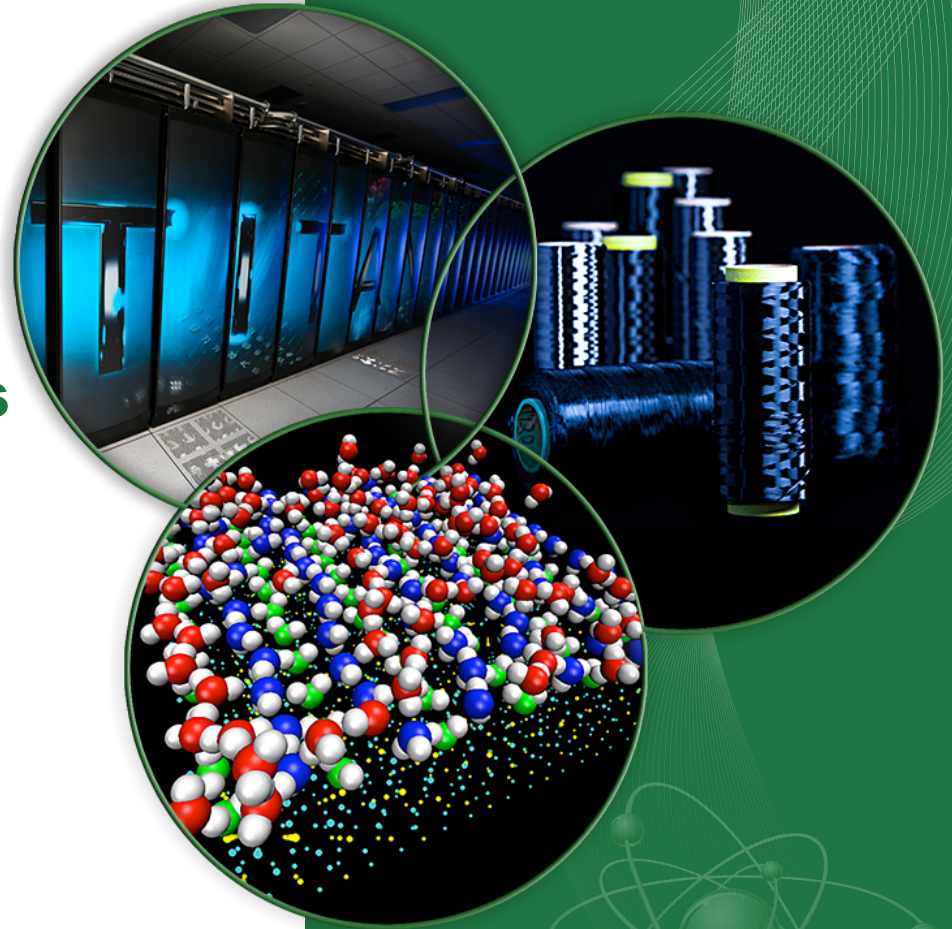
NRS Workshop 2017

CONUSS and Sychrotron Mössbauer Data Analysis

Raphaël P. Hermann

Advanced Photon Source
Argonne National Laboratory
November 16th -19th 2017

ORNL is managed by UT-Battelle
for the US Department of Energy



Rule 1: Know your audience

ONE DOES NOT SIMPLY

ASSUME

makeameme.org

- Historical perspective
- Spectral description and parameters
- Static interactions
- Time dependent interactions

Rudolf Mößbauer (1929-2011)

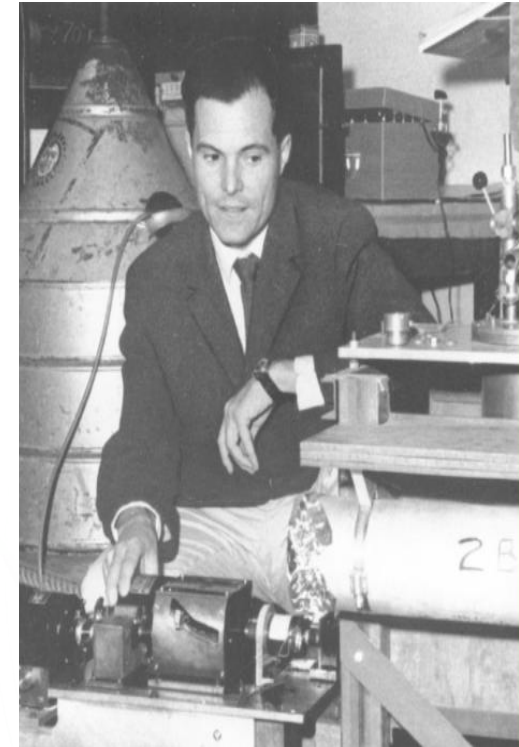
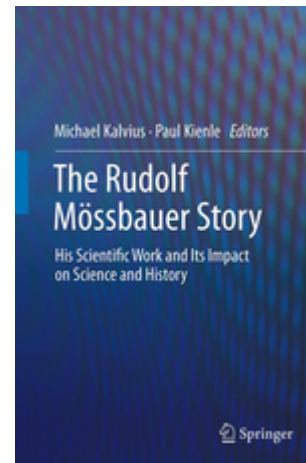
Kernresonanzfluoreszenz von Gammastrahlung in ^{191}Ir

Zeitschrift für Physik, 151, pp 124-143 (1958).

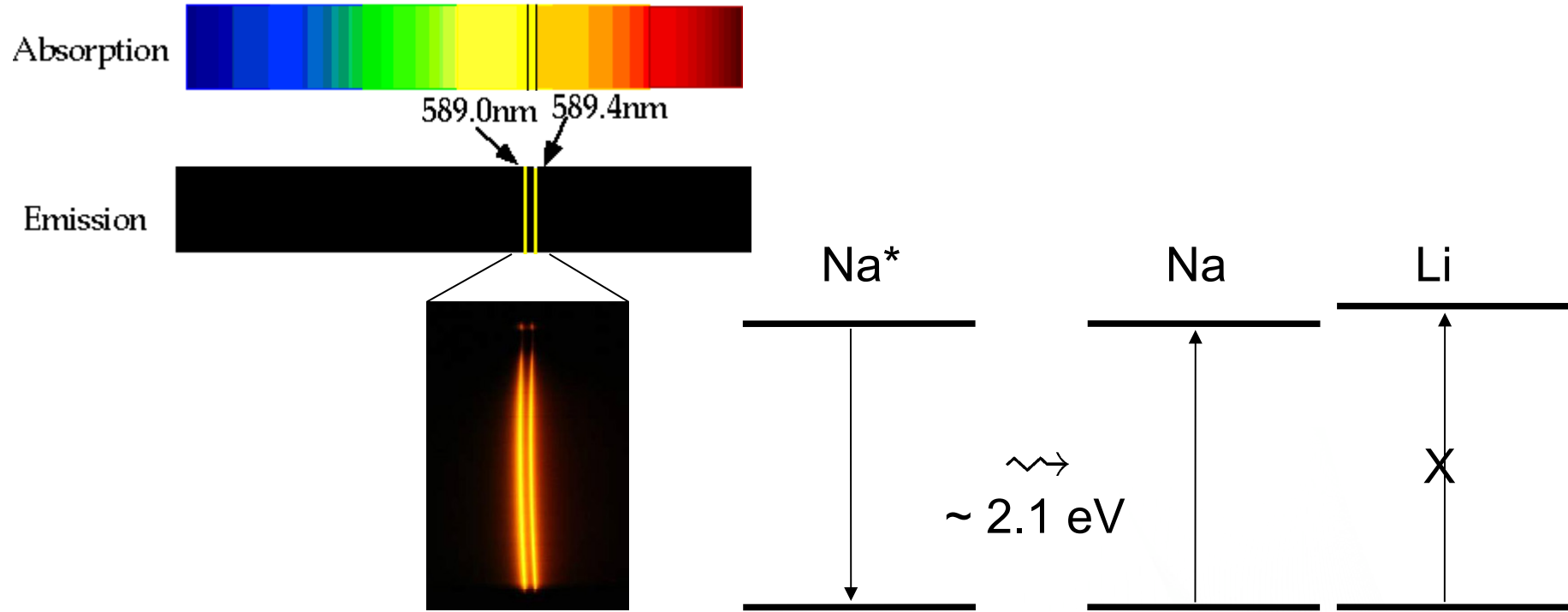
Nobel Prize in Physics, 1961.

„... young people are more often apt to attack problems with unconventional approaches, which would not be touched by older, more experienced and more knowledgeable persons.“

The Rudolf Mössbauer Story,
His Scientific Work and Its Impact on Science and History,
Kalvius, Michael, Kienle, Paul (Eds.) 2012, Springer Verlag

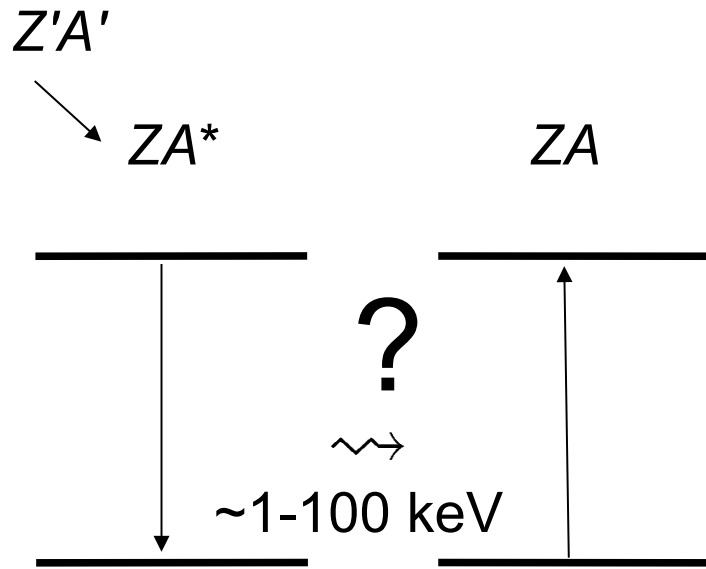


Electron transitions and resonant absorption



http://people.physics.carleton.ca/~watson/Physics/PHYS2903/2903_Quantum_Physics/PHYS2903_Bohr.html?id=0

Nuclear resonant absorption?



„As early as 1929, Kuhn had expressed the opinion that the **resonance absorption of gamma rays** should constitute the nuclear physics analogue to this optical resonance fluorescence. Here, a radioactive source should replace the optical light source. The gamma rays emitted by this source should be able to initiate the inverse process of **nuclear resonance absorption** in an absorber composed of nuclei of the same type as those decaying in the source.

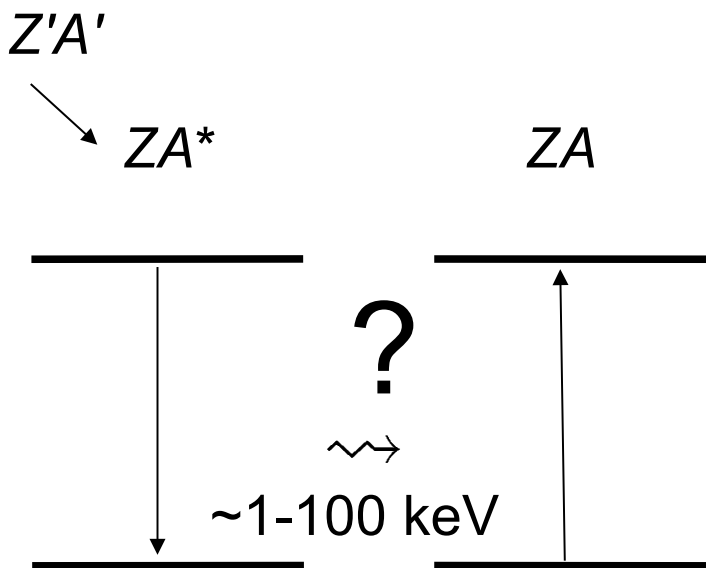
Again, the scheme (...) would hold here, but the radiative transitions would now take place between nuclear states.

Nevertheless, **all attempts in the next two decades** to find this nuclear resonance absorption **proved fruitless**. it is appropriate to consider the reasons why the discovery of nuclear resonance absorption was so long delayed.

R.L. Mössbauer, Nobel Lecture, The Nobel Foundation 1961

W. Kuhn, Phil. Mag. 8, 625 (1929)

Nuclear resonant absorption?

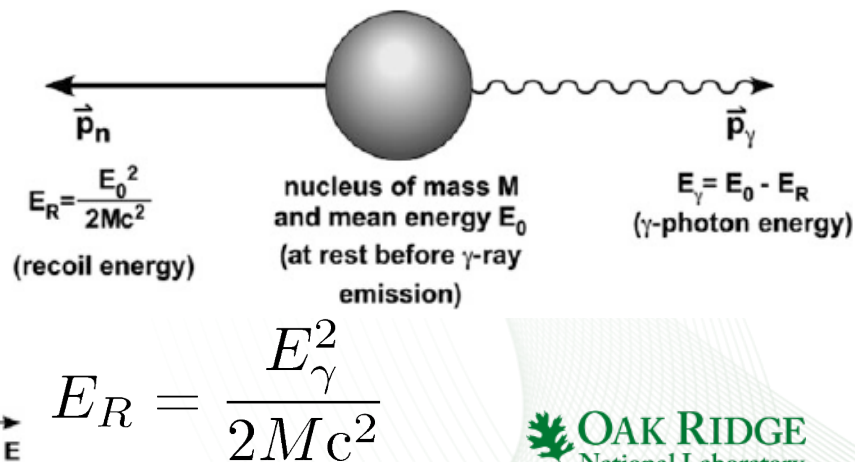
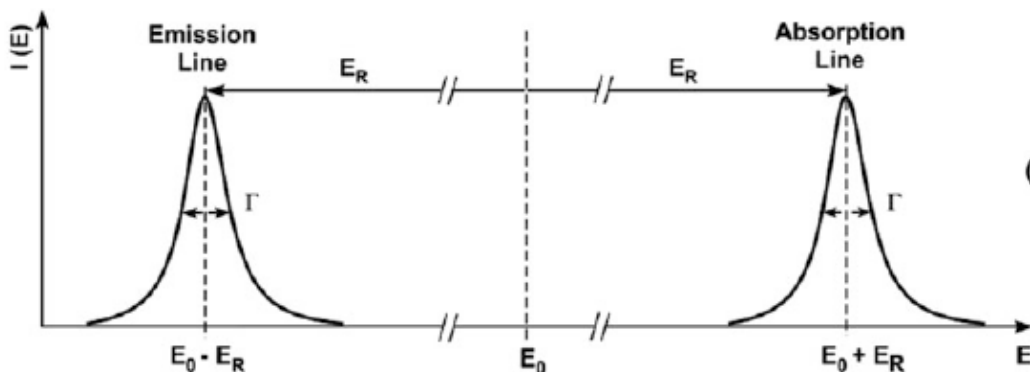


„As early as 1929, Kuhn had expressed the opinion that the **resonance absorption of gamma rays** should constitute the nuclear physics analogue to this optical resonance fluorescence. Here, a radioactive source should replace the optical light source. The gamma rays emitted by this source should be able to initiate the inverse process of **nuclear resonance absorption** in an absorber composed of nuclei of the same type as those decaying in the source. Again, the scheme (...) would hold here, but the radiative transitions would now take place between nuclear states.

Nevertheless, **all attempts in the next two decades** to find this nuclear resonance absorption **proved fruitless**. it is appropriate to consider the reasons why the discovery of nuclear resonance absorption was so long delayed.

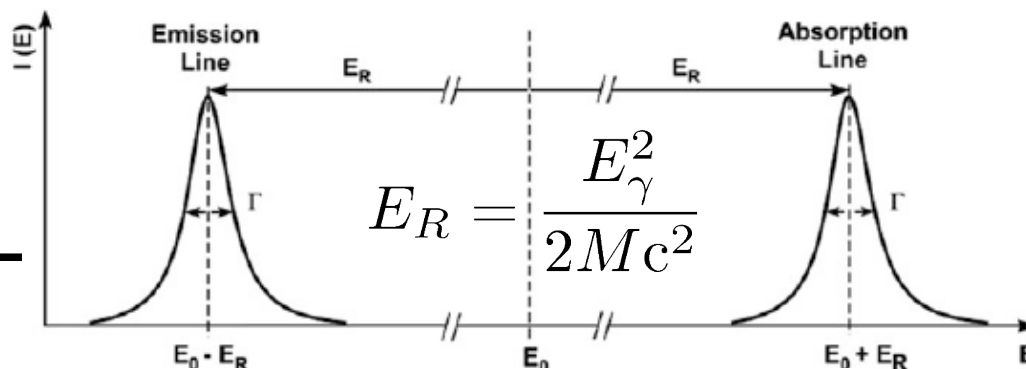
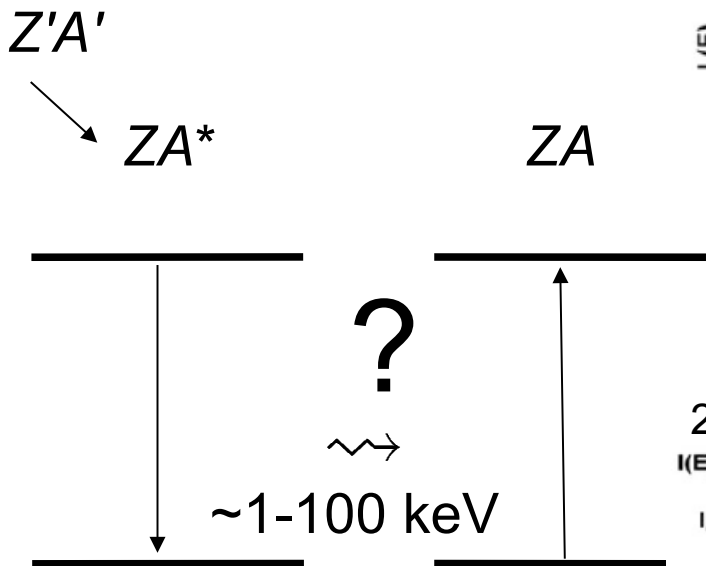
R.L. Mössbauer, Nobel Lecture, The Nobel Foundation 1961
W. Kuhn, Phil. Mag. 8, 625 (1929)

1) Conservation of momentum. Recoil energy:

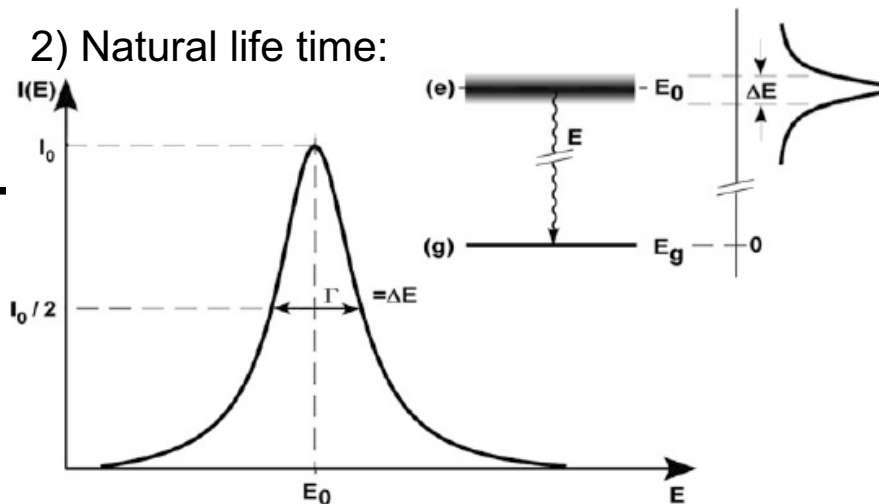


Nuclear resonant absorption?

1) Conservation of momentum. Recoil energy:



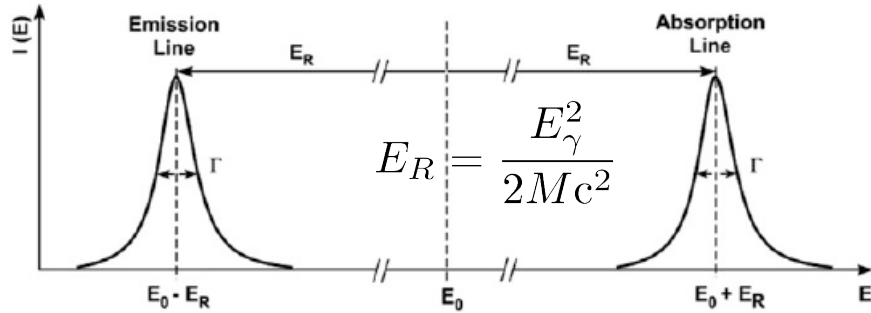
2) Natural life time:



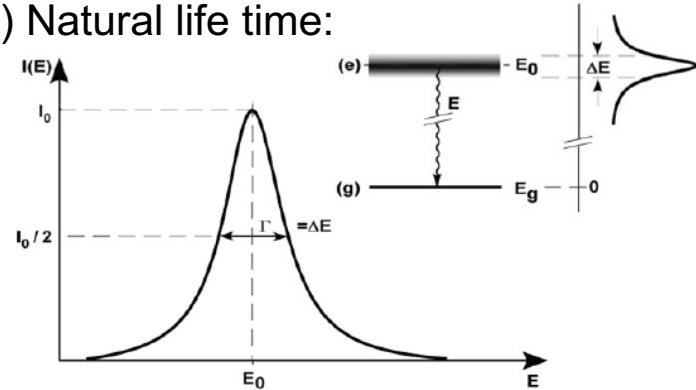
	Energy(eV)	Γ_n (eV)	E_R (eV)	$\Gamma_n/2E_R$
^{57}Fe	14400	$5 \cdot 10^{-9}$	$2 \cdot 10^{-3}$	$1,2 \cdot 10^{-6}$
Na (D-line)	2.1	$4 \cdot 10^{-8}$	$1 \cdot 10^{-10}$	220

Nuclear resonant absorption?

1) Conservation of momentum. Recoil energy:



2) Natural life time:



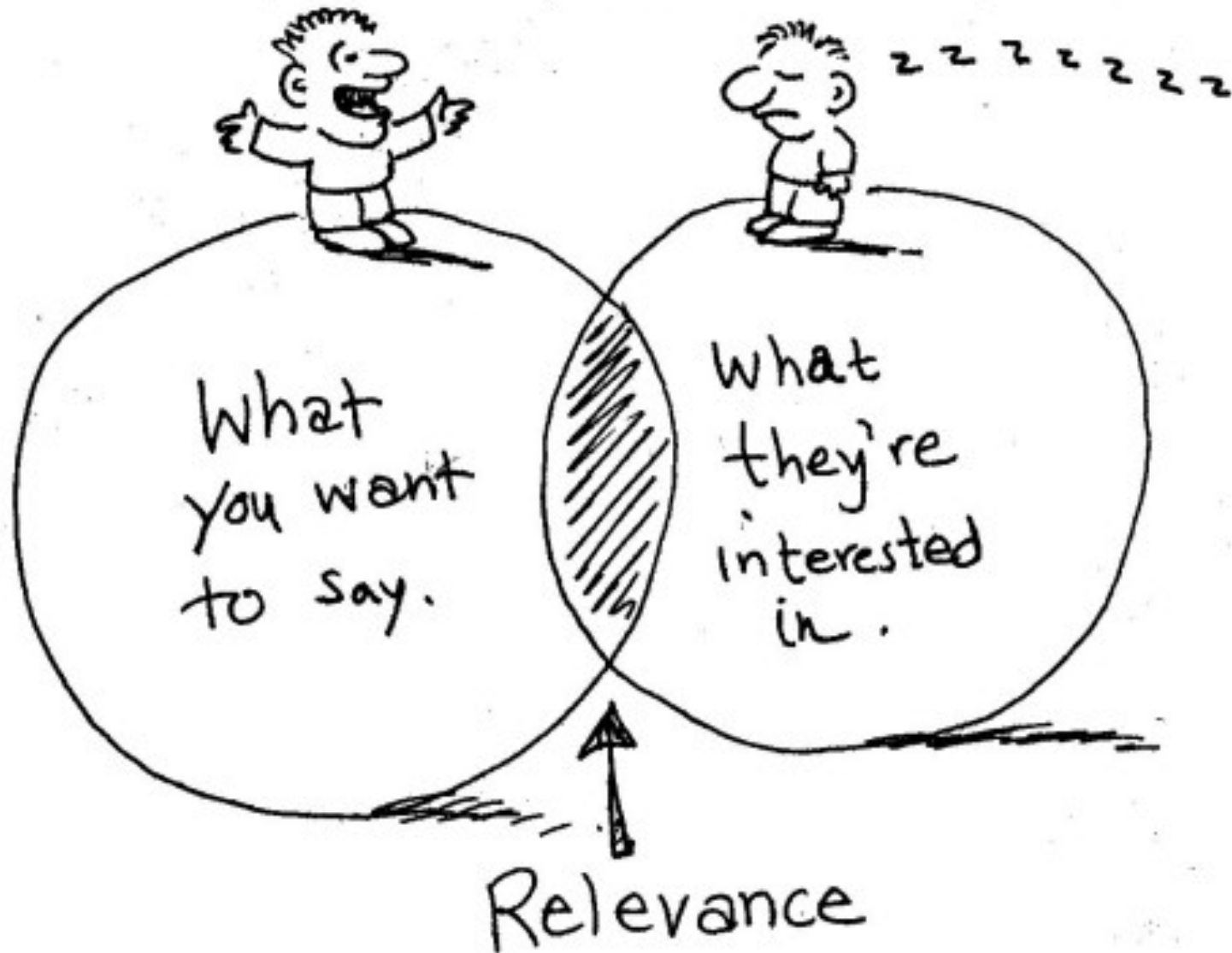
„The unsatisfactory situation with respect to nuclear resonance absorption first changed in 1951, when Moon succeeded in demonstrating the effect for the first time, by an ingenious experiment. The fundamental idea of his experiment was that of compensating for the recoil-energy losses of the gamma quanta: the radioactive source used in the experiment was moved at a suitably high velocity toward the absorber or scatterer. The displacement of the emission line toward higher energies achieved in this way through the **Doppler effect** produced a measurable nuclear fluorescence effect.“

R.L. Mössbauer, Nobel Lecture, The Nobel Foundation 1961
P.B. Moon, Proc. Phys. Soc. (London) 64, 76 (1951)

„A method first employed by Malmfors appeared to be especially suitable In this method, a broadening of the emission or absorption line, leading to a corresponding increase in the degree of overlap of the two lines, is achieved by **increasing the temperature.**“

K.G. Malmfors, Arkiv Fysik 6, 49 (1953)

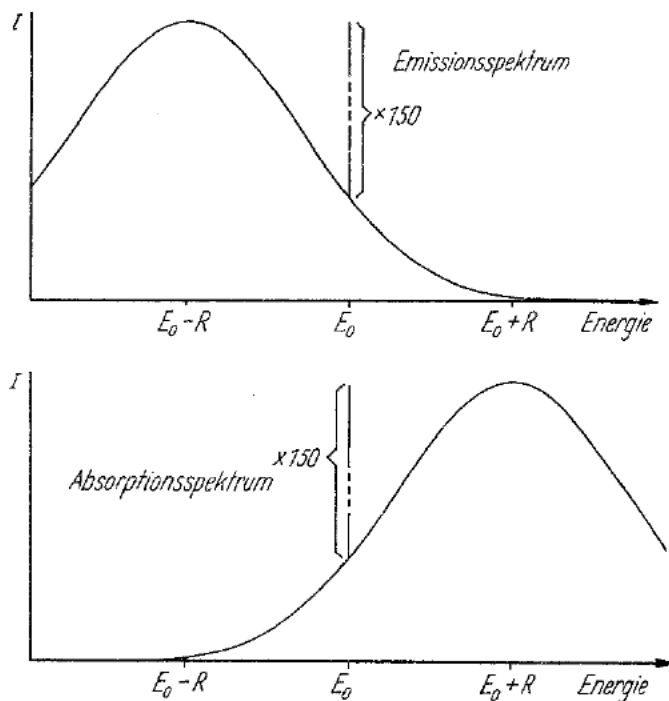
Rule 1: Know your audience



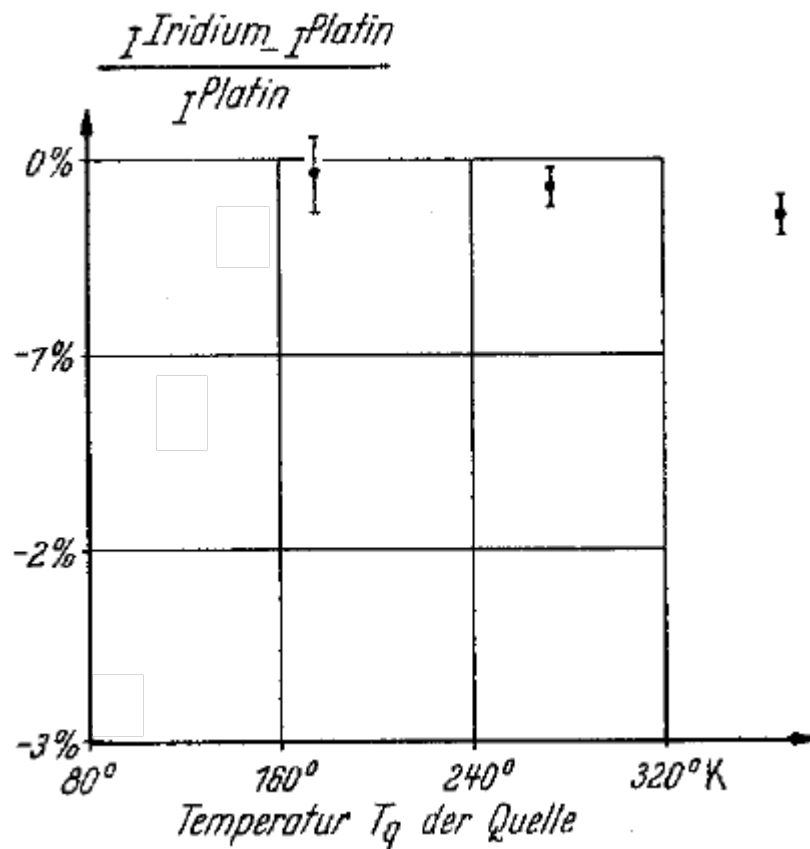
Nuclear resonant absorption?

„If the relative shift of the emission and the absorption lines resulting from the recoil-energy losses is only of the order of magnitude of the line widths, not only an increase but also a **decrease in temperature can result in a measurable change** in the nuclear absorption. My **decision** between these two possibilities was made in favour of a **temperature decrease**. It was motivated essentially by the consideration that **at low temperature, effects of chemical binding would be more likely** than at elevated temperatures.“

R.L. Mössbauer, Nobel Lecture, The Nobel Foundation 1961



^{191}Ir $E_0 = 129 \text{ keV}$

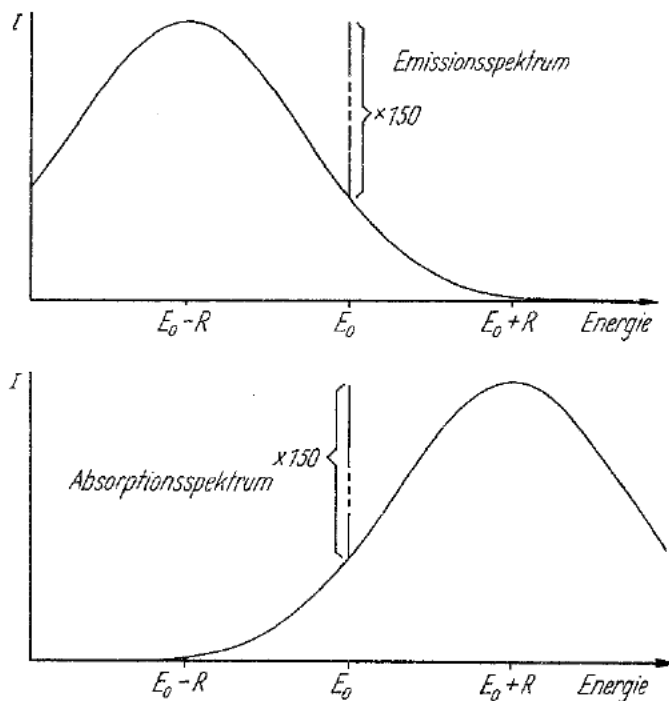


R. Mößbauer, Zeitschrift für Physik, 1958, 151, pp 124-143.

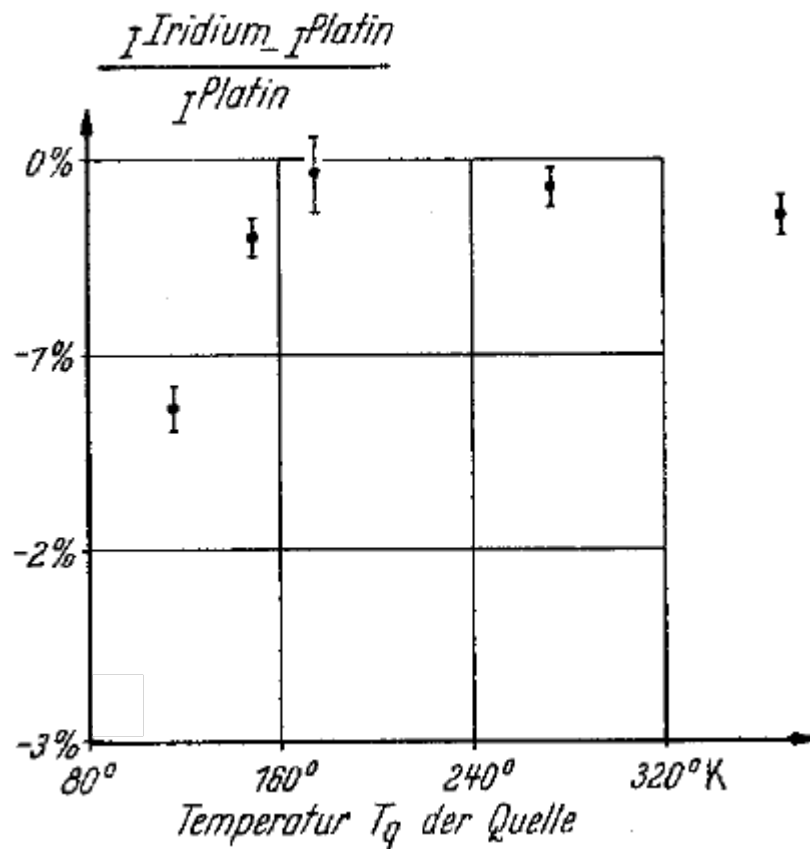
Nuclear resonant absorption?

„If the relative shift of the emission and the absorption lines resulting from the recoil-energy losses is only of the order of magnitude of the line widths, not only an increase but also a **decrease in temperature can result in a measurable change** in the nuclear absorption. My **decision** between these two possibilities was made in favour of a **temperature decrease**. It was motivated essentially by the consideration that **at low temperature, effects of chemical binding would be more likely** than at elevated temperatures.“

R.L. Mössbauer, Nobel Lecture, The Nobel Foundation 1961

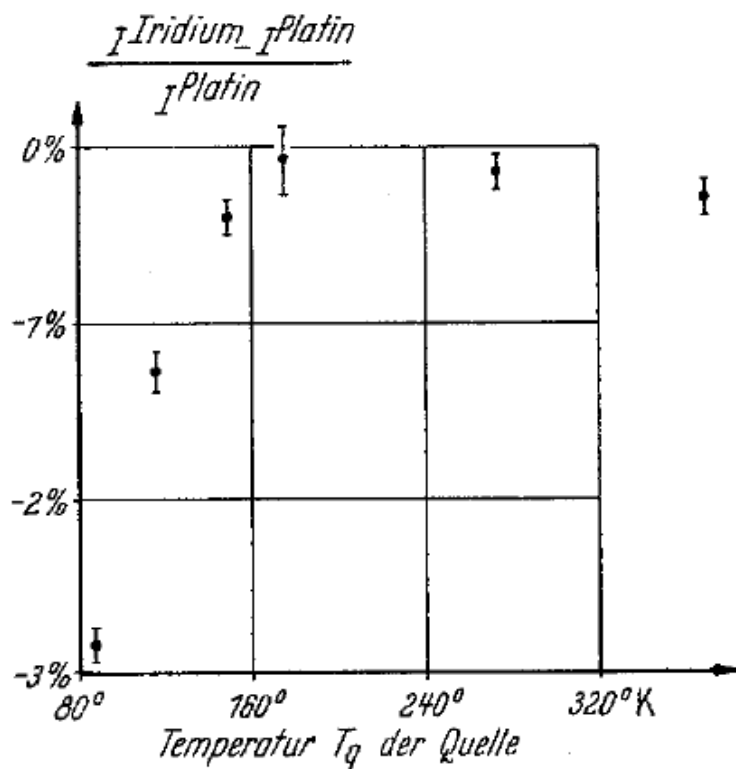


^{191}Ir $E_0 = 129 \text{ keV}$

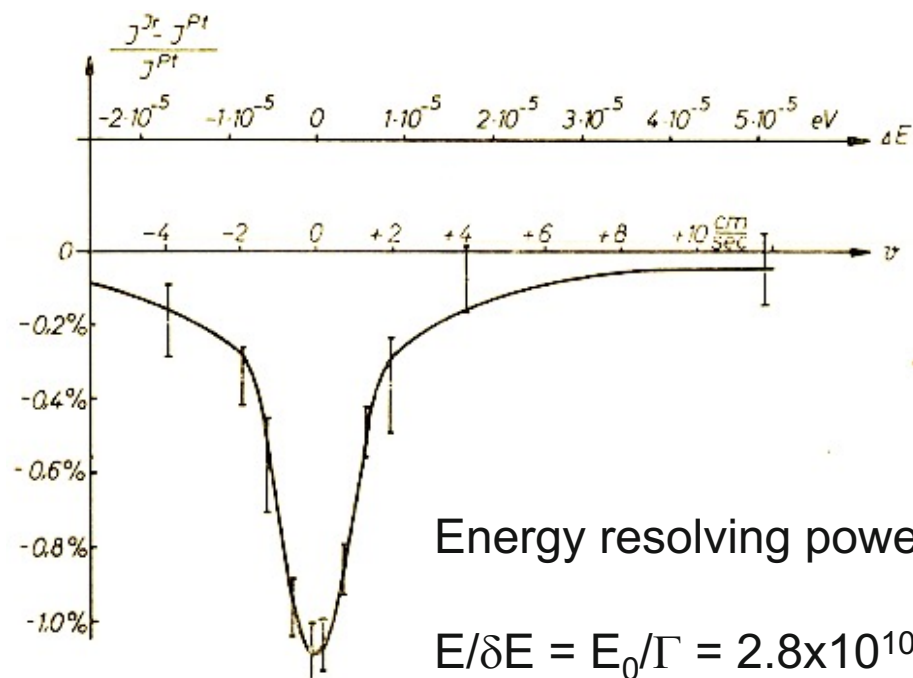


R. Mössbauer, Zeitschrift für Physik, 1958, 151, pp 124-143.

Nuclear resonant absorption?



R. Mößbauer, Zeitschrift für Physik, 1958, 151, pp 124-143.



Energy resolving power:

$$E/\delta E = E_0/\Gamma = 2.8 \times 10^{10}$$

R.L. Mößbauer, Naturwiss. 45, 538 (1958)

R.L. Mößbauer, Z. Naturforsch. 14a, 211 (1959)

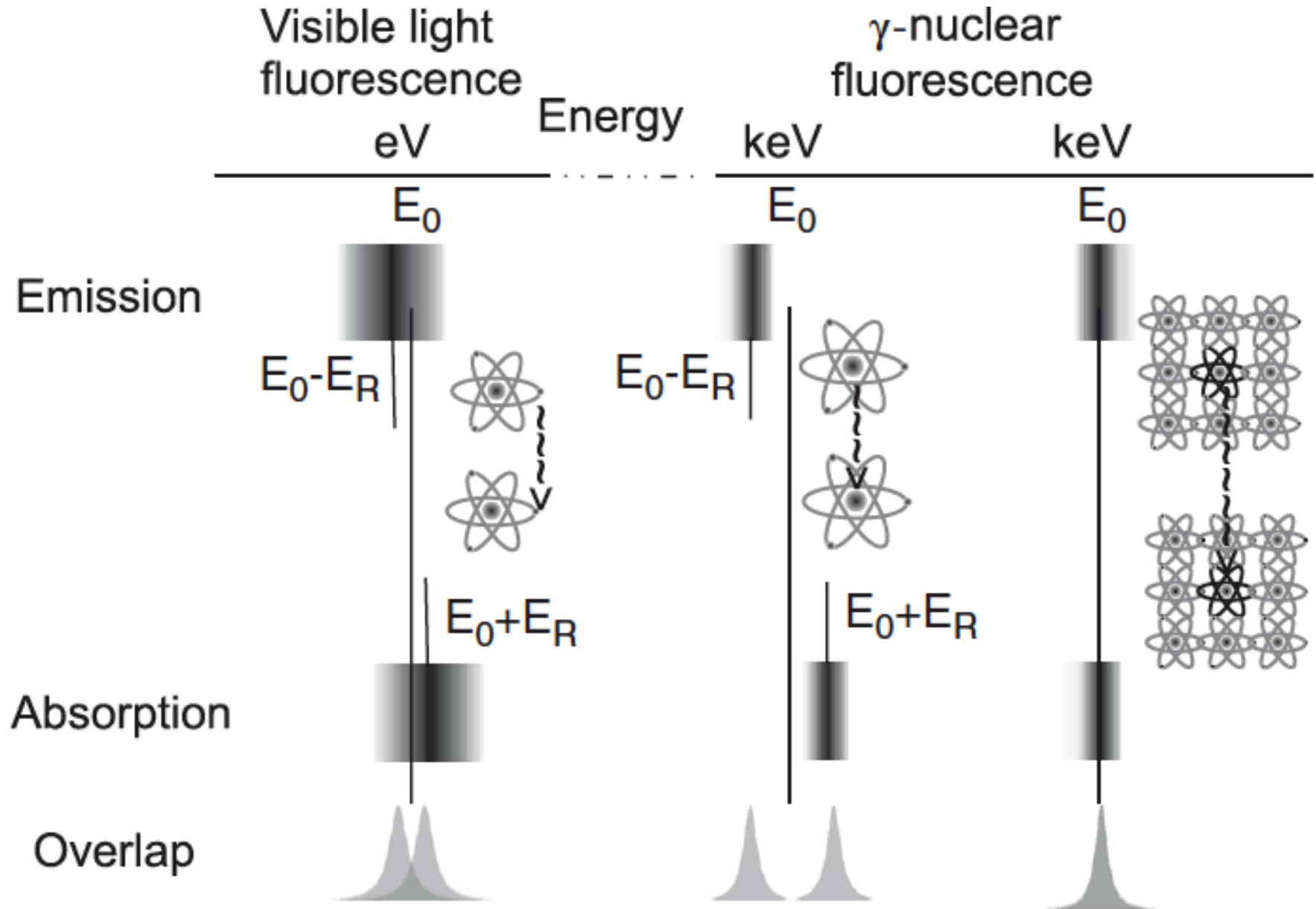
„Recoilless absorption and emission of gamma-rays“

„It is this property of the recoilless nuclear resonance absorption – namely, that it is possible by this means to measure extraordinarily small energy differences between two systems – which gave the method its significance and opened up a broad field of possible applications. Thus, the **extraordinary sharpness of the recoilless gamma lines** brought direct investigation of the **hyperfine structure** of nuclear transitions within the range of possibility.“

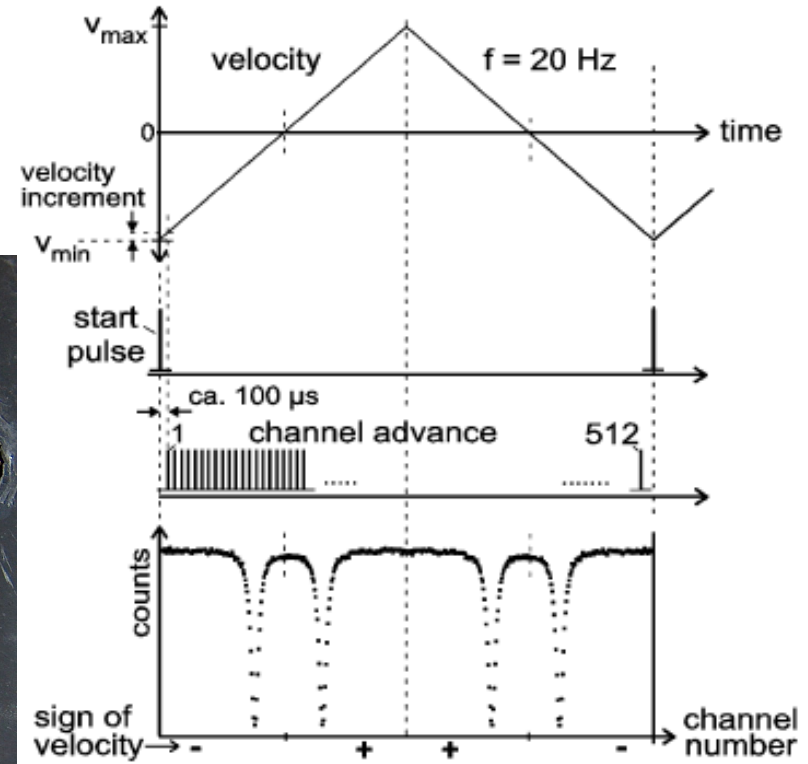
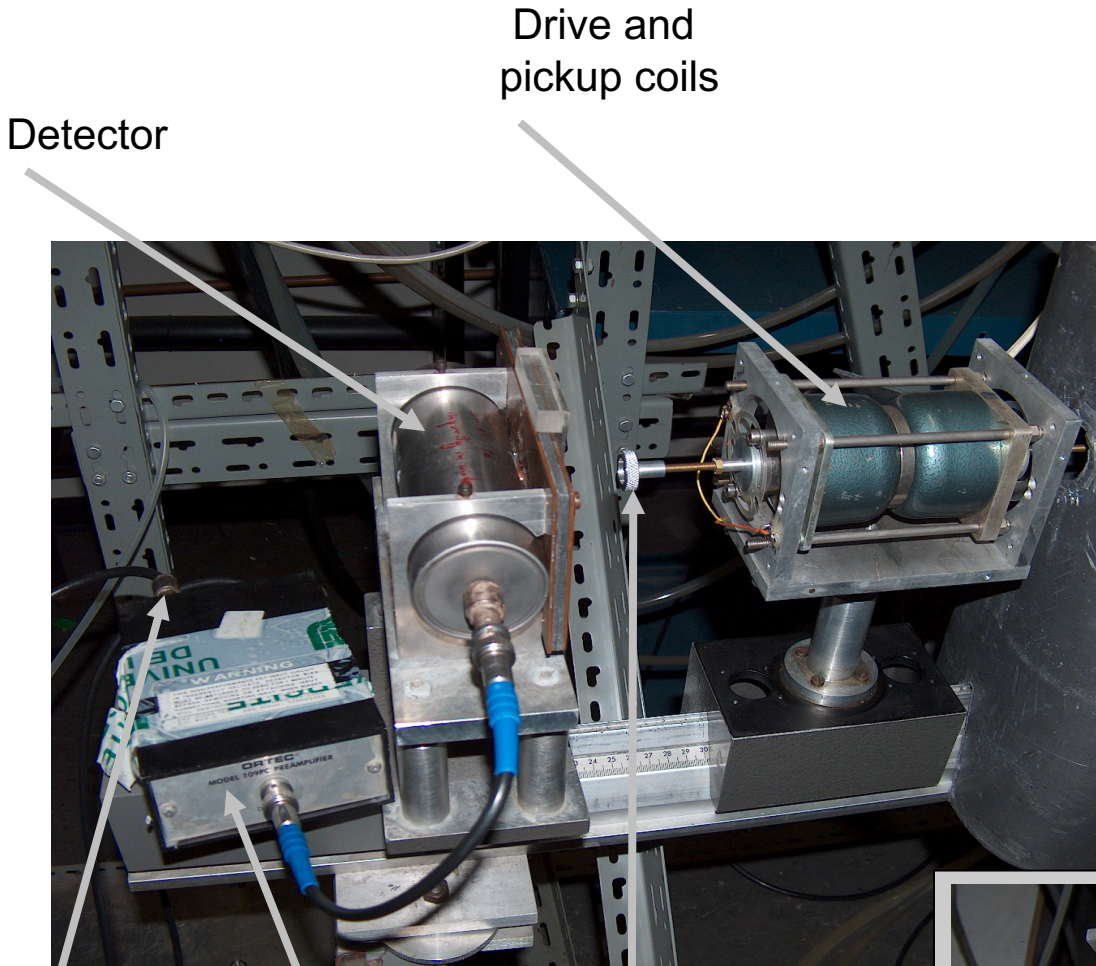
The Mößbauer effect



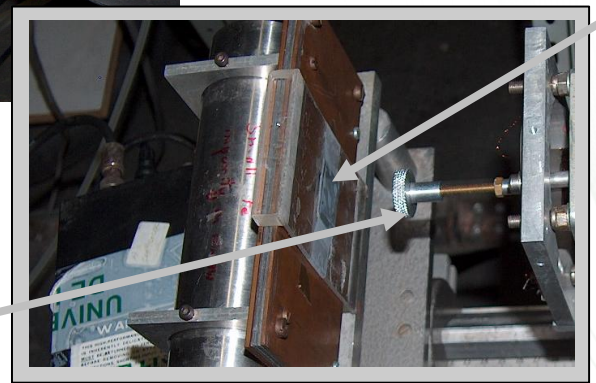
Summary



Mössbauer spectroscopy: experimental setup



Gütlich, Bill, Trautwein (eds.), 2011.



γ -ray source (e.g. ^{57}Co , $^{151\text{m}}\text{Sm}$, $^{121\text{m}}\text{Sn}$, ...)

Applications from fundamental physics to materials

Testing general relativity

APPARENT WEIGHT OF PHOTONS*

R. V. Pound and G. A. Rebka, Jr.

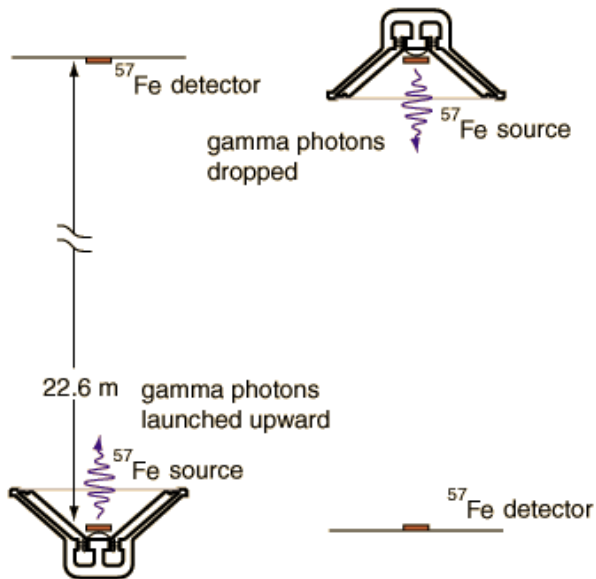
Lyman Laboratory of Physics, Harvard University, Cambridge, Massachusetts

(Received March 9, 1960)

$$(\Delta\nu)_{\text{exp}} / (\Delta\nu)_{\text{theor}} = + 1.05 \pm 0.10;$$

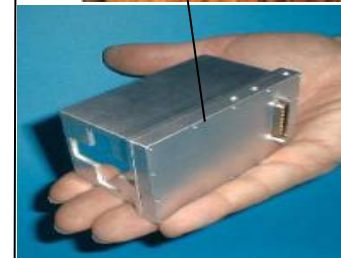
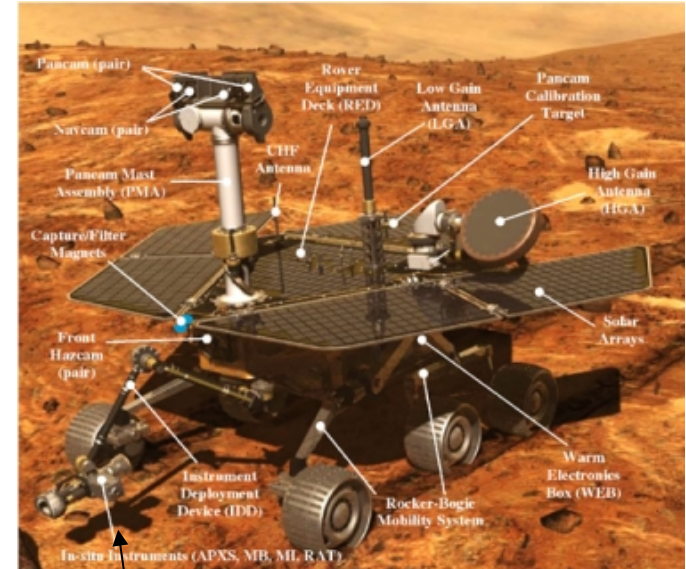
$$\Delta E = mgh = \frac{E}{c^2} gh = \frac{14.4 \text{ keV}}{c^2} g \cdot 22.6 \text{ m}$$

$$\Delta E = 3.5 \times 10^{-11} \text{ eV}$$

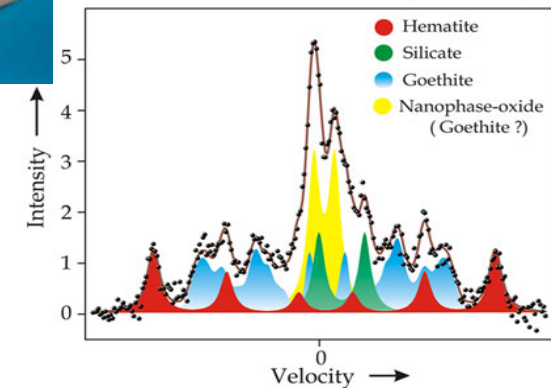


$$\left(\frac{\Delta E}{E}\right)_{\text{down}} - \left(\frac{\Delta E}{E}\right)_{\text{up}} = (5.1 \pm 0.5) \times 10^{-15}$$

Mössbauer spectroscopy on Mars



Mössbauer Spectrum of Clovis (200 - 220K)



<http://iacgu7.chemie.uni-mainz.de/klingshoefer/>

Rule 1: Know your audience

Mössbauer Spectroscopy Periodic Table

He

<http://www.medc.dicp.ac.cn/Resources.php>

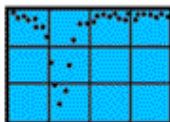
H																	He				
Li	Be															B	C	N	O	F	Ne
Na	Mg											Al	Si	P	S	Cl	Ar				
K	Ca	Sc	Ti	V	Cr	Mn	Fe	Co	Ni	Cu	Zn	Ga	Ge	As	Se	Br	Kr				
40 29.6						55 125.9	57 14.4 57 136.5		61 67.4 63 87.1		67 90.3		73 13.3 73 67.0				83 9.4				
Rb	Sr	Y	Zr	Nb	Mo	Tc	Ru	Rh	Pd	Ag	Cd	In	Sn	Sb	Te	I	Xe				
						99 140.5	99 89.4			107 93.5 109 88.0			117 158.0 118 23.9 118 88.5	121 37.1	125 35.5 125 109.0	127 57.6 129 27.8	129 39.6 131 83.2				
Cs	Ba	La	Hf	Ta	W	Re	Os	Ir	Pt	Au	Hg	Tl	Pb	Bi	Po	At	Rn				
133 81.0	133 12.3	139 165.9	176 86.3 177 113.0 178 83.1 180 93.3	181 6.2 181 106.2	180 103.7 181 113.3 182 100.1 183 48.5 183 59.1 184 111.2 186 122.3	187 134.2	190 137.2 190 150.9 190 30.2 193 138.9	191 82.4 191 129.3 195 129.7	195 98.8	197 77.4	201 32.2										
Fr	Ra	Ac																			



Number of publications

- N > 1000
- 100 < N < 1000
- 10 < N < 100
- N < 10
- Silent

Ce	Pr	Nd	Pm	Sm	Eu	Gd	Tb	Dy	Ho	Er	Tm	Yb	Lu
	141 145.4	143 97.3 142 72.0	145 51.0 147 91.1	147 122.1 149 22.5 151 85.4 152 121.8 153 35.8 154 82.0	151 21.6 153 83.4 155 105.3 156 89.0 157 54.5 157 64.0 158 79.5 160 75.3	154 123.1 155 60.0 155 88.5 155 105.3 156 89.0 157 54.5 157 64.0 158 79.5 160 75.3	159 58.0	160 86.8 161 25.7 161 43.6 161 74.6 162 80.7 164 73.4	165 94.7	164 61.4 166 80.6 167 79.3 168 79.8 170 79.3	169 8.4	170 64.3 171 99.7 171 75.9 172 78.7 174 75.5 176 82.1	175 113.8
Th	Pa	U	Np	Pu	Am	Cm	Bk	Cf	Es	Fm	Md	No	Lr
232 49.4	231 64.2	234 43.5 236 45.2 238 44.9	237 59.5	239 57.3 240 42.9	243 64.0								



Mössbauer Effect Data Center

Tel: (828) 251-6617 Fax: (828) 232-5179 Email: medc@unca.edu Web: www.unca.edu/medc

Common vs uncommon transitions

Nuclide	E_0 (keV)	τ_0 (ns)	a (%)	I_g	I_e	α	σ_n /kbarn	σ_n/σ_{ph}
^{187}Os	9.777	3.43	1.6	$1/2^-$	$3/2^-$	264.	194.4	5.84
^{57}Fe	14.4129	141.	2.14	$1/2^-$	$3/2^-$	8.18	2464.0	428.58
^{151}Eu	21.5412	14.0	47.8	$5/2^+$	$7/2^+$	28.0	242.6	29.06
^{149}Sm	22.5015	10.3	13.8	$7/2^-$	$5/2^+$	29.2	120.1	17.29
^{119}Sn	23.8793	25.6	8.58	$1/2^+$	$3/2^+$	5.22	1380.5	562.59
^{125}Te	35.4920	2.14	6.99	$1/2^+$	$3/2^+$	14.0	259.0	44.11
^{121}Sb	37.1292	4.99	57.3	$5/2^+$	$7/2^+$	11.11	195.4	40.26
^{129}Xe	39.5813	1.47	26.4	$1/2^+$	$3/2^+$	12.31	234.7	47.24
^{61}Ni	67.408	7.60	1.19	$3/2^-$	$5/2^-$	0.139	709.1	7046.
^{73}Ge	68.752	2.51	7.76	$9/2^+$	$7/2^+$	0.227	337.5	2121.
^{197}Au	77.351	2.76	100.	$3/2^+$	$1/2^+$	4.36	38.1	56.22
^{191}Ir	82.407	5.89	37.3	$3/2^+$	$1/2^+$	10.9	15.1	6.20
^{155}Gd	86.546	9.13	14.7	$3/2^-$	$5/2^+$	0.434	341.7	304.61
^{99}Ru	89.571	28.8	12.7	$5/2^+$	$3/2^+$	1.498	81.2	315.04

R. Hermann, *Mössbauer Spectroscopy*, p.443-484, in Handbook of Solid State Chemistry, Eds. Dronskowski, Kikkawa, and Stein, 2017 Wiley-VCH

- Historical perspective
- Spectral description and parameters
- Static interactions
- Time dependent interactions

Lattice dynamics

Probability for recoilless absorption or emission of gamma-rays:

Lamb-Mössbauer factor: $f = \exp\left[-\langle x^2 \rangle E_\gamma^2 / (\hbar c)^2\right]$

Single particle – incoherent – absorption

In a solid the recoil is distributed to the crystal → negligible as $M \gg m_{\text{nucleus}}$
and to the lattice vibrations → quantized in phonons.

The Lamb-Mössbauer factor quantifies the 0-phonon probability.

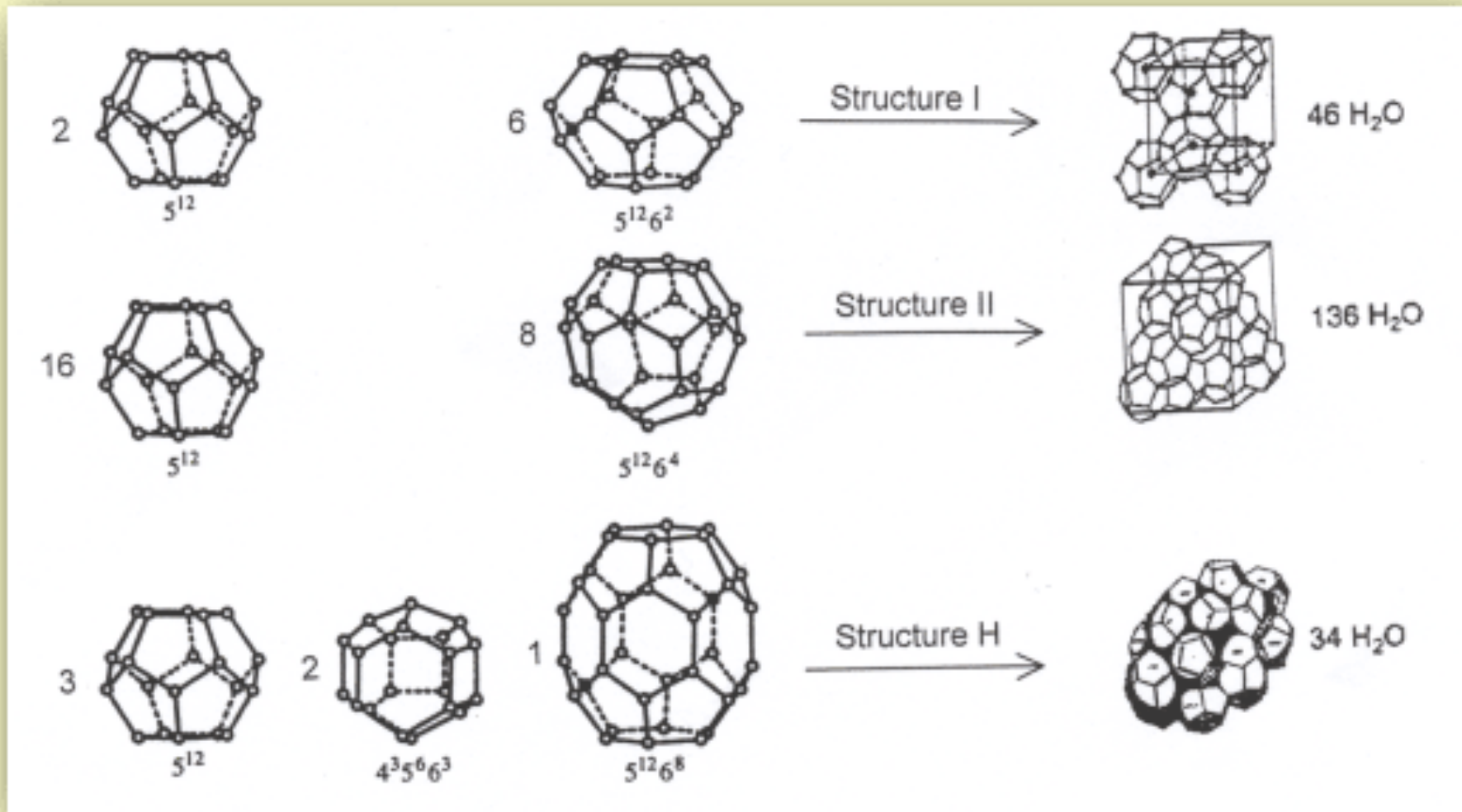
$$f_{DW} = \exp(-\langle \mathbf{u} \cdot \mathbf{q} \rangle^2)$$

$$|\mathbf{q}| = 4\pi \sin\theta/\lambda$$

Similar, but not to be confused with the Debye-Waller factor:

Pair distribution function – coherent – scattering

Guest dynamics in clathrates



<http://www.calstatela.edu/dept/chem/ba/researchtops-gashy.htm>

<http://www.calstatela.edu/dept/chem/ba/researchtops-gashy.htm>

Guest dynamics in clathrates

THE JOURNAL OF CHEMICAL PHYSICS

VOLUME 49, NUMBER 4

15 AUGUST 1968

Dynamics of Krypton Atoms in Clathrate by the Mössbauer Technique*

Y. HAZONY

Department of Chemical Engineering, Princeton University, Princeton, New Jersey

AND

S. L. RUBY

Physics Division, Argonne National Laboratory, Argonne, Illinois

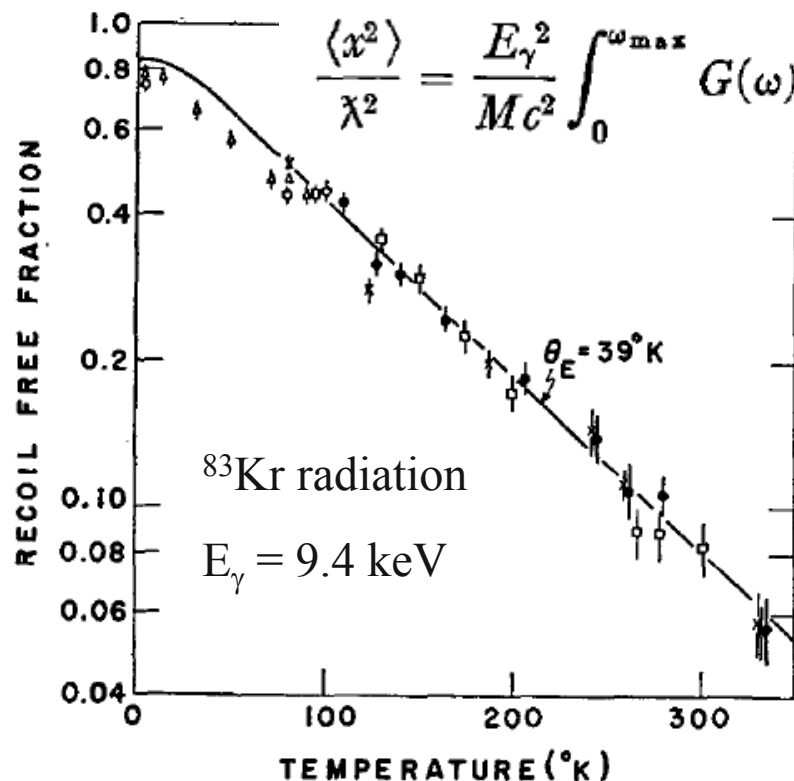


FIG. 1. Experimental results for the recoil-free fraction f vs temperature for Kr in HQ clathrate. The solid curve is that calculated for a particle in a harmonic well, for which $x^2/\lambda^2 = (E^2/2mc^2) (k\theta)^{-1} (1+e^{-u})^{-1} (1-e^{-u})^{-1}$, $\mu = \theta/T$, $\theta = 39^\circ\text{K}$.

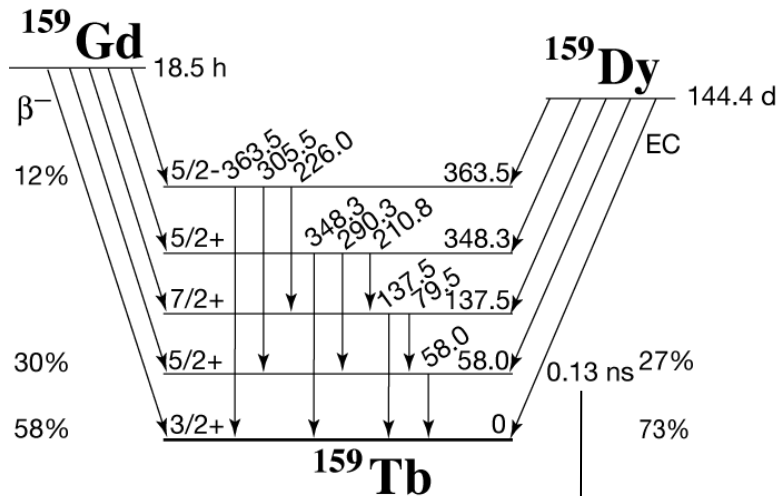
The hydroquinone (HQ) clathrate structure provides a solid "cagework" in which a variety of atoms or even small molecules may be trapped.¹ Since the guest atoms and molecules are confined mainly by the repulsive forces of the walls of the cages, this structure has been considered as an ideal case for the study of the cell model, which is used in statistical thermodynamics to describe the behavior of liquid and solid solutions. A large amount of experimental and theoretical work has been performed on the dynamics of the trapped molecules as well as on the nature of their interaction with the walls.

The theoretical analysis of the thermodynamic properties of these compounds is usually based on the cell model. In this approximation, the interaction between the trapped molecule and the cage is represented by a static potential well and the vibrations of the molecule in the cell are assumed to be completely decoupled from the dynamics of the host lattice as well as from the other guest molecules in the adjacent cells.²

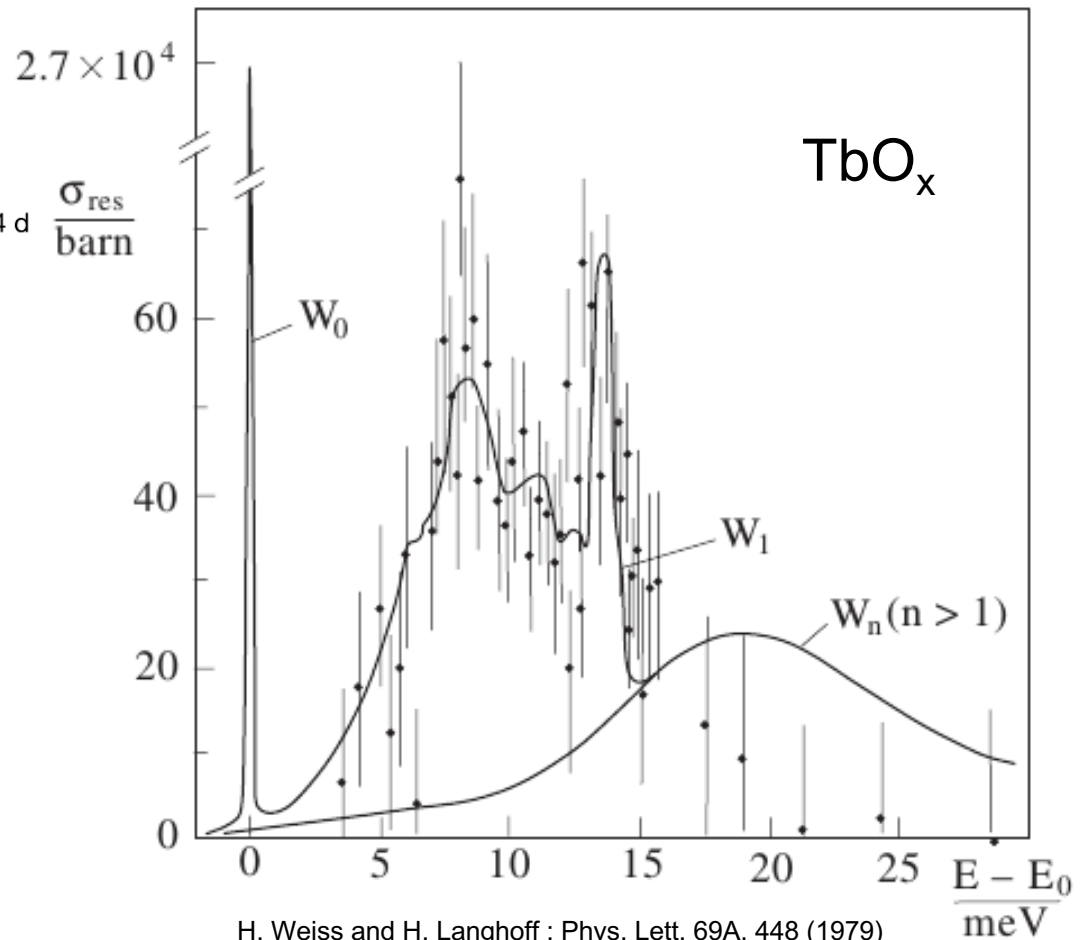
Accessing phonon modes

If Doppler velocity is increased:

$$E - E_0 = E_0 \cdot v/c \sim 16.7 \text{ meV, for } 100 \text{ m/s and } E_0 = 50 \text{ keV}$$

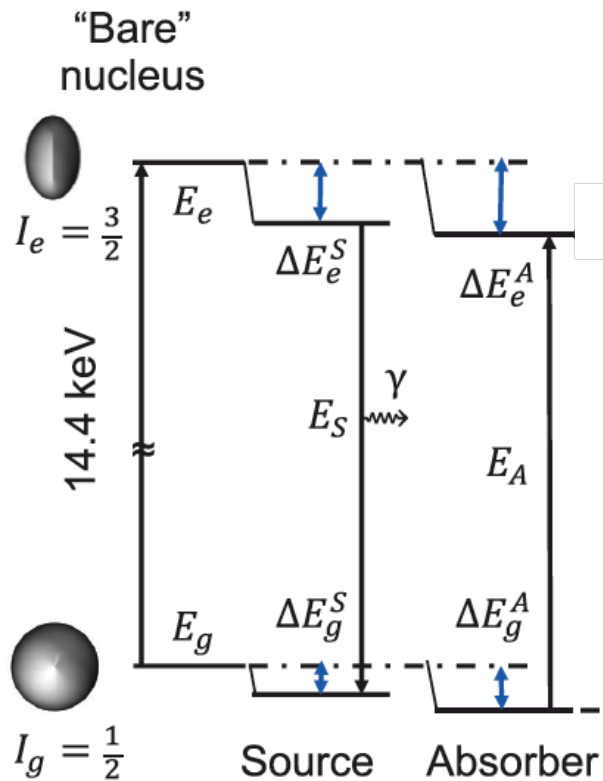


Heisenberg relation: $\Gamma = 5 \mu\text{eV}$



H. Weiss and H. Langhoff : Phys. Lett. 69A, 448 (1979)

Electric monopole: isomer shift

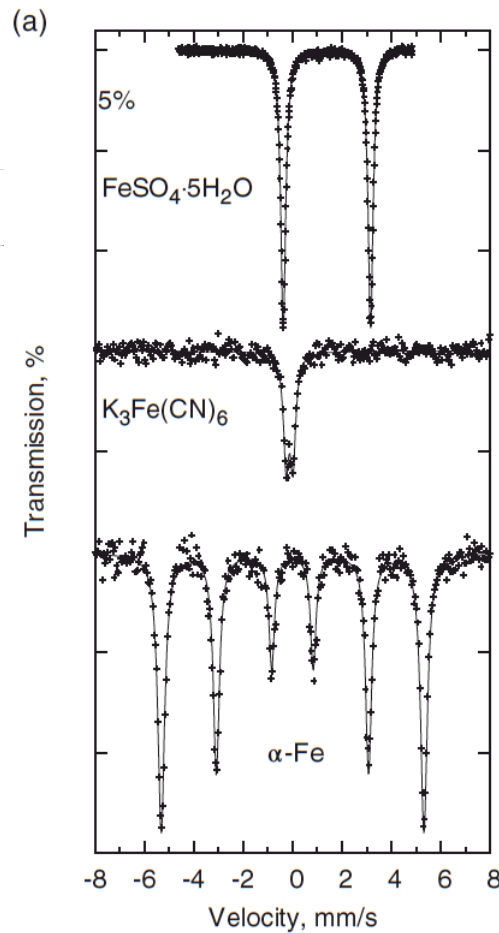


$$\delta = E_S - E_A$$

$$= (\Delta E_e^S - \Delta E_g^S)$$

$$- (\Delta E_e^A - \Delta E_g^A)$$

Isomer shift

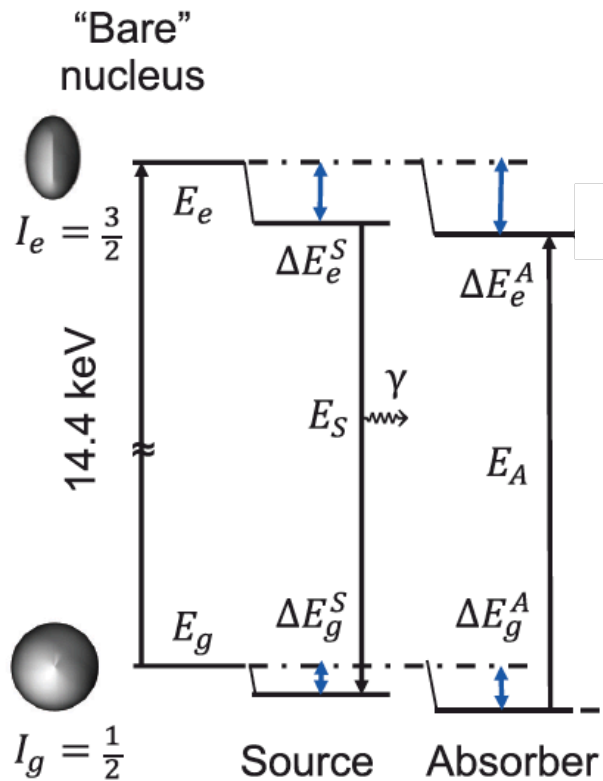


Sample property

$$\delta = E_A - E_S = \frac{2\pi}{5} Z e^2 (\rho_A(0) - \rho_S(0)) [R_e^2 - R_g^2]$$

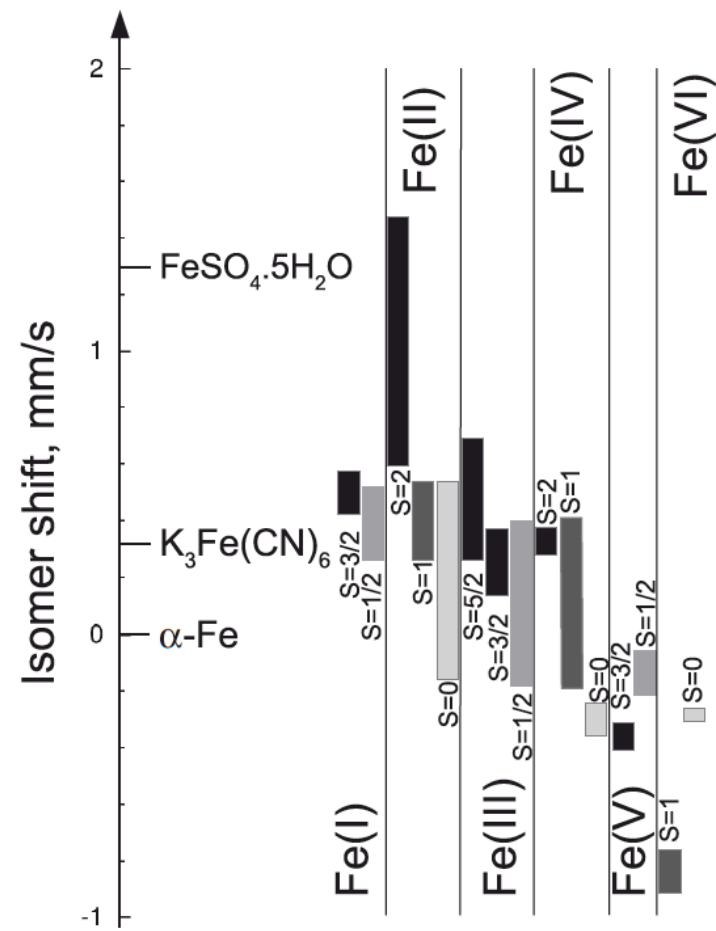
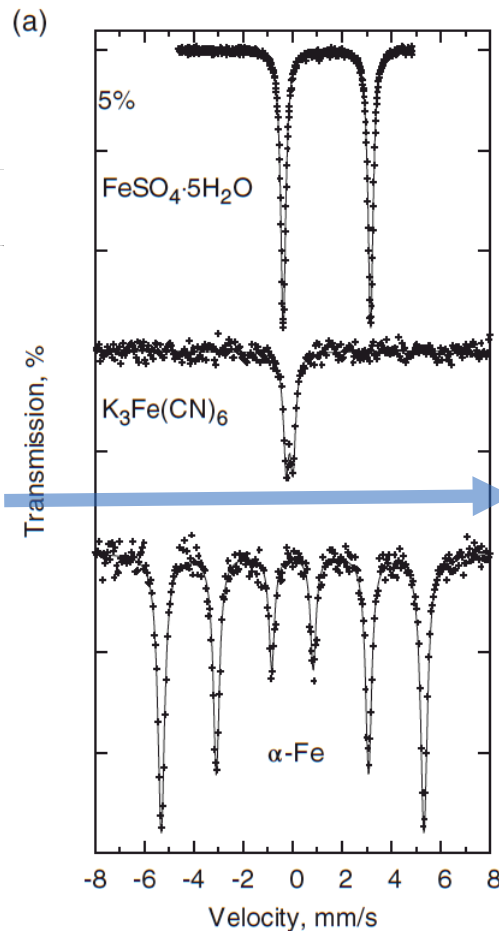
Electric monopole: isomer shift

^{57}Fe



$$\delta = E_S - E_A = (\Delta E_e^S - \Delta E_g^S) - (\Delta E_e^A - \Delta E_g^A)$$

Isomer shift



Sample property

$$\delta = E_A - E_S = \frac{2\pi}{5} Ze^2 (\rho_A(0) - \rho_S(0)) [R_e^2 - R_{gg}^2]$$

TEMPERATURE-DEPENDENT SHIFT OF γ RAYS EMITTED BY A SOLID

B. D. Josephson

Trinity College, Cambridge, England

(Received March 11, 1960)

Recent experiments by Mössbauer¹ have shown that when low-energy γ rays are emitted from nuclei in a solid a certain proportion of them are unaffected by the Doppler effect. It is the purpose of this Letter to show that they are nevertheless subject to a temperature-dependent shift to lower energy which can be attributed to the relativistic time dilatation caused by the motion of the nuclei.

Let us regard the solid as a system of interacting atoms with the Hamiltonian

$$H = \sum p_i^2/2m_i + V(r_1, r_2, \dots).$$

The Mössbauer effect is due to those processes in which the phonon occupation numbers do not change. It might appear that in such cases the energy of the solid is unaltered, but this is not so, as the nucleus which emits the γ ray changes its mass, and this affects the lattice vibrations. Suppose the nucleus of the i th atom emits a γ ray of energy E , its mass changing by $\delta m_i = -E/c^2$.

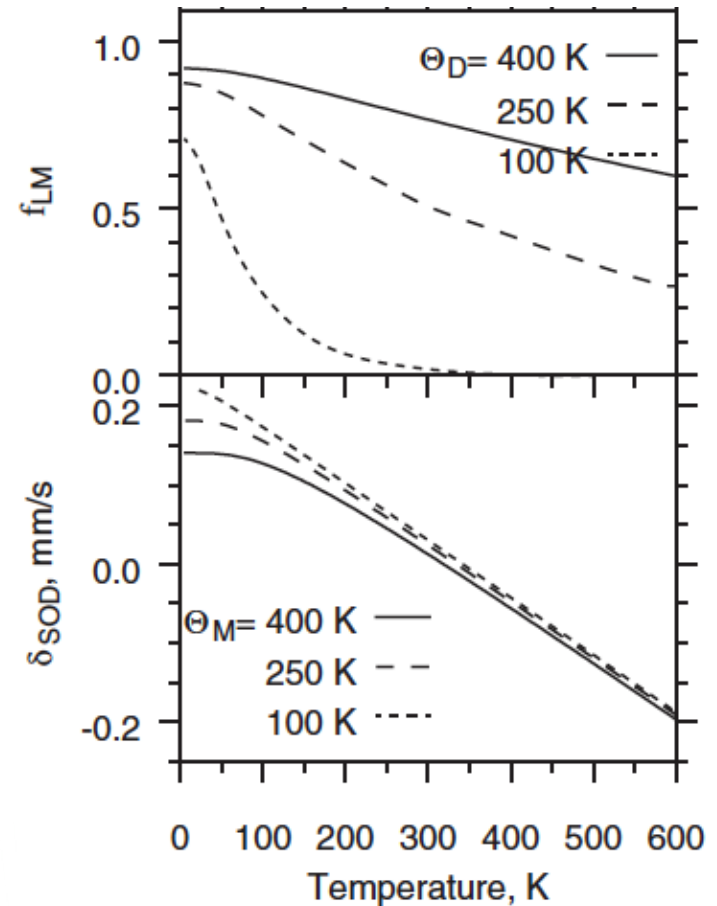
The change in energy, δE , of the solid is given by

$$\begin{aligned} \delta E &= \langle \Delta H \rangle = \delta \langle p_i^2/2m_i \rangle = -\delta m_i \langle p_i^2/2m_i^2 \rangle \\ &= (\delta m_i/m_i) T_i = (E/m_i c^2) T_i, \end{aligned}$$

where T_i is the expectation value of the kinetic energy of the i th atom. The energy of the γ ray must accordingly be reduced by δE so there is a shift of relative magnitude $\delta E/E = T_i/m_i c^2$. The same formula can be deduced by regarding the shift as due to a relativistic time dilatation.

To estimate T_i we make the following assumptions: (i) The atoms all have the same mass, and the kinetic energy is equally distributed among them. (ii) The kinetic energy is half the total lattice energy, i.e., we assume that the forces coupling the atoms are harmonic. Under these assumptions $T_i/m_i = \frac{1}{2}U$, where U is the lattice energy per unit mass. The relative shift is thus given by $\delta E/E = U/2c^2$. For Fe at 300°K

$$f_{LM} = \exp(-k^2 \cdot \langle x^2 \rangle)$$



$$\delta_{SOD} = -\langle v^2 \rangle / 2c$$

VOLUME 4, NUMBER 7

PHYSICAL REVIEW LETTERS

APRIL 1, 1960

this has the value 8×10^{-13} . Clearly a compensating shift would occur for absorption provided source and absorber were identical and at the same temperature. A small difference in temperature between source and absorber leads to a relative shift per degree given by $\delta E/E = C_p/2c^2$ where C_p is the specific heat. For Fe at 300°K this is $2.2 \times 10^{-15}/^\circ\text{K}$. This is sufficient for it to be necessary to take it into account in accurate experiments using the resonance absorption of

γ rays, such as those to measure the gravitational red shift.^{2,3}

I would like to thank Dr. Ziman, Professor O. R. Frisch, and Dr. W. Marshall for helpful discussions.

¹R. L. Mössbauer, Z. Physik 151, 124 (1958).

²R. V. Pound and G. A. Rebka, Phys. Rev. Letters 3, 554 (1959).

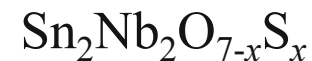
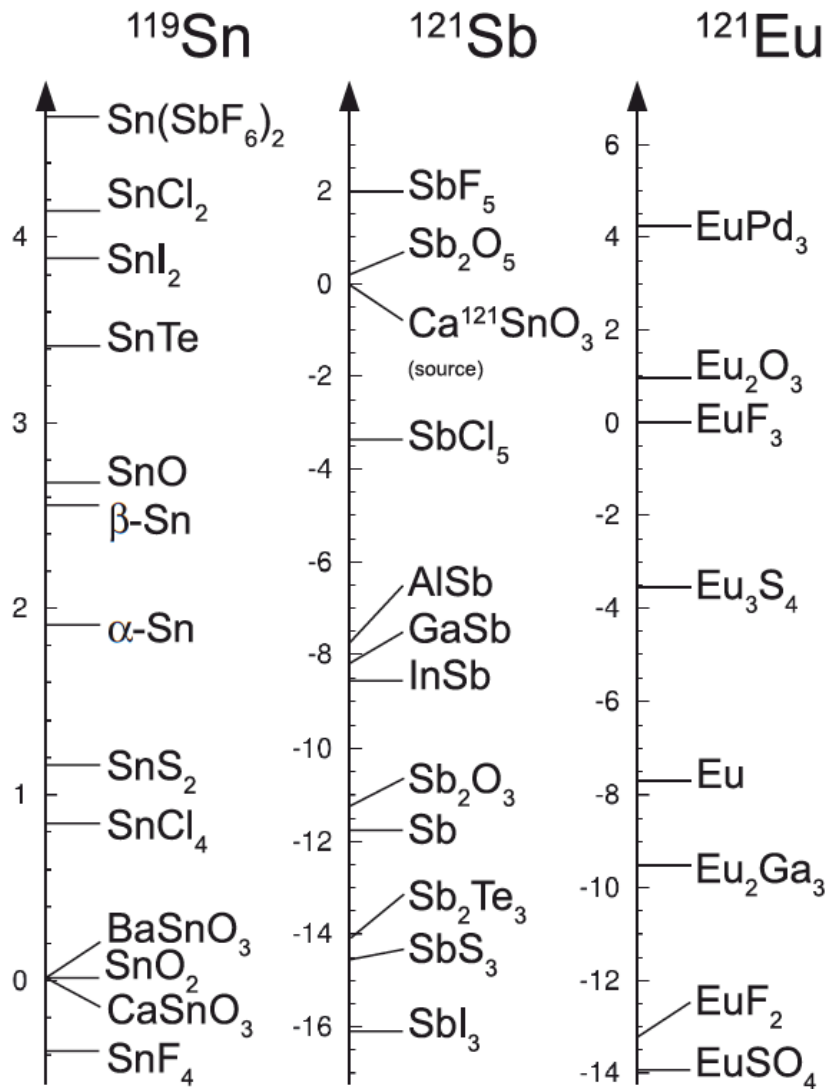
³T. E. Cranshaw, J. P. Schiffer, and A. B. Whitehead, Phys. Rev. Letters 4, 163 (1960).

UPPER LIMIT FOR THE ANISOTROPY OF INERTIAL MASS FROM NUCLEAR RESONANCE EXPERIMENTS*

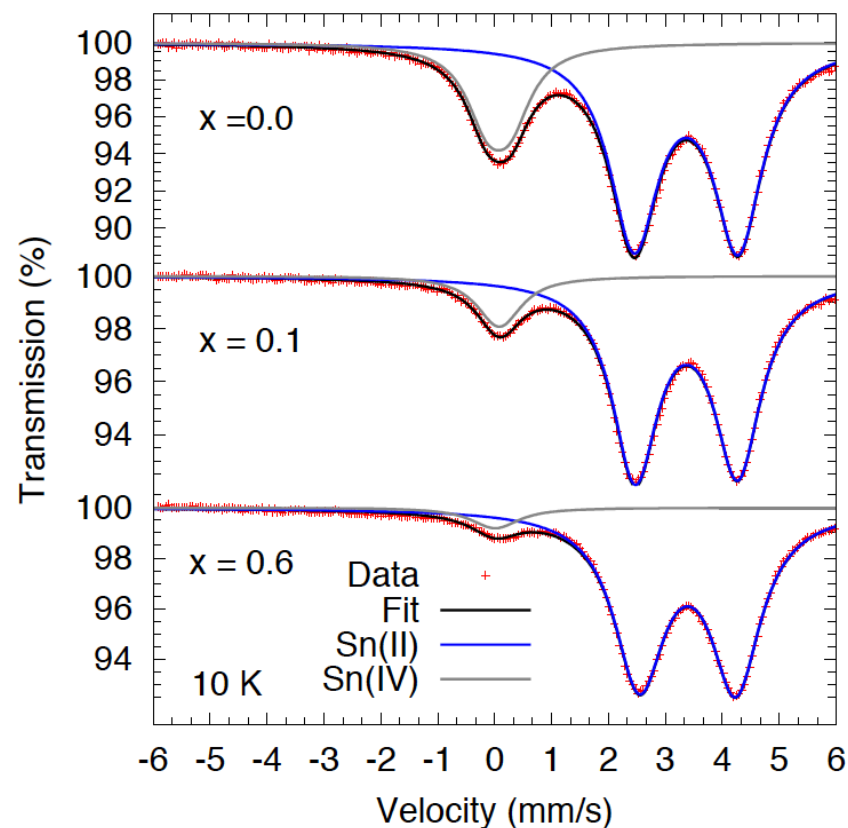
V. W. Hughes, H. G. Robinson, and V. Beltran-Lopez
Gibbs Laboratory, Yale University, New Haven, Connecticut

(Received March 2, 1960)

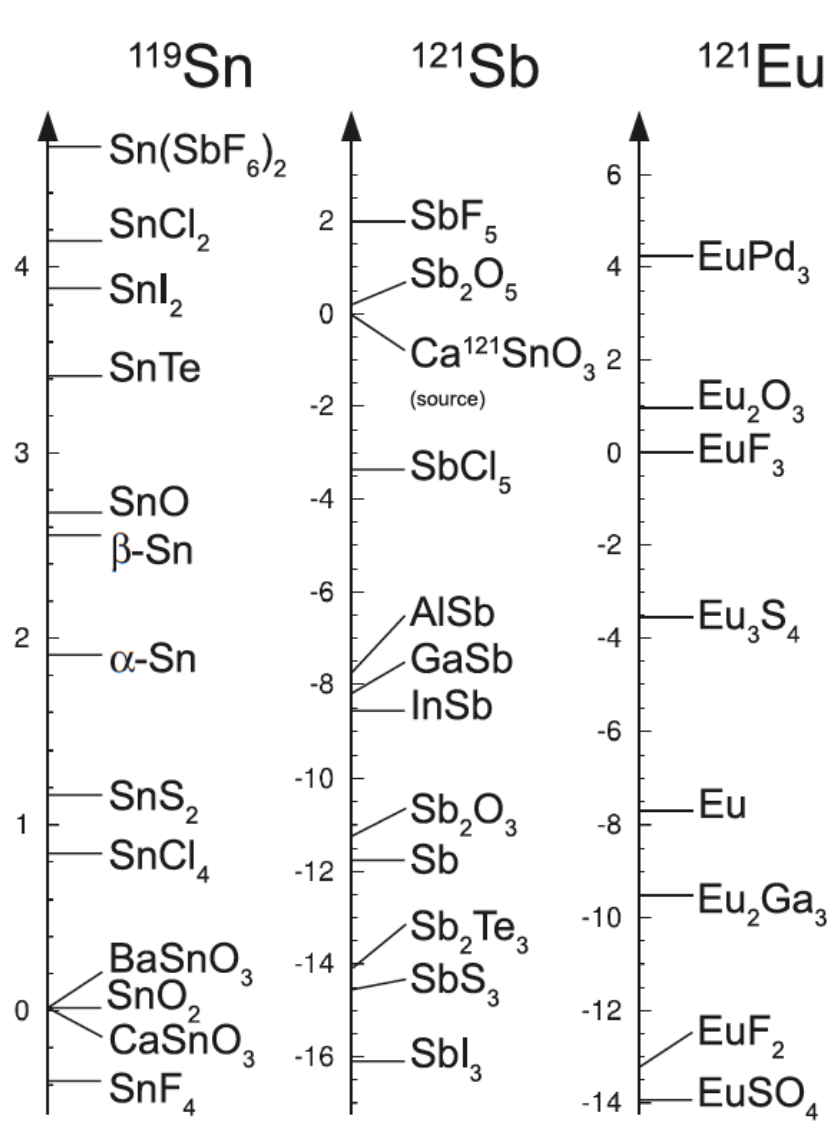
Electric monopole: isomer shift



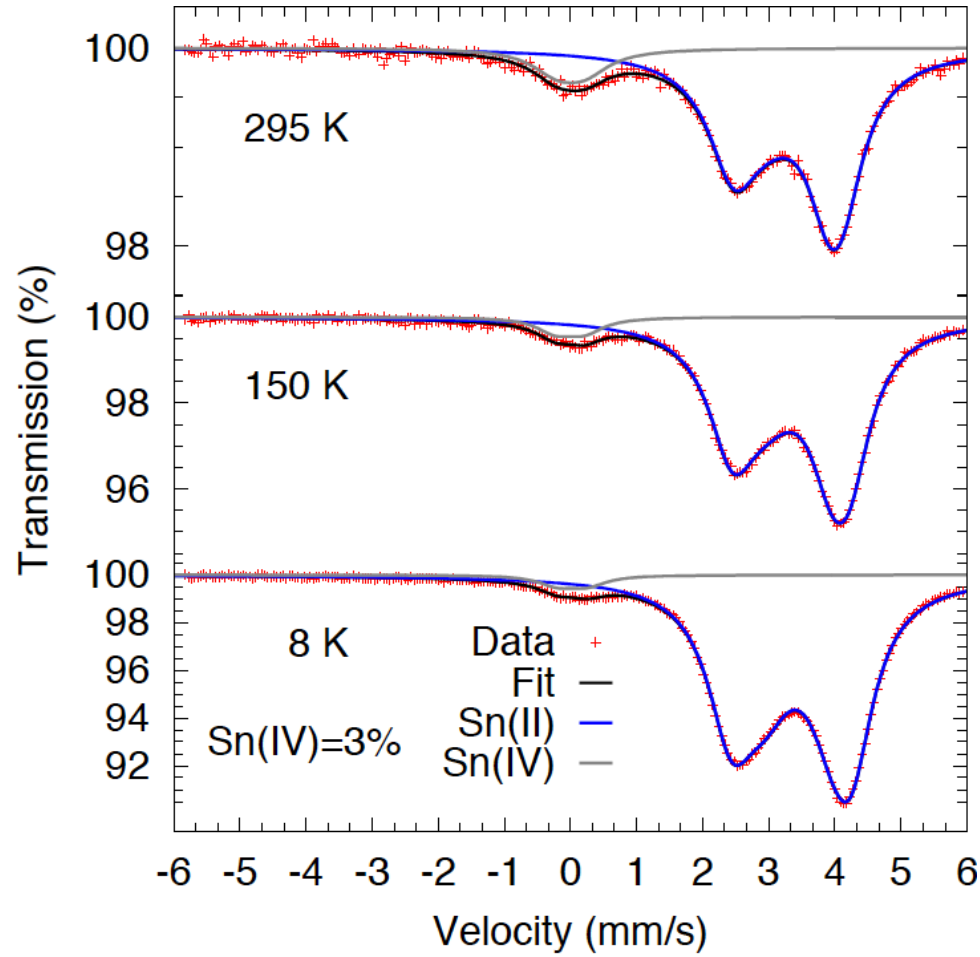
Coll. M Subramanian, Oregon State



Atomic fractions: temperature dependence

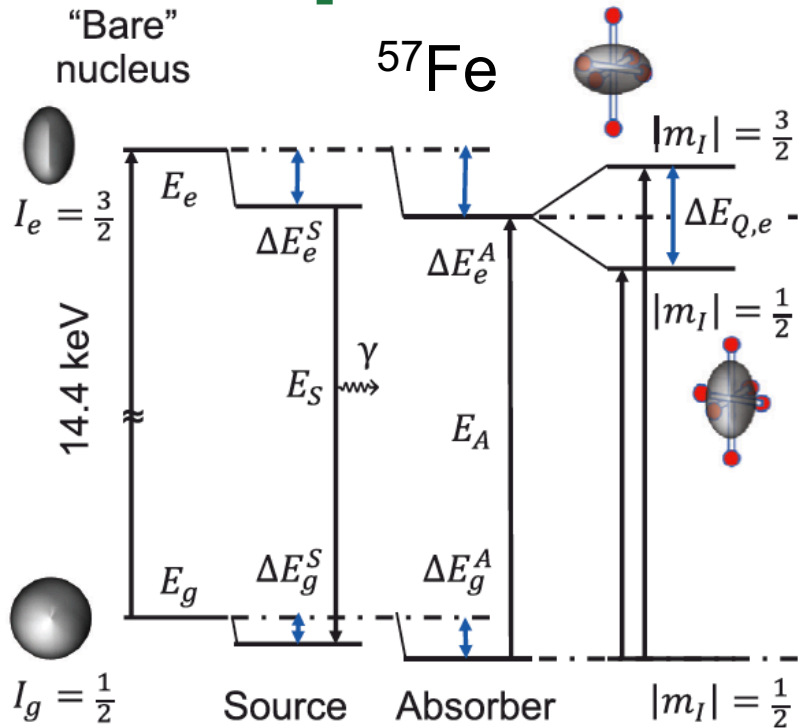


Coll. M Subramanian, Oregon State



Quadrupole interaction

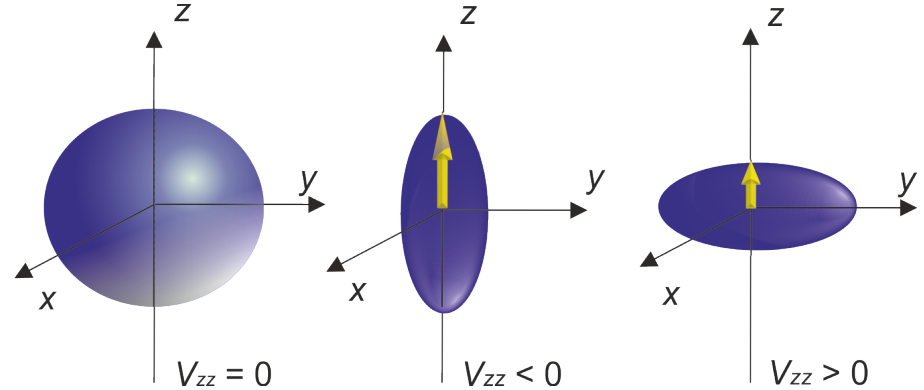
$$\eta = \frac{V_{xx} - V_{yy}}{V_{zz}}$$



$$\begin{aligned} \delta &= E_S - E_A \\ &= (\Delta E_e^S - \Delta E_g^S) \\ &\quad - (\Delta E_e^A - \Delta E_g^A) \end{aligned}$$

Isomer shift Quadrupole splitting

$$\hat{H}_{(g,e)}^Q = \sum_{ij} Q^{ij} V_{ij} = \frac{eQ_{(g,e)}}{I \cdot (2I - 1)} (V_{zz} \hat{I}_z^2 + V_{yy} \hat{I}_y^2 + V_{xx} \hat{I}_x^2)$$



<http://www.advancedmaterialsgroup.edu.rs/wp-content/uploads/2013/07/Slika-1.2.1-EFG.png>

$$E_{g,e}^Q(I, m_I) = \frac{eQ_{g,e} V_{zz}}{4I_{g,e} \cdot (2I_{g,e} - 1)} [3m_I^2 - I \cdot (I + 1)] \sqrt{(1 + \eta^2/3)}$$

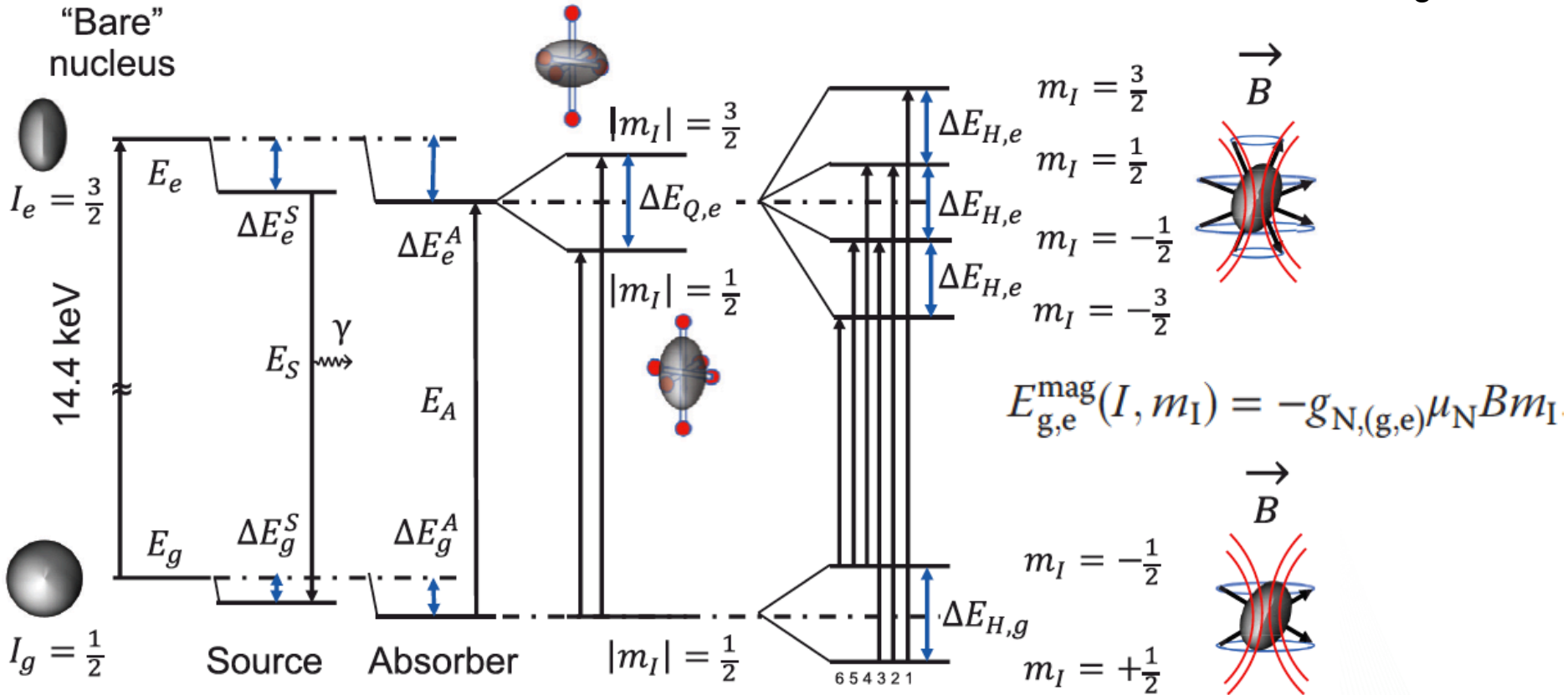
1) Lattice contribution → point symmetry + point charges located on surrounding atoms.

2) Valence electron contribution → crystal field + orbital term (essential for transition metals)

Magnetic Zeeman interaction

$$\hat{\mathcal{H}}_{(g,e)}^{\text{mag}} = -\hat{\mu} \cdot \hat{\mathbf{B}} = -g_{N,(g,e)}\mu_N \hat{\mathbf{I}} \cdot \hat{\mathbf{B}}$$

- Magnetically ordered materials
- Applied magnetic field in diamagnets
- Transferred fields on non magnetic ions



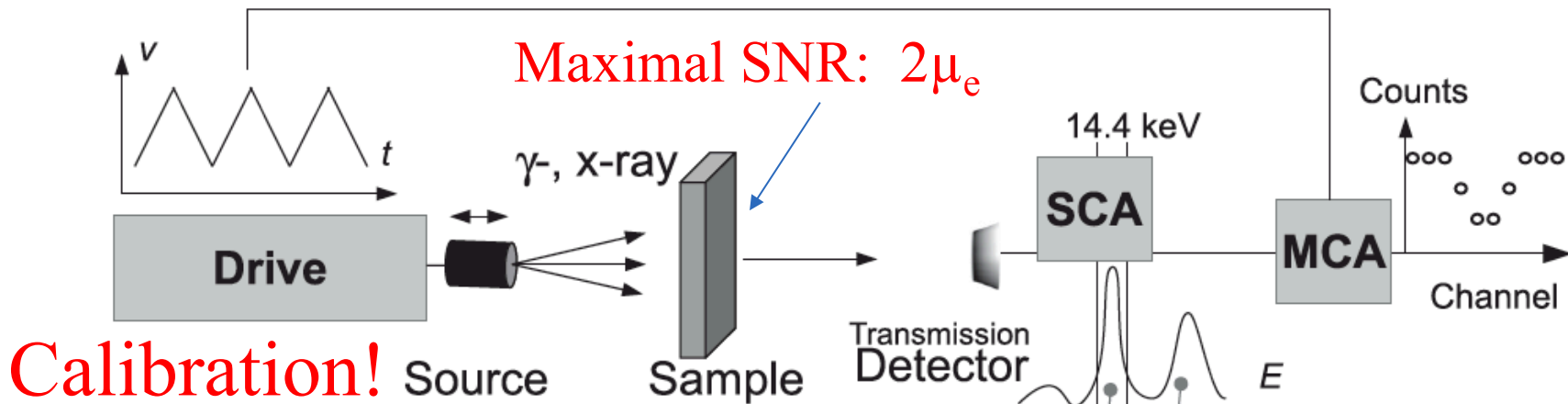
$$\begin{aligned} \delta &= E_S - E_A \\ &= (\Delta E_e^S - \Delta E_g^S) \\ &\quad - (\Delta E_e^A - \Delta E_g^A) \end{aligned}$$

Isomer shift

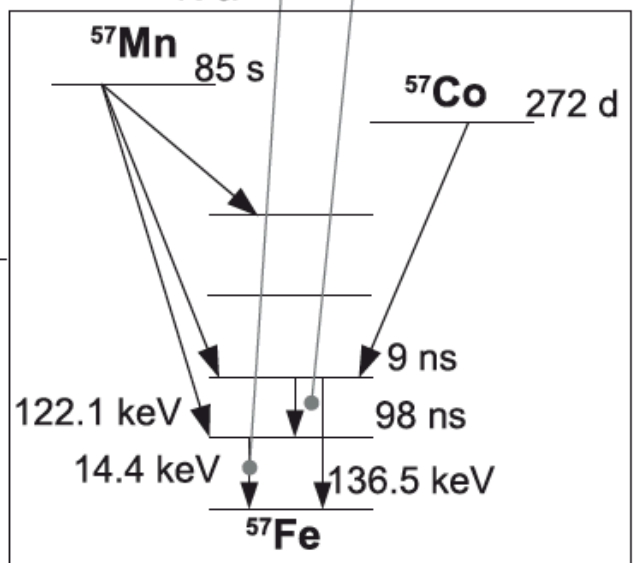
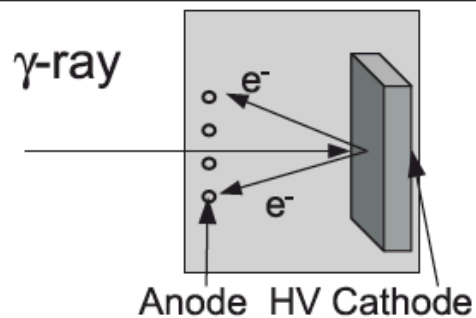
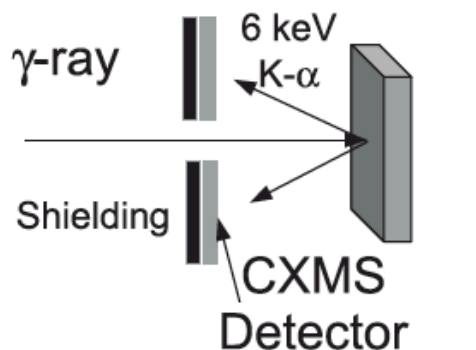
Quadrupole splitting

Magnetic hyperfine splitting

Technique and optimization

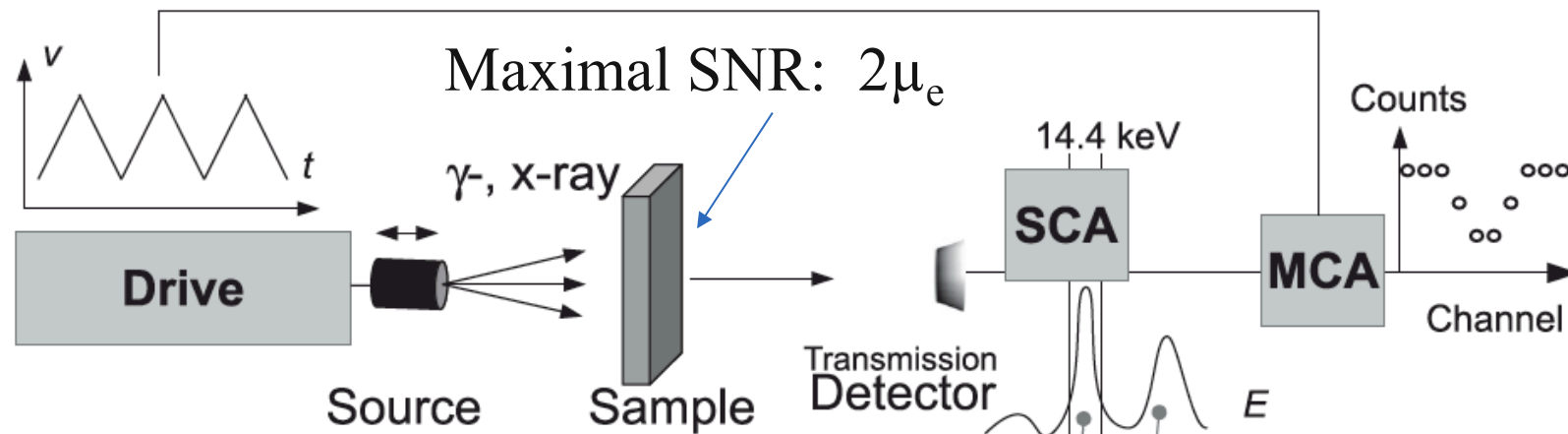


Calibration!



$$t^{-1} = f_{LM} \cdot n_a \cdot \sigma_n = f_{LM} \cdot a \cdot \rho / m_M \cdot f_{at} \cdot N_A \cdot \sigma_n$$

Technique and optimization



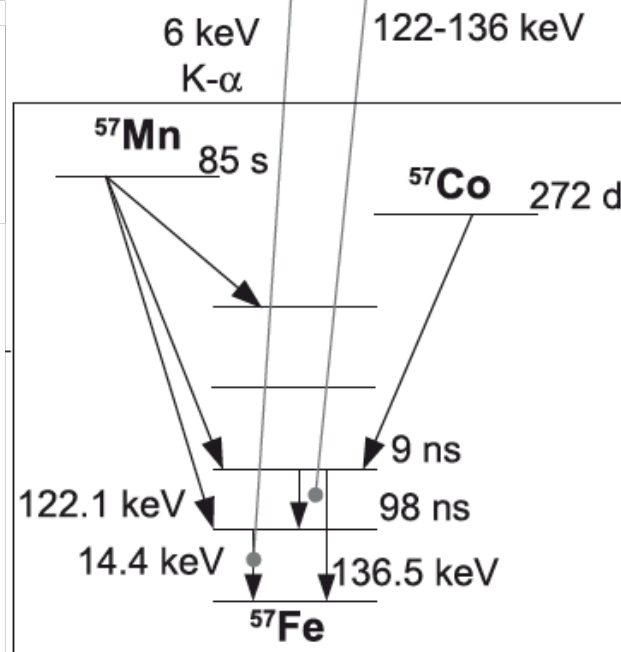
Natural thickness: t

$$t^{-1} = f_{LM} \cdot n_a \cdot \sigma_n$$

$$= f_{LM} \cdot a \cdot \rho / m_M \cdot f_{at} \cdot N_A \cdot \sigma_n$$

$$T^{295 K}_{Fe-\alpha} \sim 11 \mu m$$

! Broadening: $\Gamma \sim (1+0.135t)\Gamma_0$



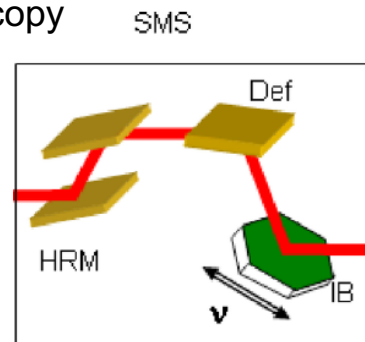
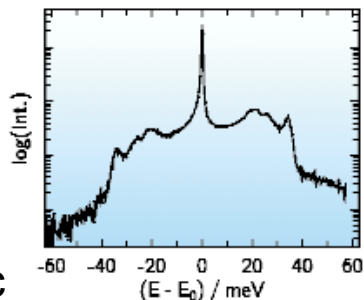
Choose wisely! -> e.g. programm mossthick

Nuclear resonance scattering

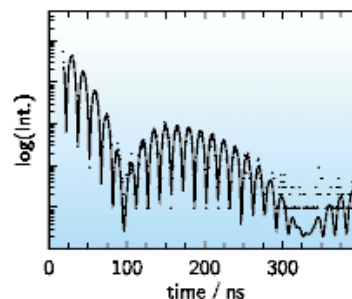
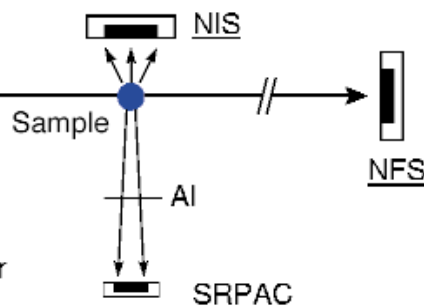
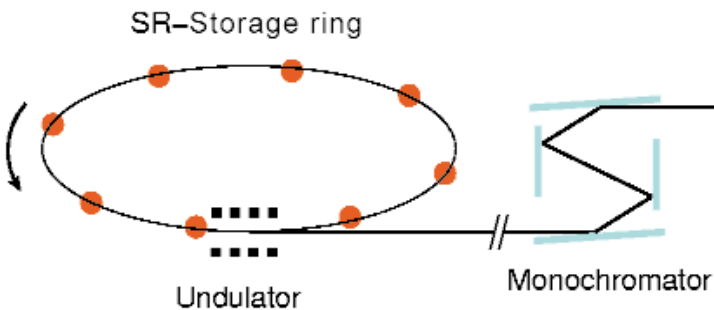
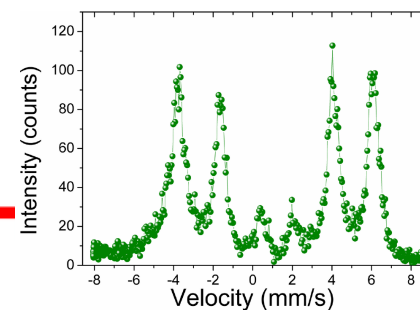
- = Time or Energy Domain Synchrotron Mössbauer Spectroscopy
- + Phonon Assisted Nuclear Resonance Absorption
- + Synchrotron Radiation Perturbed Angular Correlation
- + ...

+ polarized beam.

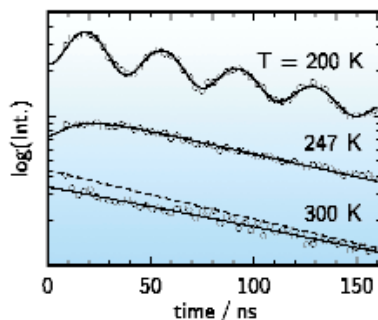
With recoil
→ inelastic



Potapkin et al. J. Synchrotron Rad. (2012). 19, 559–569

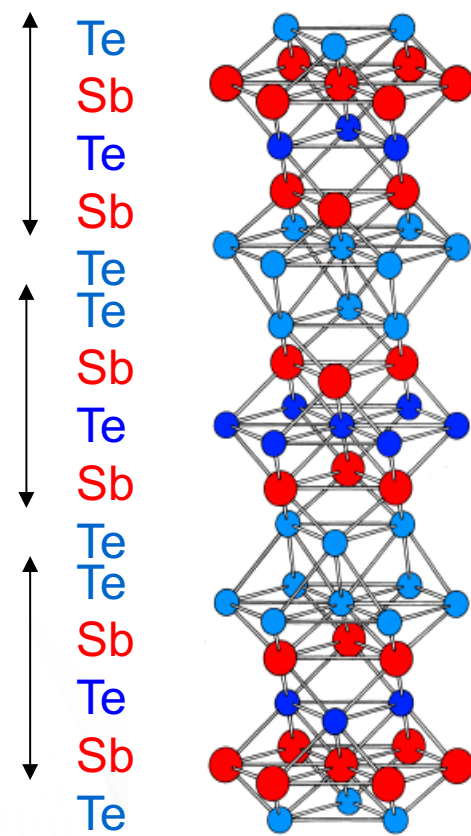
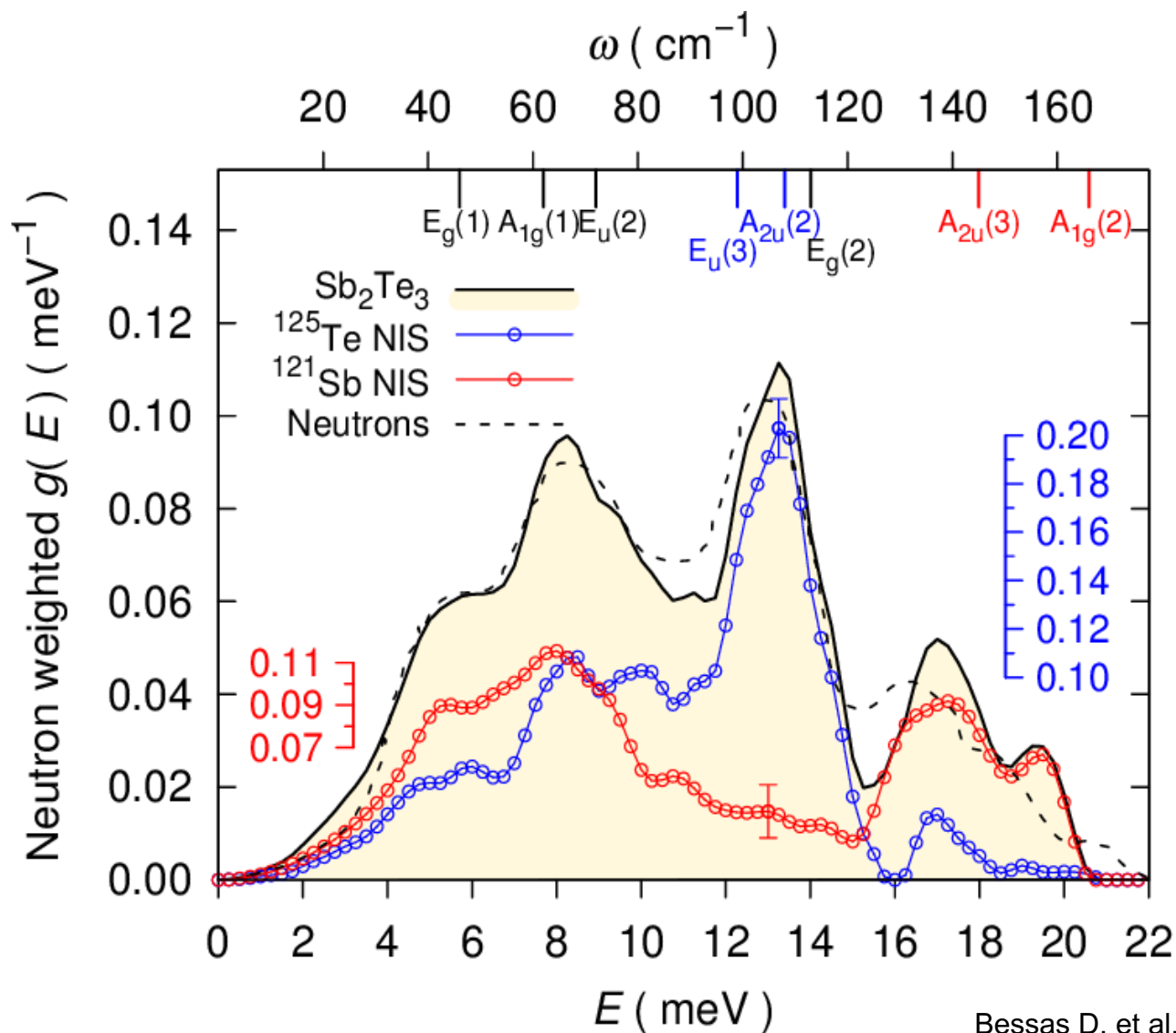


Without recoil



Rotational dynamics

Sb₂Te₃ phonon spectroscopy



Bessas D. et al., *Phys. Rev. B* **86**, 224301 (2012).

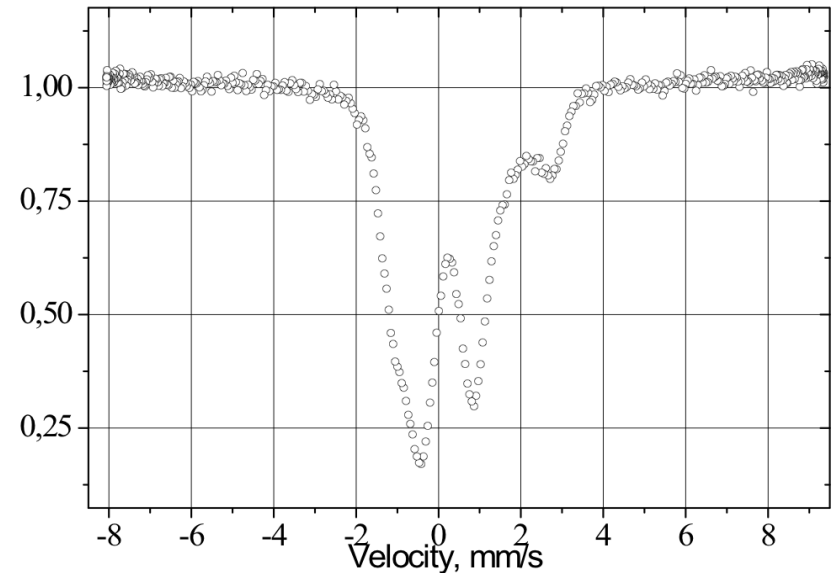
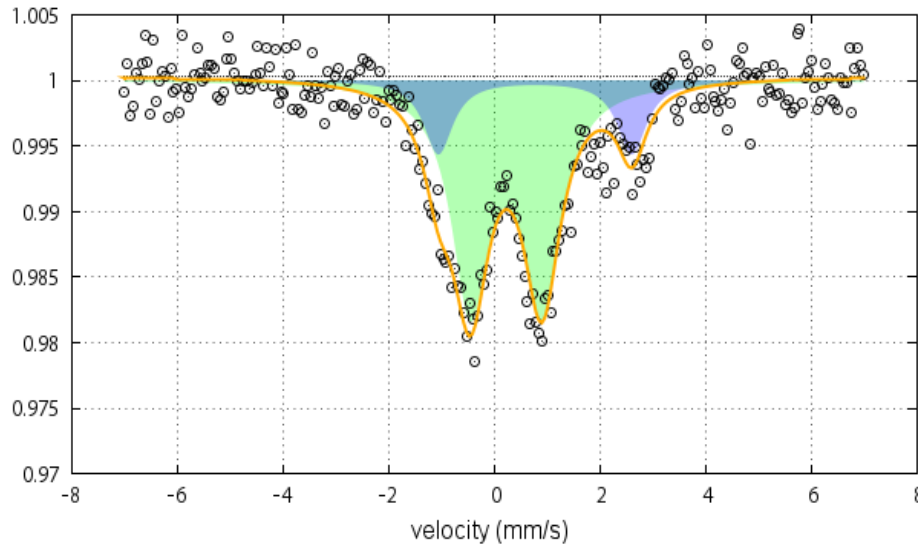
Synchrotron Mössbauer Spectroscopy

Energy domain

Small samples → direct benefit from beam size

Perovskite at 94 GPa measured with a conventional source and with SMS
(same sample, same diamond anvil cell)

Pv P~94 GPa after 1 week with point drive



Measuring time ~ 10^4 min (one week)

Measuring time ~ 10 min

SMS is three orders of magnitude faster

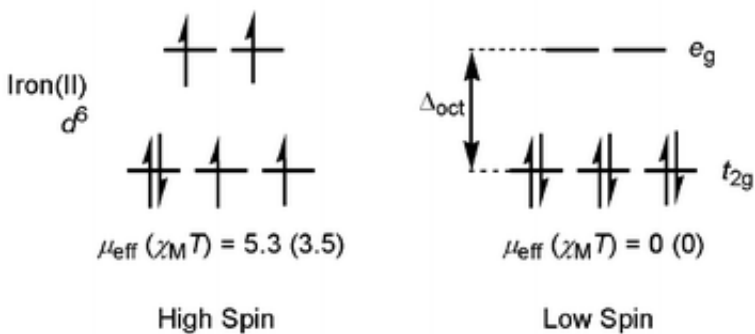
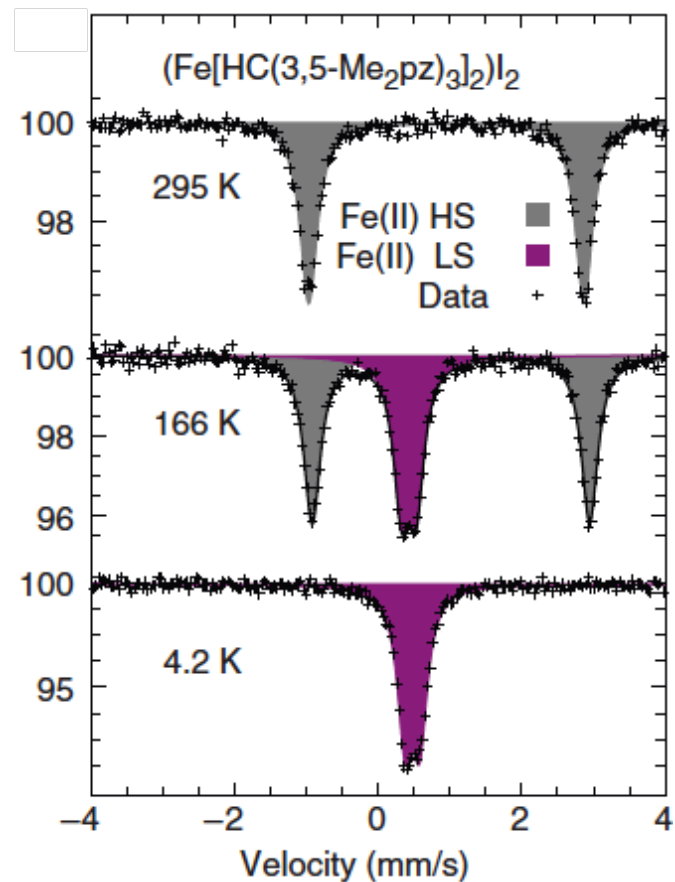
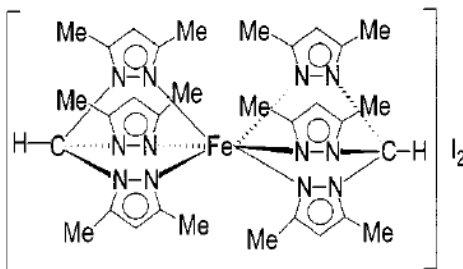
V. Potapkin, A.I. Chumakov, G.V. Smirnov, *et al.* (2012) *J. Synchrotron Rad.* (2012). 19, 559-569

- Historical perspective
- Spectral description and parameters
- Static interactions
- Time dependent interactions

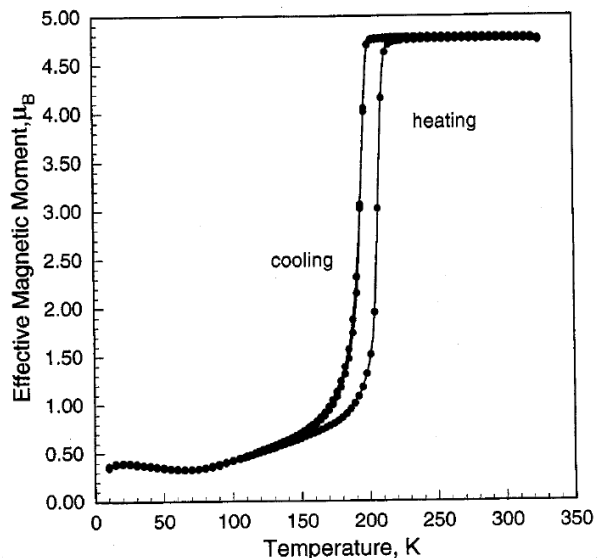
Spin cross over in $\{\text{Fe}[\text{HC}(3,5\text{-Me}_2\text{pz})_3]_2\}\text{I}_2$

Reger, D. L. *et al.*, *Eur. J. Inorg. Chem.* **2002**, 1190–1197 (2002).

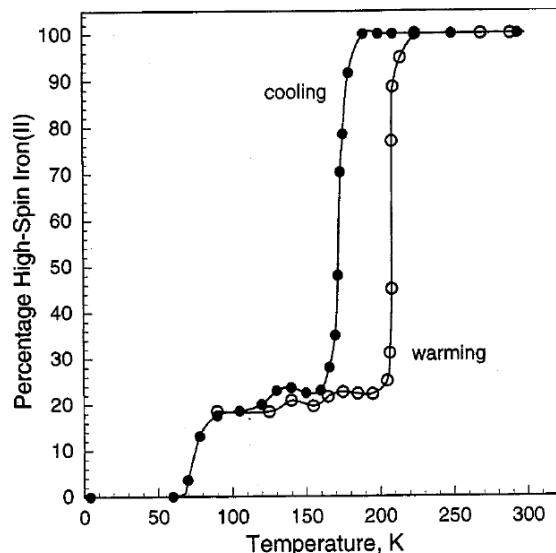
Interest: memory, color change



Magnetometry



Mössbauer



Oxidation states: Ba_2FeO_4 and Ba_3FeO_5

Interest: Oxidation agent and battery cathode

Delattre et al., Inorg. Chem. **41**, 2834-2838 (2002)

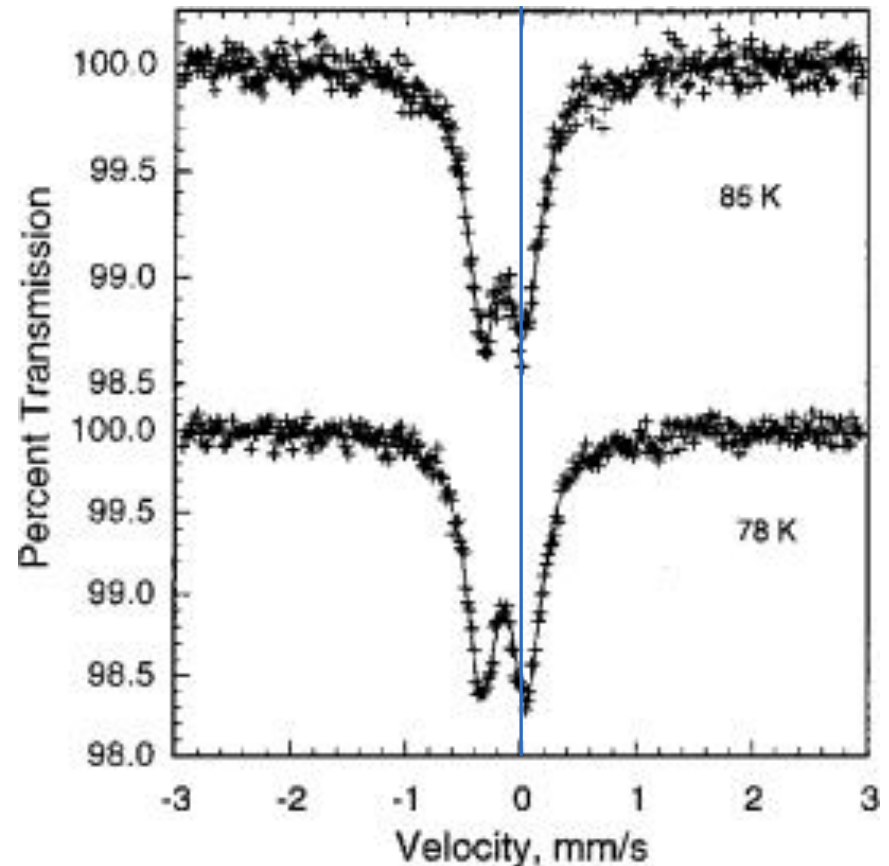
compound	T, K	$\delta, \text{mm/s}^a$	$\Delta E_Q, \text{mm/s}$
Ba_2FeO_4	295	-0.244	0.33
	225	-0.185	0.34
	155	-0.169	0.35
	85	-0.152	0.36
Ba_3FeO_5	295	-0.225	0.35
	240	-0.204	0.34
	190	-0.199	0.37
	140	-0.168	0.40
	90	-0.150	0.39
	78	-0.142	0.39

Fe(IV)

-> magnetometry: $\mu_{\text{eff}} = 4.89 \mu_B$

Fe(IV) spin only moment: $4.9 \mu_B$

In contrast, isostructural Ba_3FeS_5 features Fe(III)
and the reduced iron yields a hole in the $\text{S}^{2-} 3p^6$ band.



Screening synthesis conditions

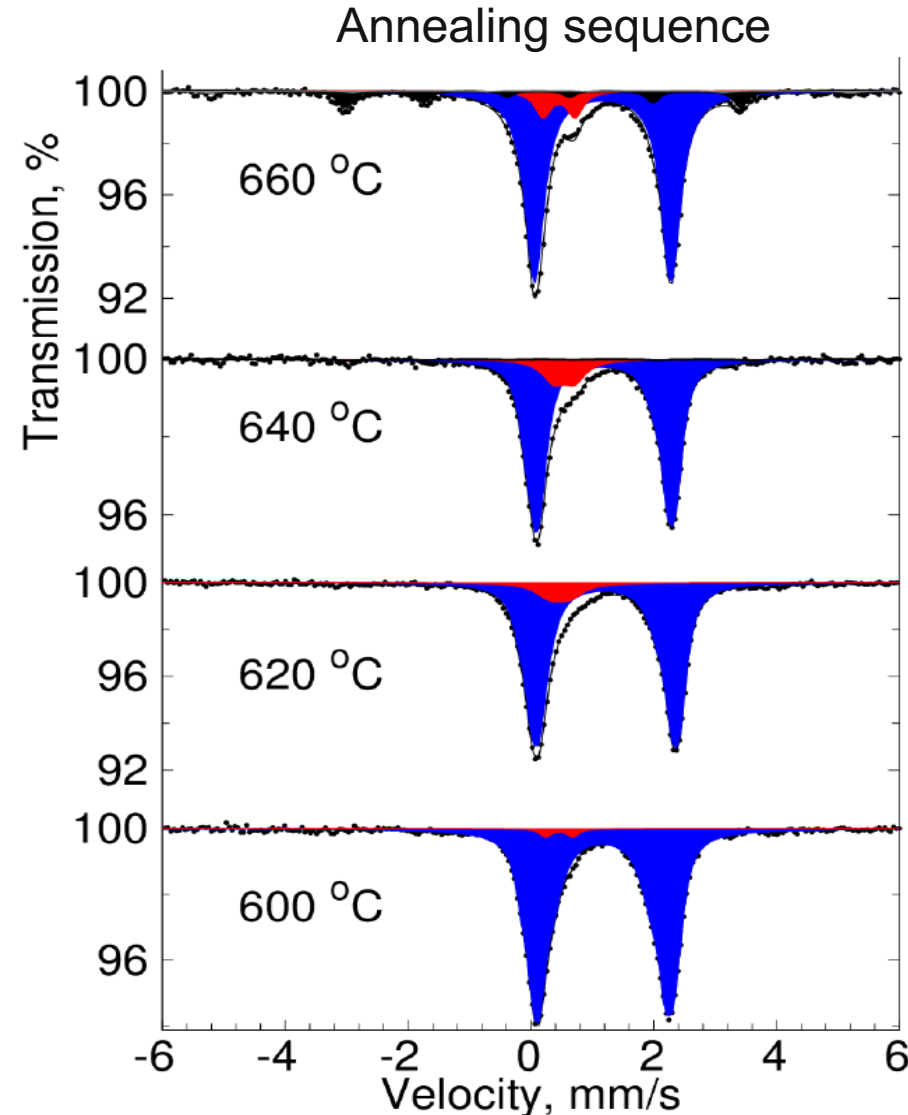
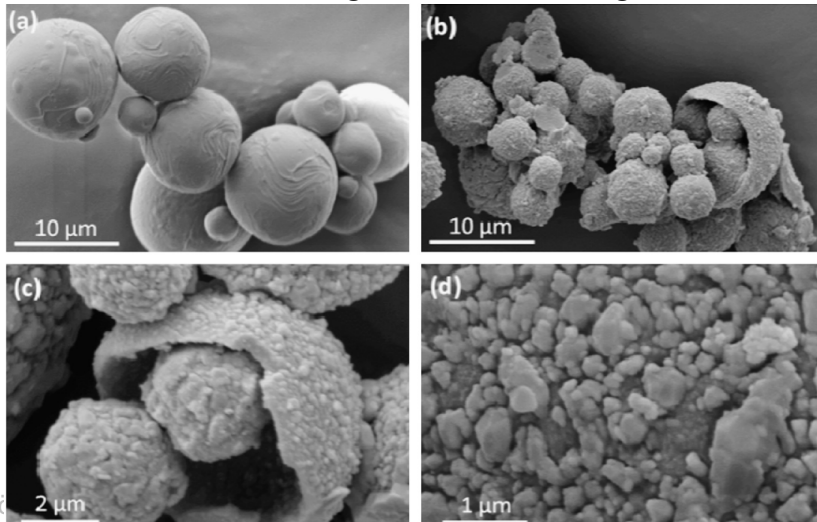
NaFePO₄F/carbon powder synthesis by spray drying
Application: cathode material for Li-, Na-ion batteries

Synthesis parameters:

- Fe (II) citrate + NH₄H₂PO₄, NaF and NaOH + deionized water
- final iron concentration of 0.1 mol/l
- solution spray-dried:
 - 25 ml/min feed rate
 - 140°C inlet temperature
- annealing at 600°C

Optimised with “live” Mössbauer spectral feedback for Fe(II)/Fe(III) content

Before annealing After annealing at 600 °C



Screening synthesis conditions

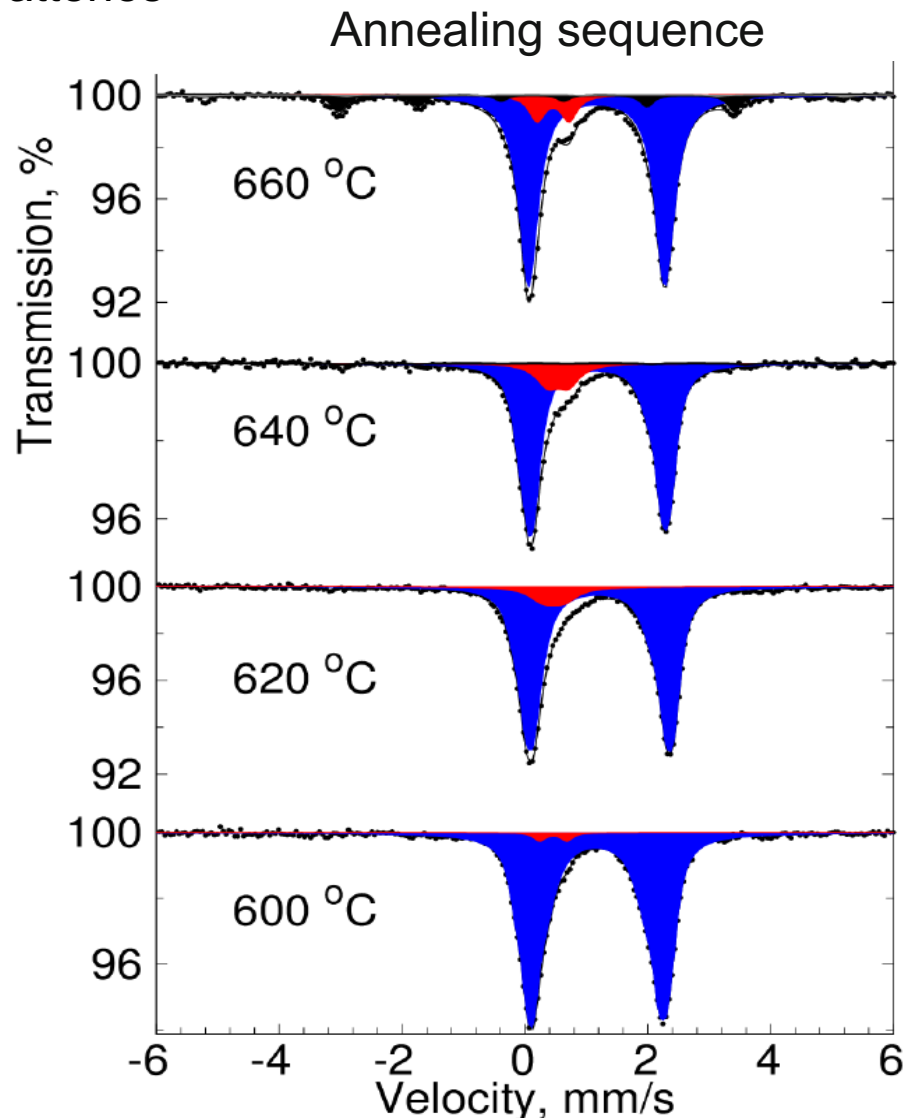
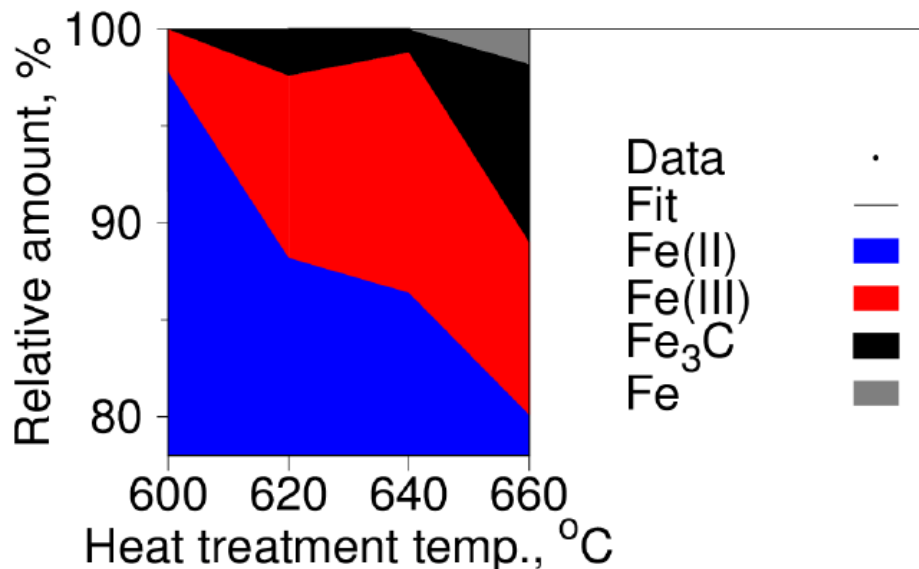
NaFePO₄F/carbon powder synthesis by spray drying

Application: cathode material for Li-, Na-ion batteries

Synthesis parameters:

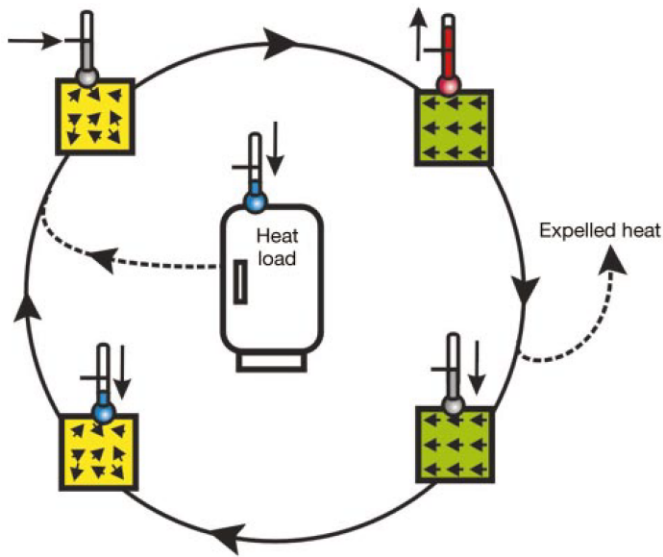
- Fe (II) citrate + NH₄H₂PO₄, NaF and NaOH + deionized water
- final iron concentration of 0.1 mol/l
- solution spray-dried:
 - 25 ml/min feed rate
 - 140°C inlet temperature
- annealing at 600°C

Optimised with “live” Mössbauer spectral feedback for Fe(II)/Fe(III) content



Brisbois et al., *Materials Letters* **130** (2014), 263.

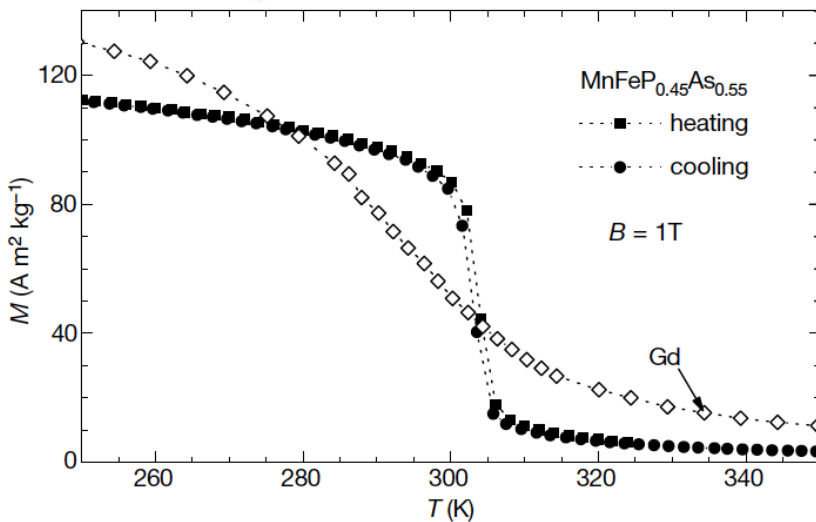
Magnetocaloric $\text{FeMnP}_{1-x}\text{As}_x$



The application of a magnetic field aligns the magnetic moments, reduces the magnetic entropy and increases the (lattice) temperature.

The removal of the magnetic field yields a randomization of the moments, increases the spin entropy and decreases the (lattice) temperature.

The sharp magnetic transition in $\text{FeMnP}_{1-x}\text{As}_x$ yields a cooling efficiency of $\sim 20 \text{ J/K/kg}$ similar to Gd for operation around $\sim 300 \text{ K}$.



Jan. 2015: product presented
CES Las Vegas
Material: FeMn(P,Si)

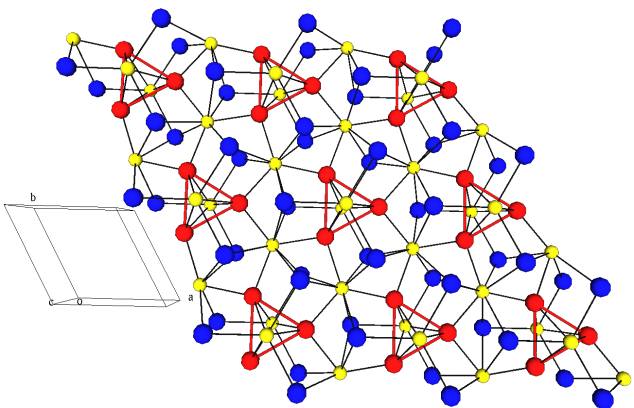
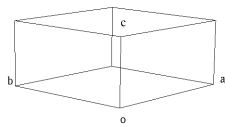
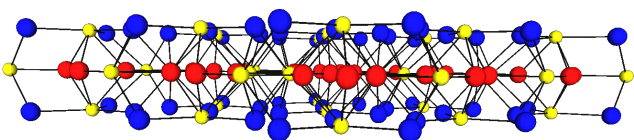
Haier | **BASF** We create chemistry | **Astronautics** Corporation of America

Developed the world's first
Magnetic Cooling domestic
appliance.

Tegus O., Brück E., Buschow K. H. J., and de Boer F. R., Nature **415**, 150 (2002).

FeMnP_{1-x}As_x structure

Iron and manganese layers perpendicular *c*
Iron has four P or As near-neighbors.



Triangular iron groups in the *ab* plane.

The 5% component corresponds to iron that occupies the manganese site.

The paramagnetic and ferromagnetic states coexist over a range of ~10 K.

The hyperfine field at 301 K is only slightly smaller than at 225 K.

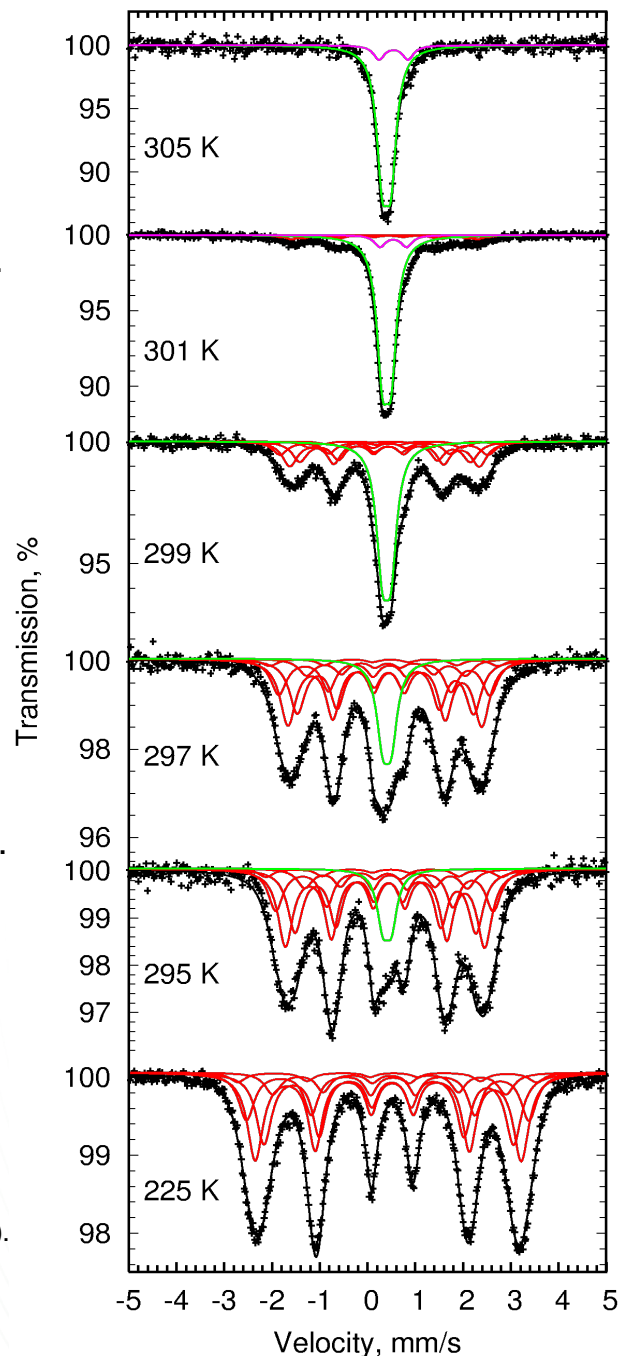
The magnetic transition is first-order in agreement with the magnetization.

The ferromagnetic subspectra correspond to the binomial P and As near-neighbor distribution components.

$$P(n) = C_4^n x^n (1-x)^{4-n}$$

Malaman *et al.*, J. Phys.: Cond. Matter **8**, 8653 (1996).
Hermann *et al.*, Phys Rev B **70**, 214425 (2004)

(I) FeMnP_{0.45}As_{0.55}



Incommensurate magnetism

The **ferromagnetic subspectra** are constrained, except relative area.

The **antiferromagnetic subspectra** are fitted by taking into account

the binomial distribution, (poor fits ...)

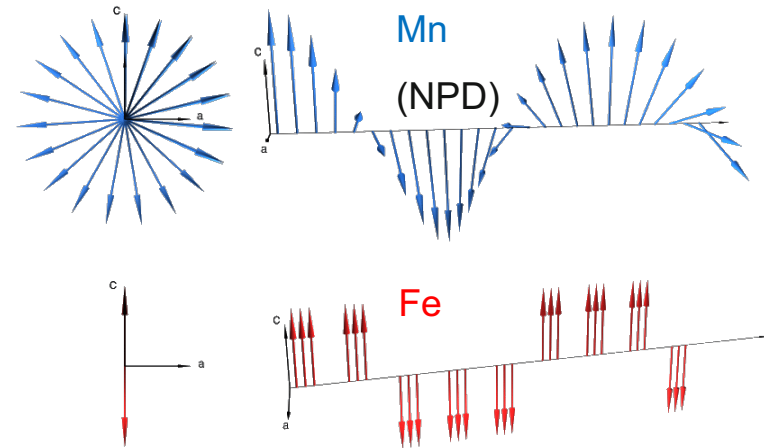
the incommensurate antiferromagnetic structure, (poor fits ...)

$$H_{AF} = C\mu \sin \theta,$$

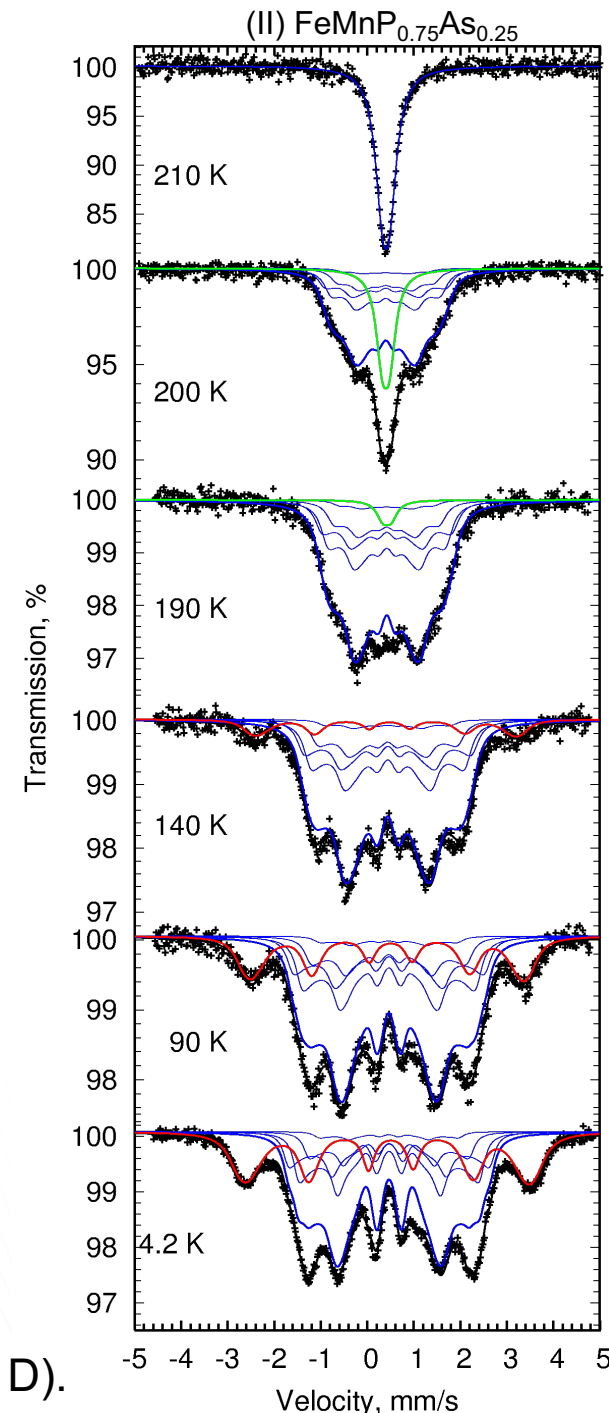
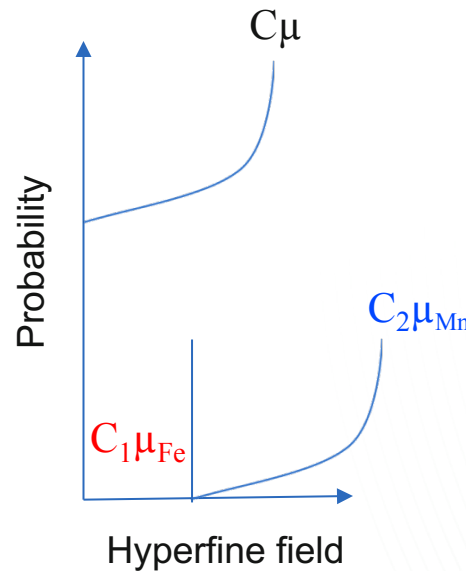
and the contribution from the **two** magnetic sub-lattices. (good fits)

$$H_{AF} = C_1\mu_{Fe} + C_2\mu_{Mn} \sin \theta$$

The last addition introduces a single free parameter.

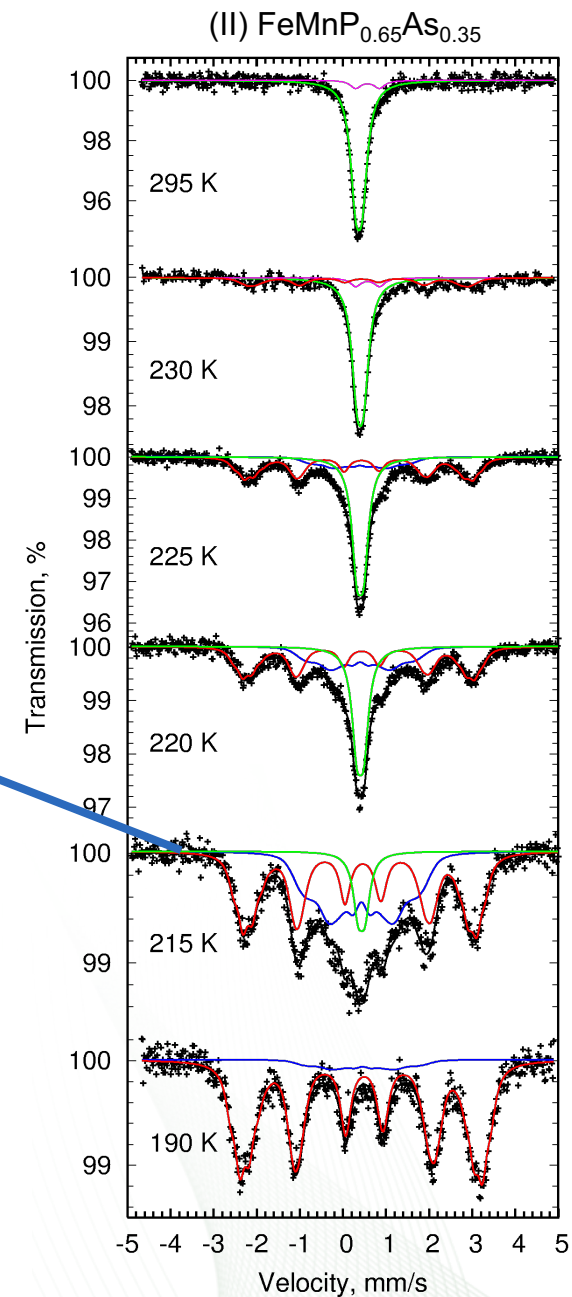
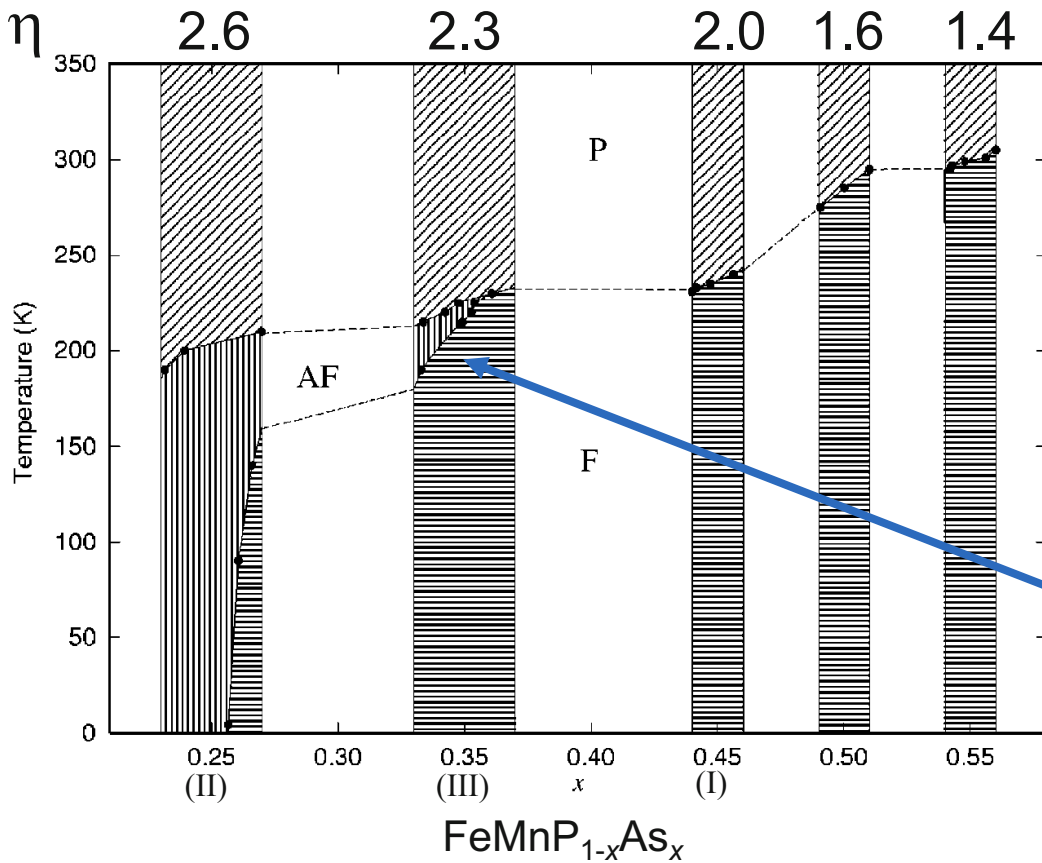


Hermann et al., Phys Rev B **70**, 214425 (2004)



$$\theta = 2\pi \cdot x_M / a_M, \text{ position of the nucleus/magnetic lattice constant (1D).}$$

Magnetic phase diagram



Magnetic triple point: the **ferromagnetic**, **antiferromagnetic**, and **paramagnetic** phases coexist at $T \sim 220$ K.

Spectra for $x = 0.55, 0.50, 0.45, 0.35,$ and 0.25 can be summarized in a phase diagram by assuming a compositional inhomogeneity, Δx .

The order of the transition, $\eta > 1$, indicating first order character. (Bean and Rodbell model for magnetostriction exchange)

Carbodiimides – new pseudooxides



- 3D non-oxidic extended frameworks, new class of materials
- $-N=C=N-$ (-2) is among the shortest and simplest bridging anions
- linear geometry is at variance with $-O-$ bridging
- how is magnetic exchange between transition metals or rare-earth affected?



Historically: main use as calcium cyanamide as fertilizer.

In contact with water: $CaNCN + 3 H_2O \rightarrow 2 NH_3 + CaCO_3$

Also used in steelmaking \rightarrow introduces nitrogen

Magnetic properties

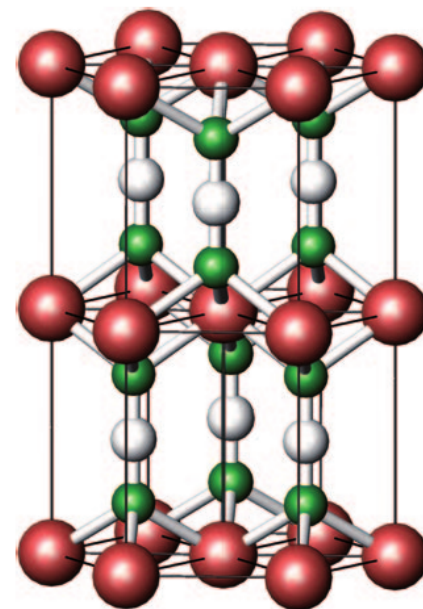
→ MnNCN, CoNCN, NiNCN and CuNCN are „nitrogen based pseudo-oxides“ [4]
MnO, CoO, NiO, and CuO.

→ Gapped insulators: MnNCN is green, FeNCN dark red, CoNCN orange-brown,
NiNCN light-brown, close to *MO* compounds

→ [NiAs] and not [NaCl] type structure, for FeNCN, close to delafossite CuFeO₂.

→ Néel temperatures

	- O ⁻²	- NCN ⁻²
Mn ⁺²	119 K [1]	30 K [2]
Fe ⁺²	198 K [3]	350 K [4]
Co ⁺²	289 K [1]	255 K [4]
Ni ⁺²	524 K [1]	360 K [4]



[1] G. Srinivasan *et al.*, Phys. Rev. B **28**, 6542 (1983).

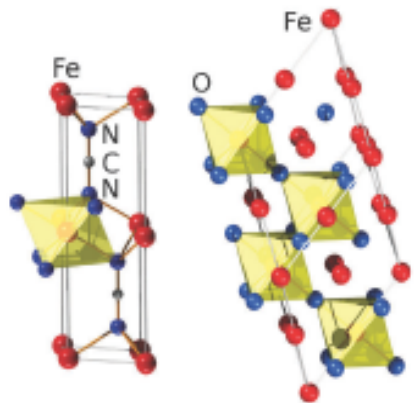
[2] X. Liu *et al.*, Inorg. Chem. **44**, 3001–3003 (2005).

[3] G. Kugel *et al.*, Phys. Rev. B **16**, 378–385, (1977).

[4] X. Liu *et al.*, Chem. Eur. J. **15**, 1558 – 1561 (2009).

[5] M. Krott *et al.*, Inorg. Chem. **46**, 2204–2207 (2007).

Mössbauer spectra of FeNCN

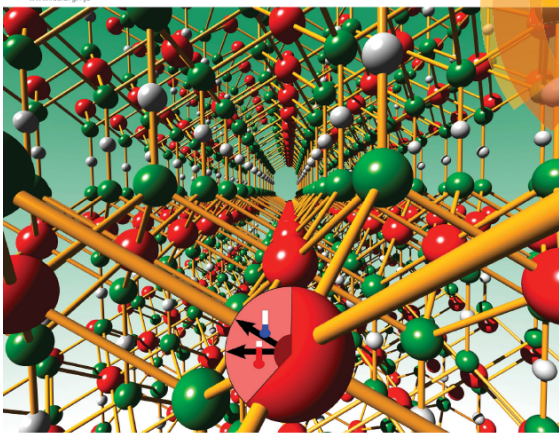


Volume 38 | Number 10 | October 2014 | Pages 4633–5098

NJC

New Journal of Chemistry
www.rsc.org/njc

A journal for new directions in chemistry



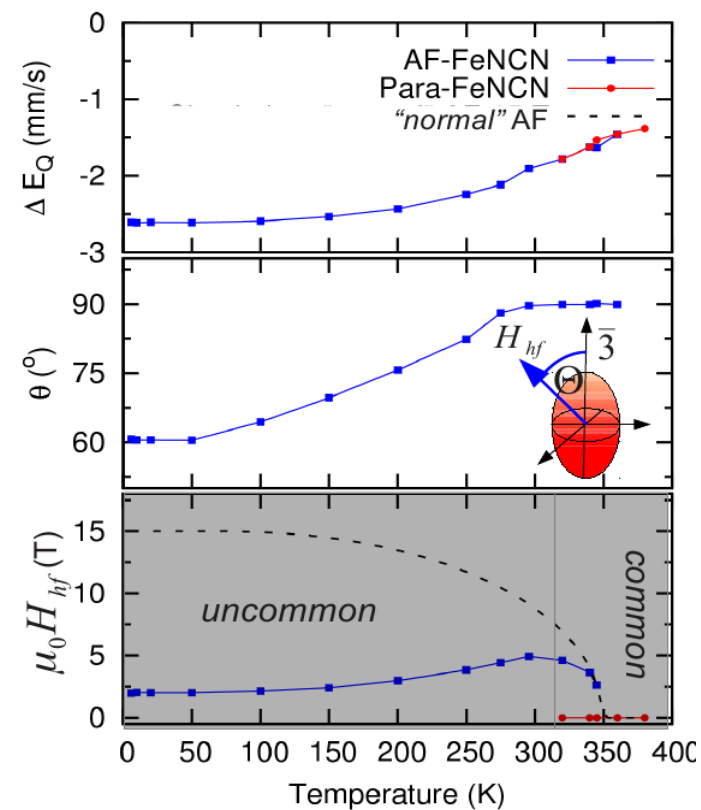
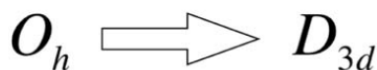
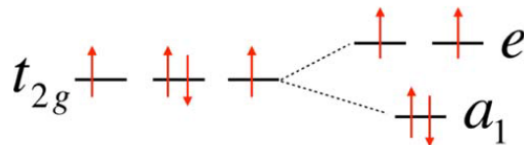
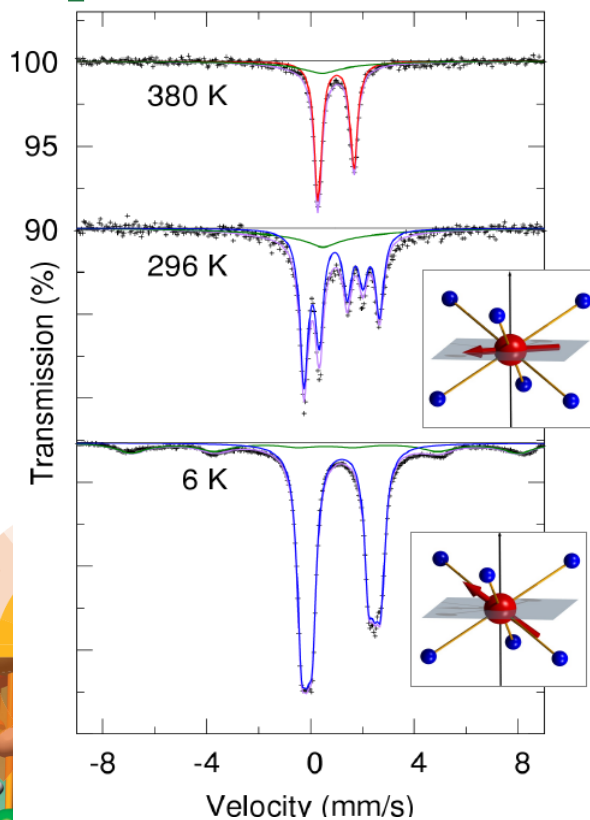
ISSN 1144-0546



PAPER
M. Herlitschke et al.
Magnetism and lattice dynamics of FeNCN compared to FeO



M. Herlitschke, *et al.*
New J. Chem., 2014, 38, 4670



Thermal activation:

change of ΔE_Q

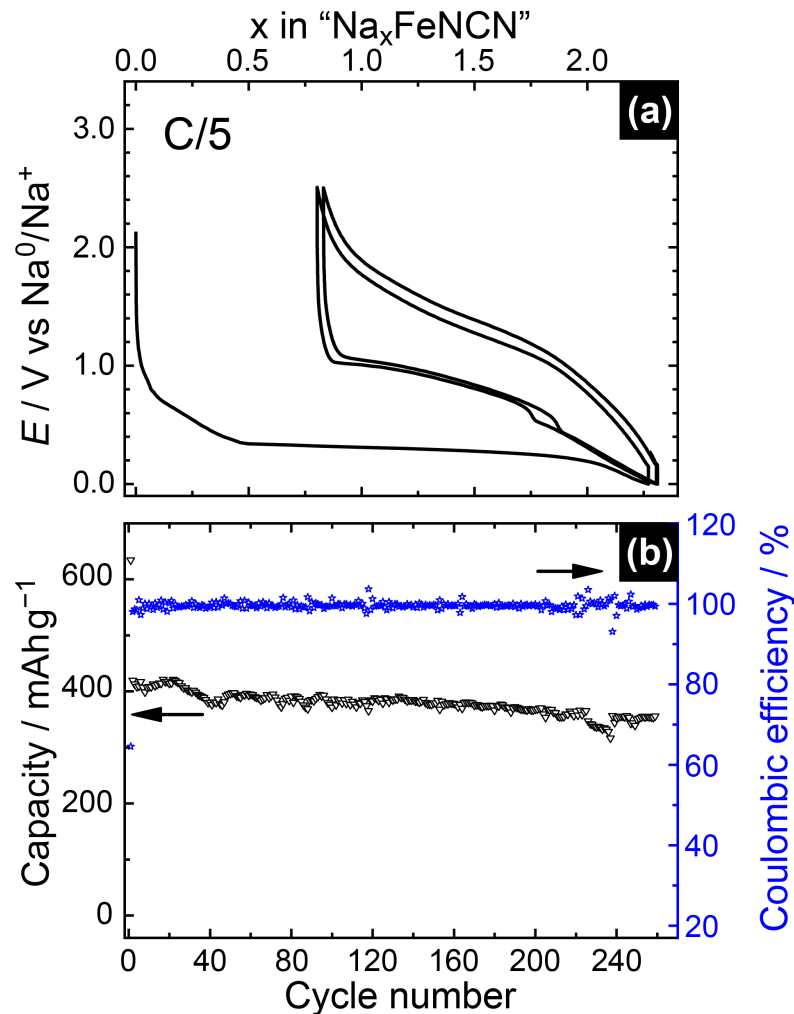
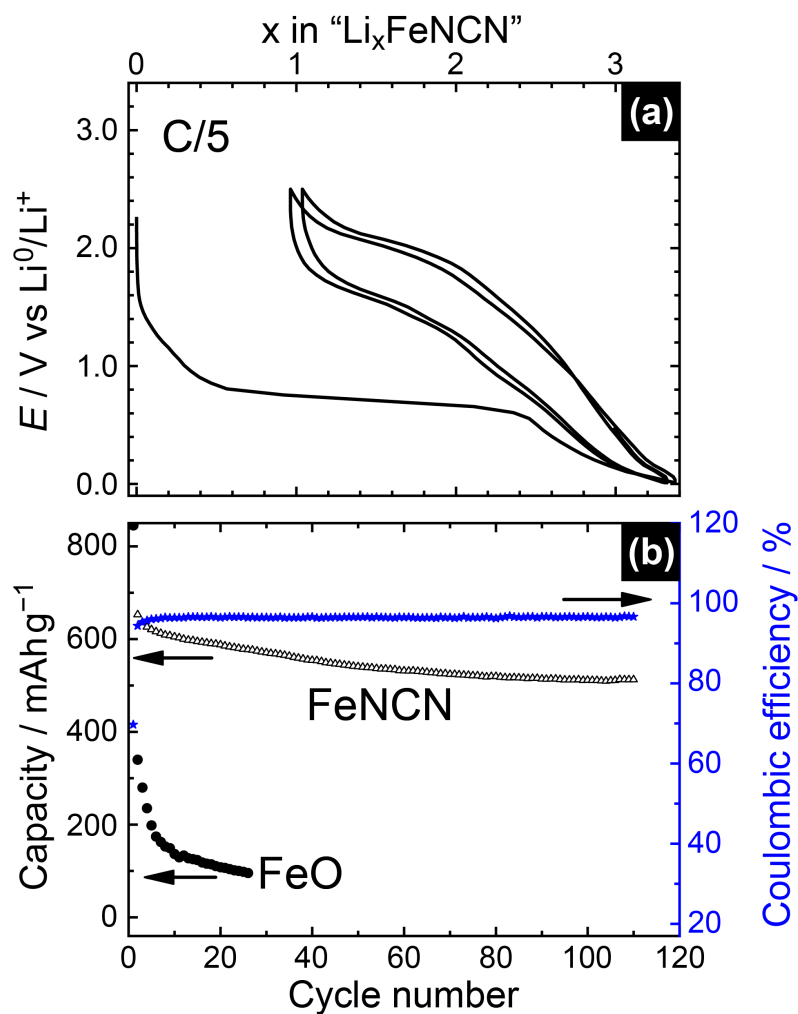
Orbital moment arises
(degenerated by excitations)

Dipole interaction changes

Tchougréeff *et al.*, *Int. J. of Quantum Chem.* **116**, 282–294 (2016)

“Transition-metal carbodiimides as new molecular negative electrode materials for Li- and Na-ion batteries with excellent cycling properties”

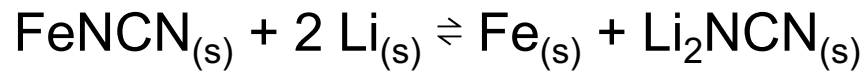
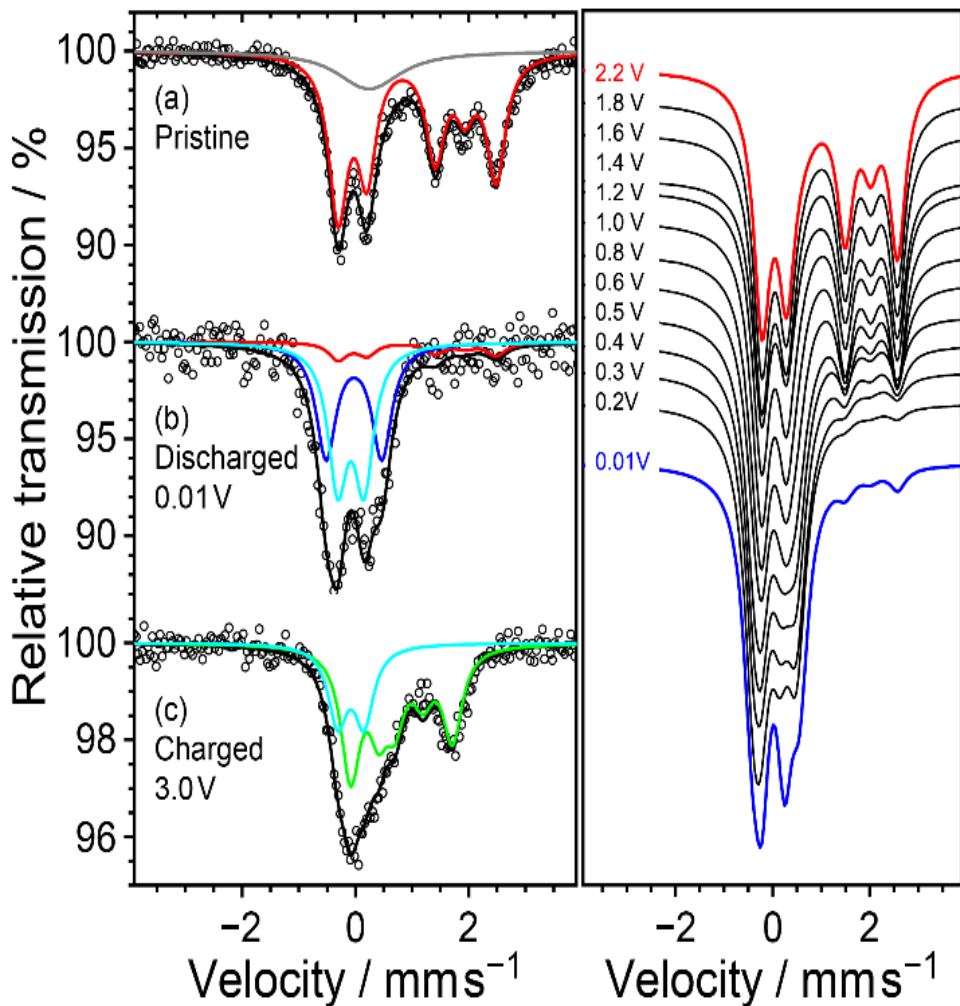
M. T. Sougrati et al., Angewandte Chemie, accepted Feb. 2016



Analogous reactions for MnNCN, ZnNCN and Cr₂(NCN)₃

“Transition-metal carbodiimides as new molecular negative electrode materials for Li- and Na-ion batteries with excellent cycling properties”

M. T. Sougrati et al., *Angewandte Chemie*, accepted Feb. 2016



Analogous reactions for MnNCN, ZnNCN and Cr₂(NCN)₃



Electrochemical cell for *Operando* XRD and Mössbauer studies developed by Leriche et al. (*J. Electrochem. Soc.* Vol. 157 (2010))

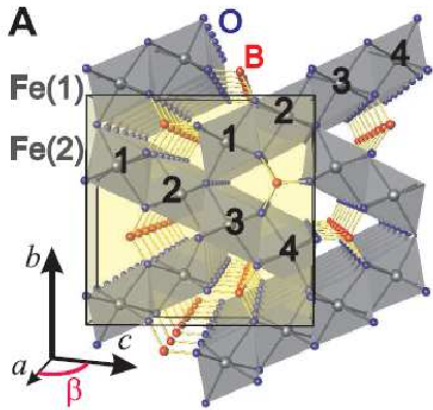
M. T. Sougrati, A. Darwiche, L. Monconduit, L. Stievano, R. P. Hermann, A. Mahmoud, M. Herlitschke, R. Dronskowski, X. Liu, *Metal Carbodiimides and Metal Cyanamides as New Active Electrode Materials*, EP15305888 (2015), European Patent pending.

- Historical perspective
- Spectral description and parameters
- Static interactions
- Time dependent interactions

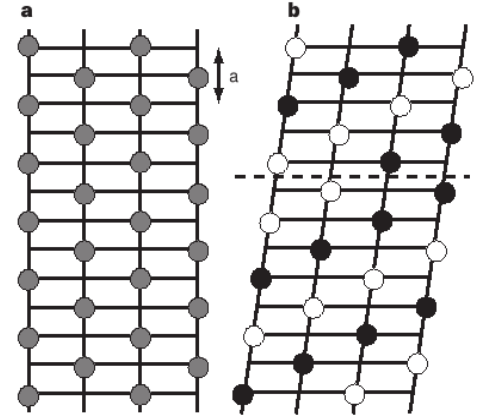
Charge order / electron hopping in Fe_2OBO_3

Evidence: Mössbauer spectroscopy, change in resistivity

Proposed structure [Atfield *et al.*, Nature **396**, 655 (1998)]

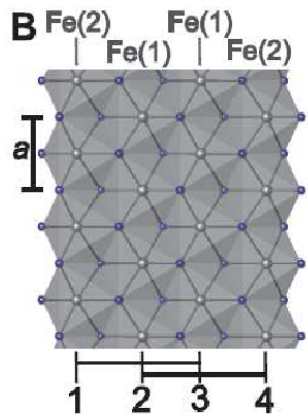


(from powder data)

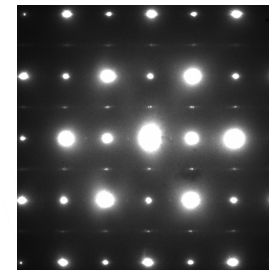
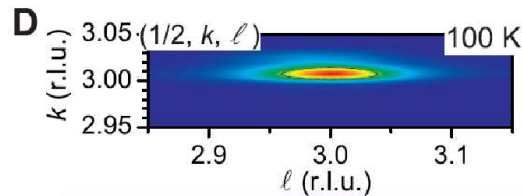


Single crystal growth [Angst, 2005; ORNL]

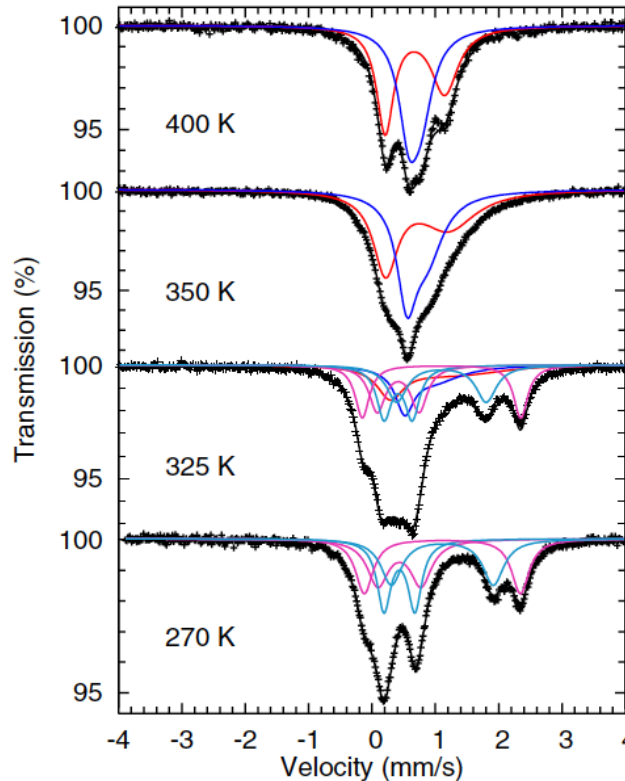
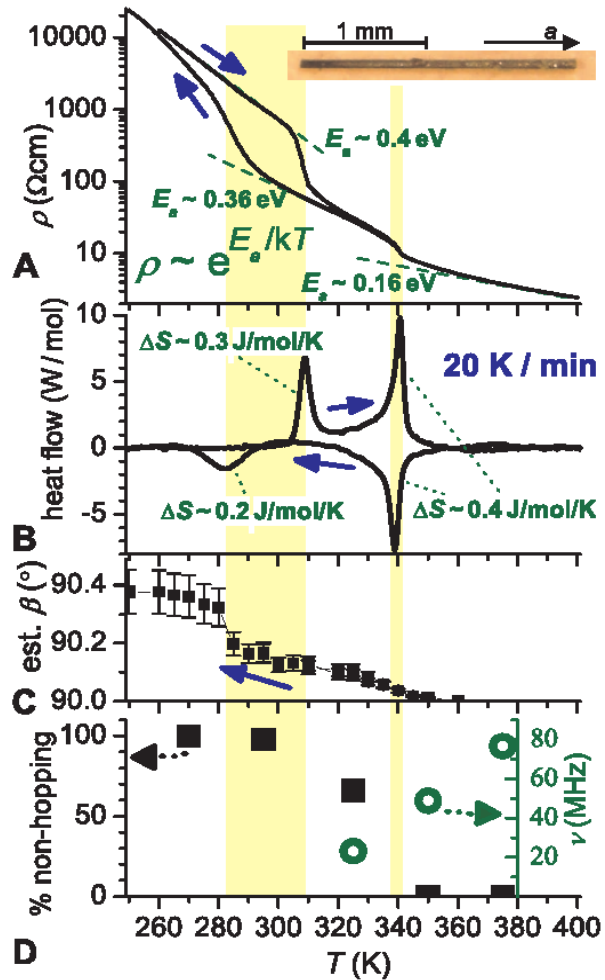
Single crystal diffraction: detailed structure



Synchrotron radiation and electron scattering: CO peaks!



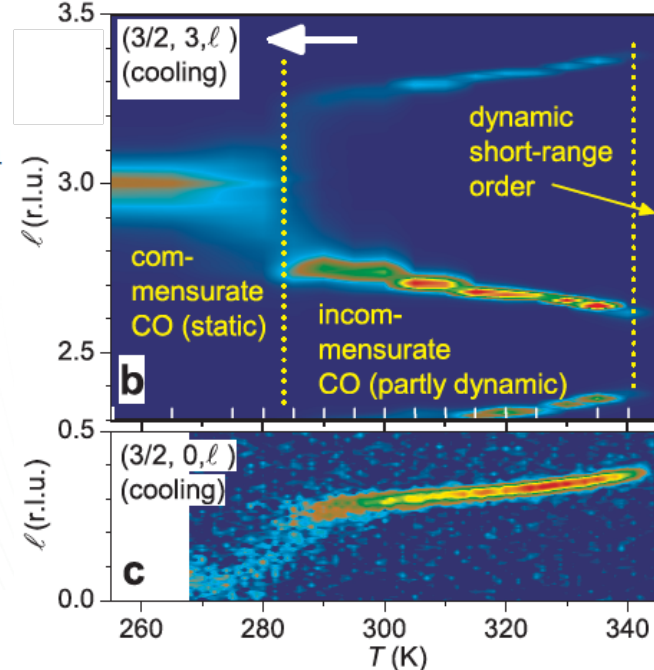
Charge order / electron hopping in Fe_2OBO_3



Electron hopping
 I, IV — red
 II, III — blue

No electron hopping
 I, IV — magenta
 II, III — cyan

Fit total — black line
 Data — '+'



Intermediate phase: 300-340 K,
 incommensurate charge order

Angst, M. *et al.*, *Phys. Rev. Lett.* **99**, 256402 (2007).

Angst, M. *et al.*, *Phys. Rev. Lett.* **99**, 086403 (2007).

Guest dynamics in $AGa_{16}Ge_{30}$ clathrates

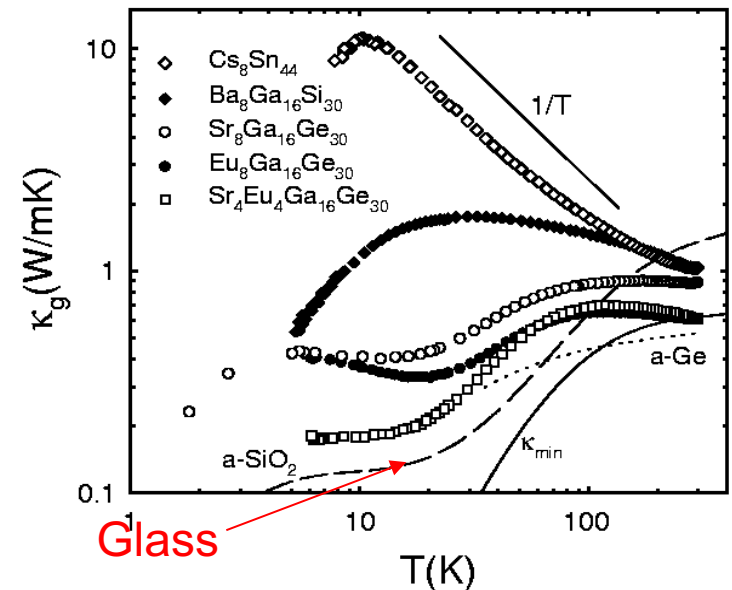
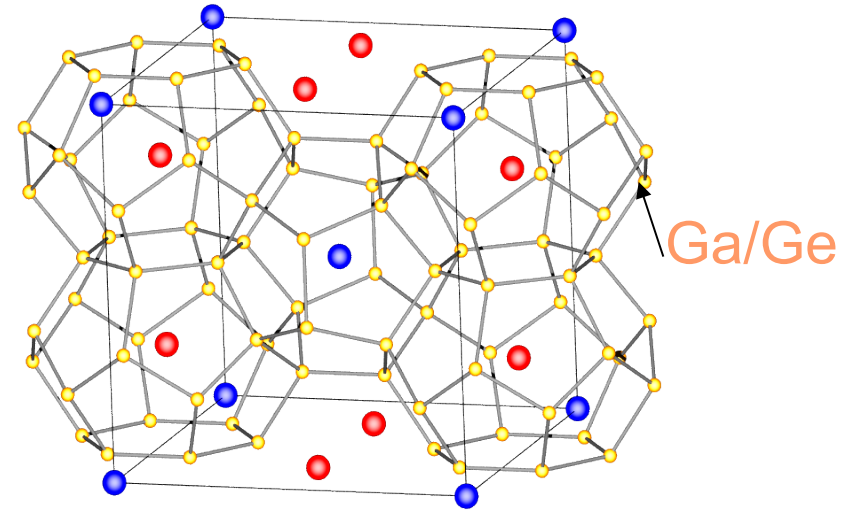
2a A(I) and 6d A(II) sites are occupied by either Ba, Eu, or Sr.

The structure consists of stacked **small cages** with A(I) and **large cages** with A(II) on/near the center.

Filled clathrate are interesting as

- potential thermoelectric materials,
- model systems for caged atoms.

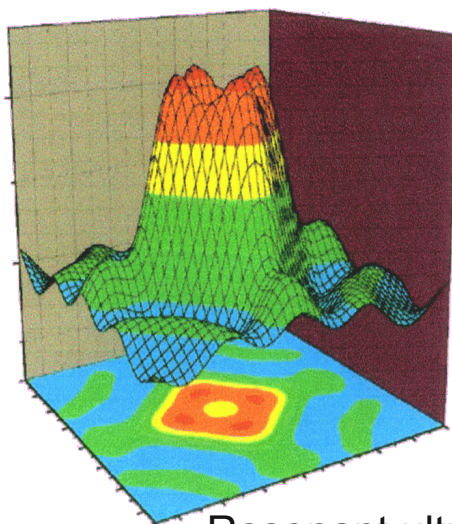
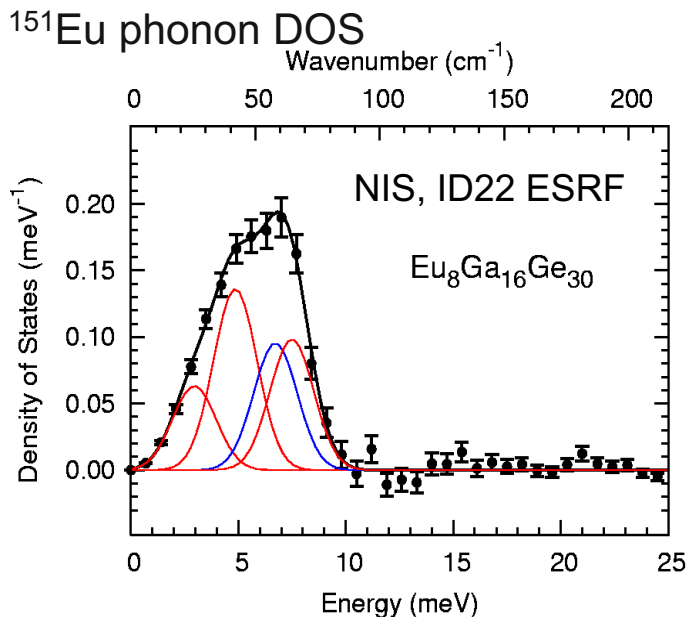
Low, anomalous thermal transport.



Cohn *et al.*, *PRL* **82**, 779 (1999)

Potential landscape

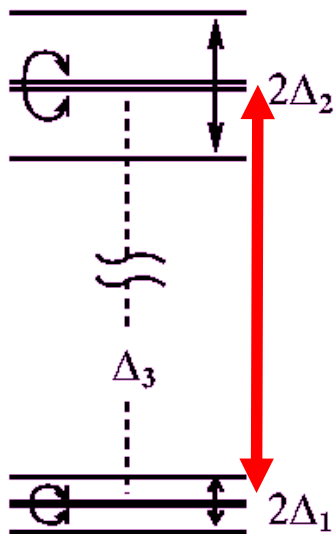
Sales B. C., Chakoumakos B. C., Jin R., Thompson J. R., and Mandrus D., *Phys. Rev. B* **63**, 245113 (2001).



Static or dynamic disorder
in the ground state?

Resonant ultrasound spectroscopy response

Hermann et al., *Phys. Rev. B* **72**, 174301 (2005)

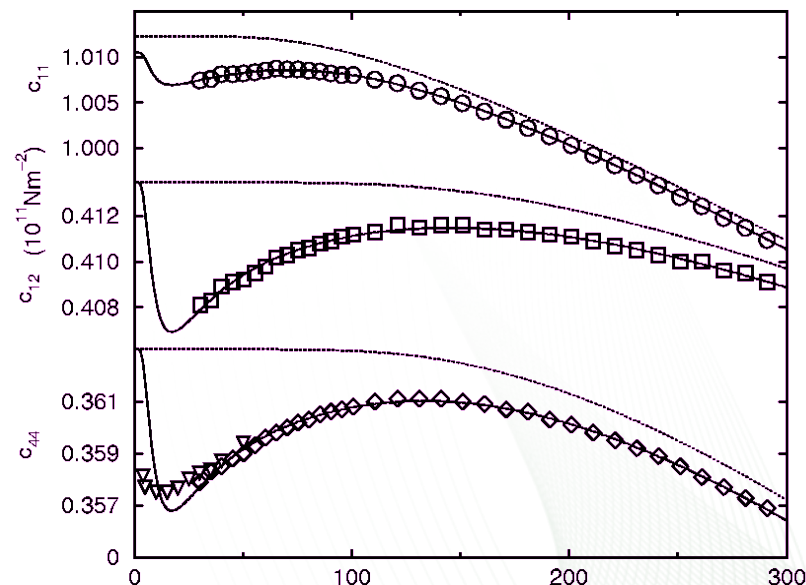


$\sim 3 \text{ meV}$

50 mK

$\sim 4.3 \mu\text{eV}$

$\sim 1 \text{ GHz}$



Zerec I., Keppens V., McGuire M. A., Mandrus D., Sales B. C., and Thalmeier P., *Phys. Rev. Lett.* **92**, 185502 (2004).

Mössbauer spectra

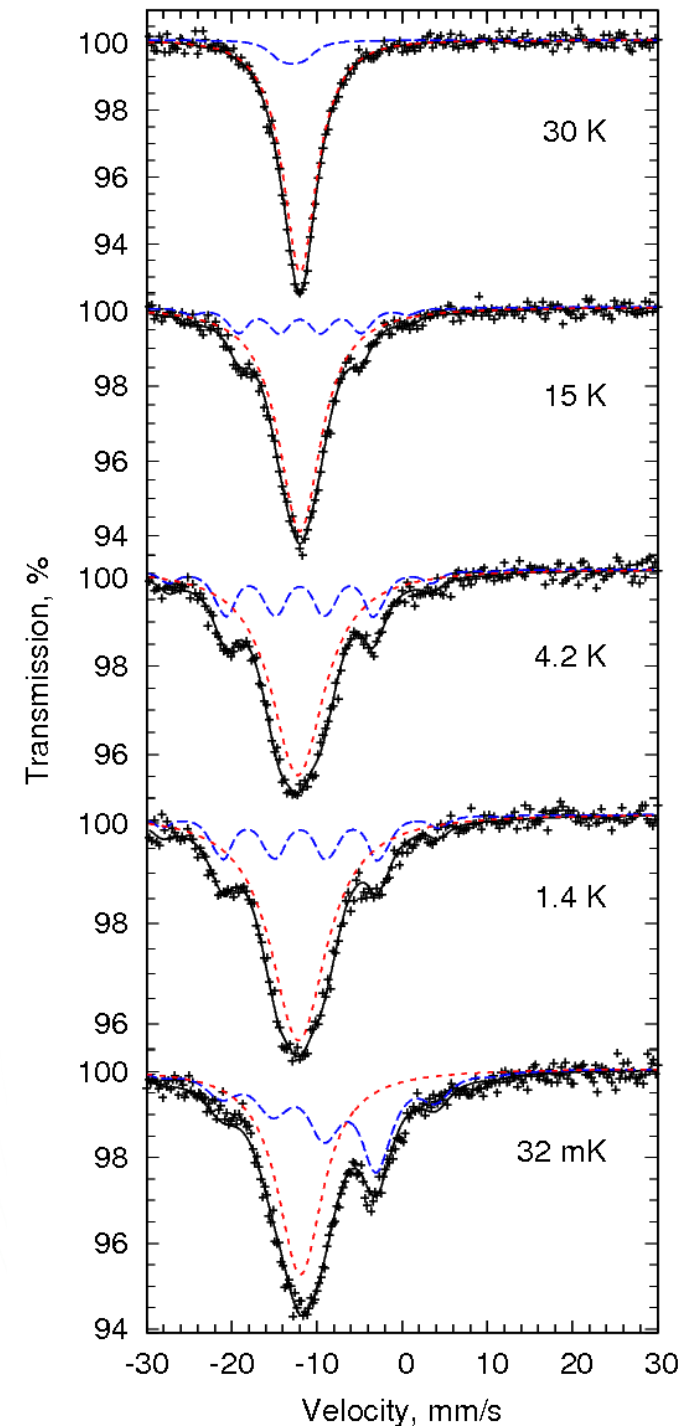
Eu(I) and **Eu(II)** Eu^{2+} spectral components overlap.

Eu(I) exhibits magnetic splitting with $T_c \sim 30$ K.

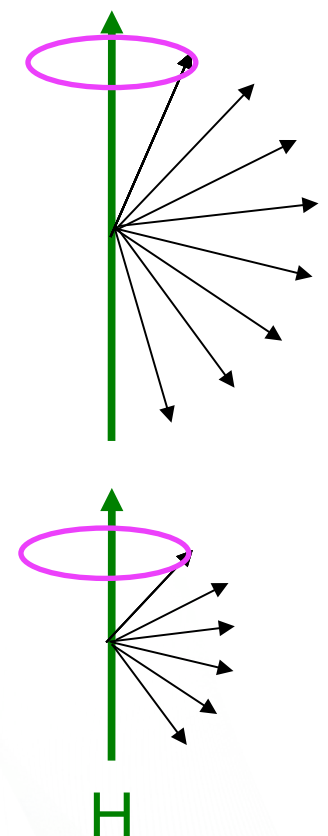
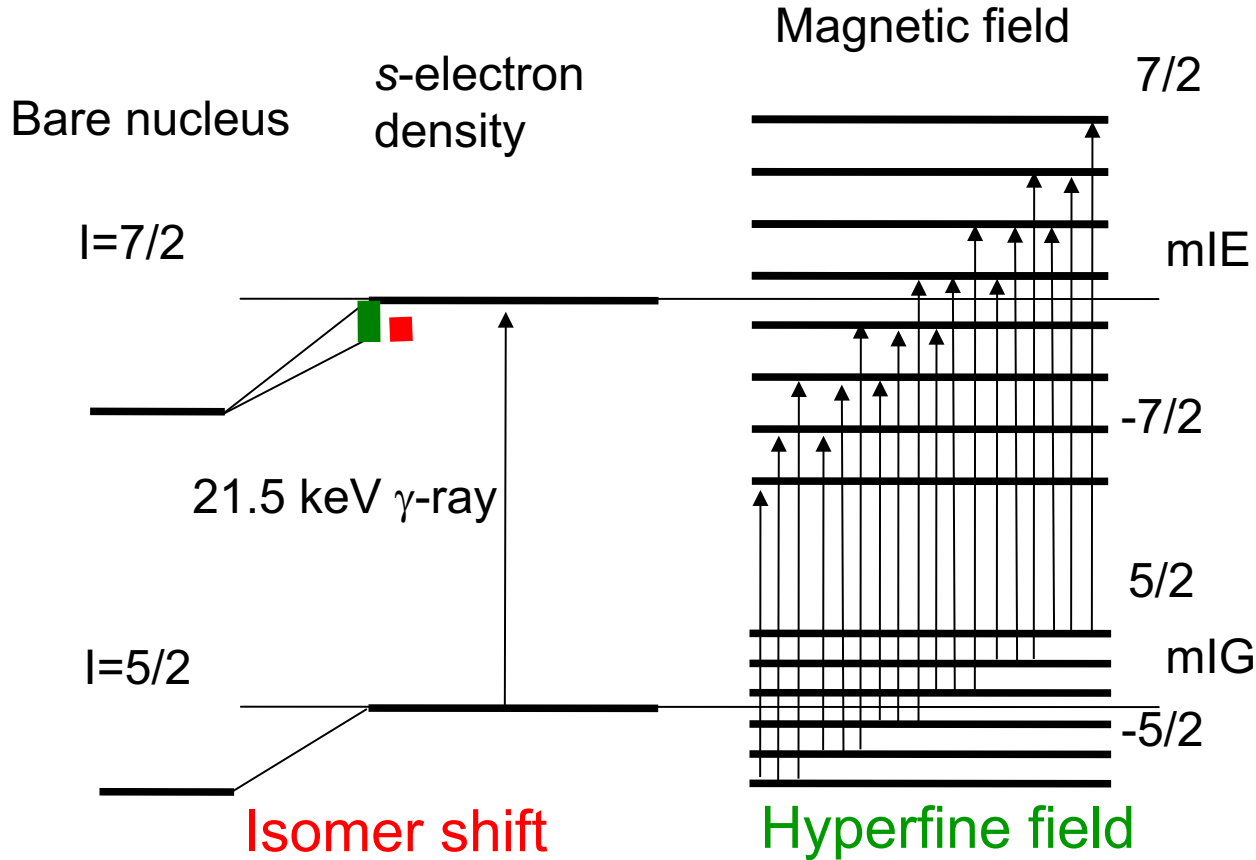
Eu(II) exhibits no magnetic splitting even at 32 mK.

Neutron diffraction and magnetization measurements indicate $7 \mu_B$ moments for **all** Eu.

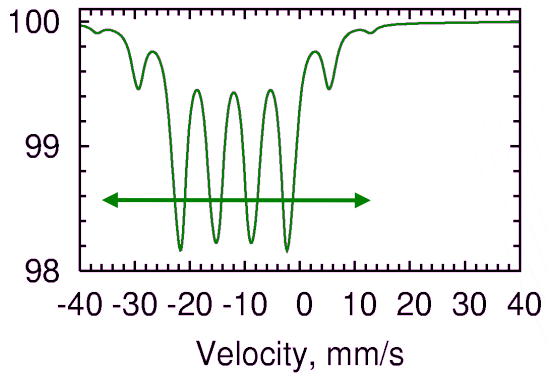
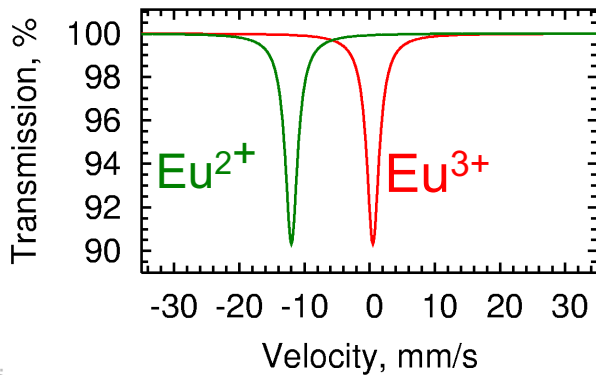
Hypothesis: we observe jump diffusion or tunneling induced magnetic relaxation.



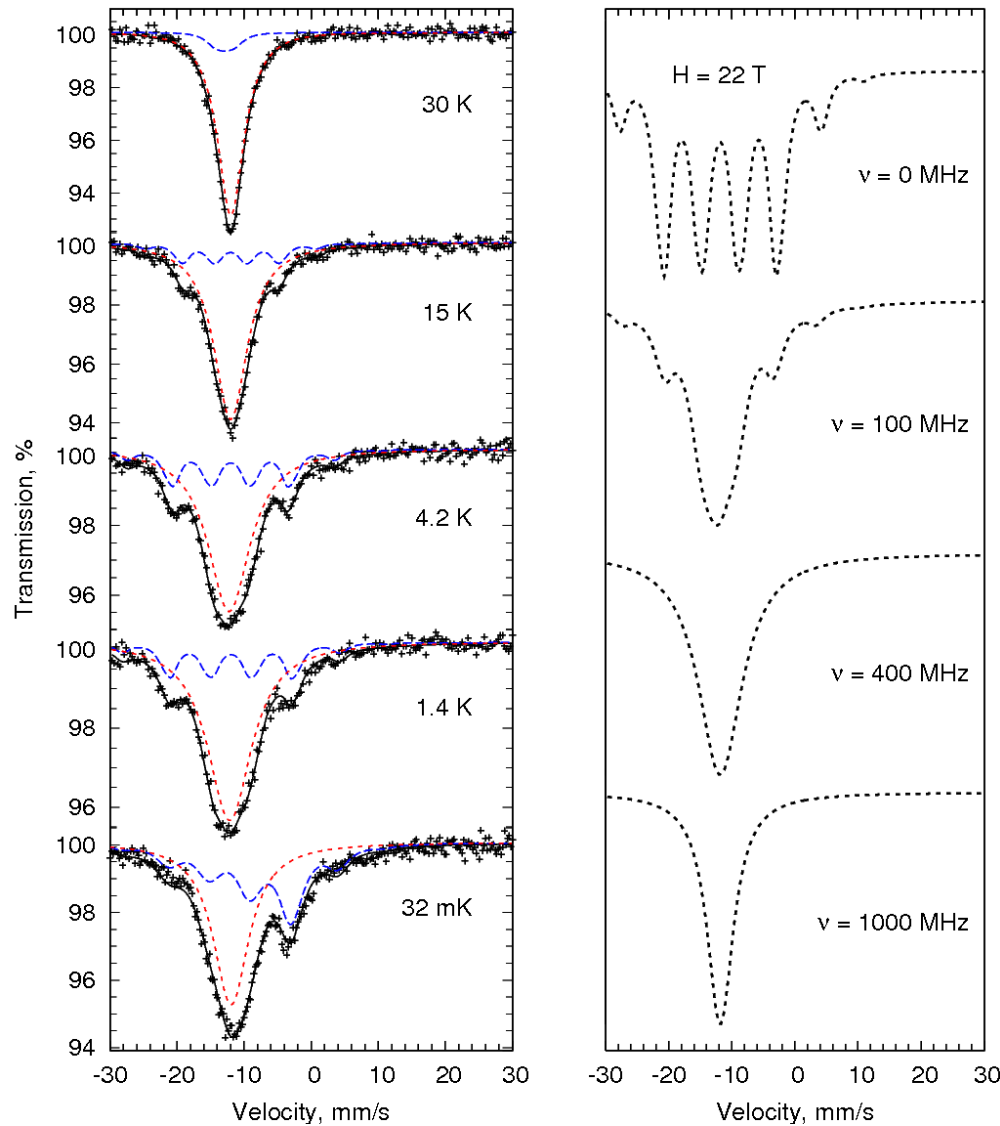
Larmor precession, ^{151}Eu



Larmor precession

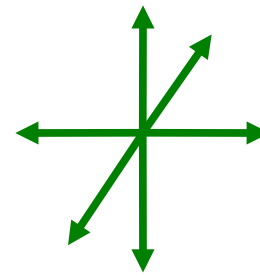


Relaxation spectra

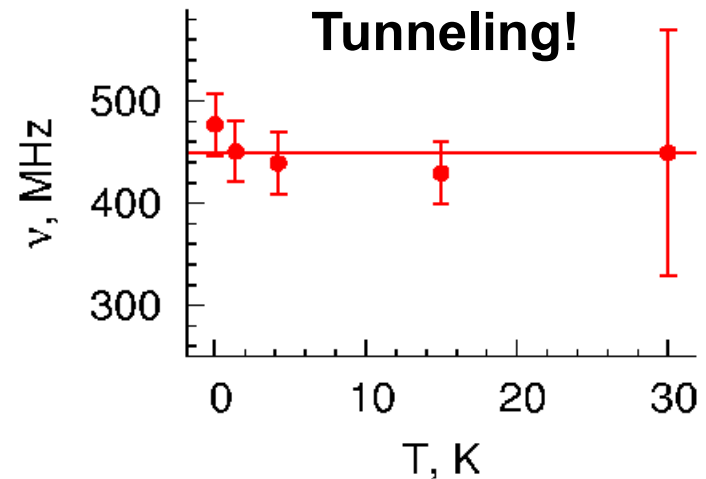
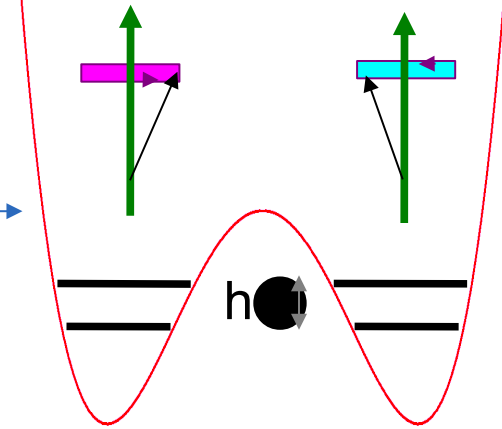


S. Dattagupta and M. Blume, *Phys. Rev. B* 10,4540 (1974).

Isotropic relaxation

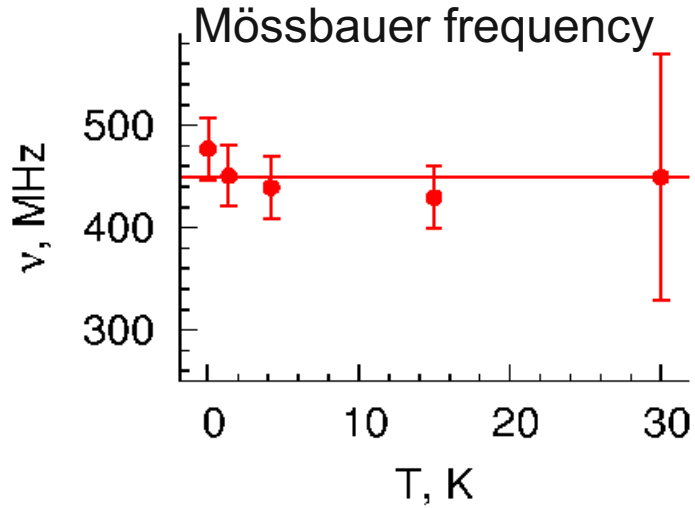


Phase is lost



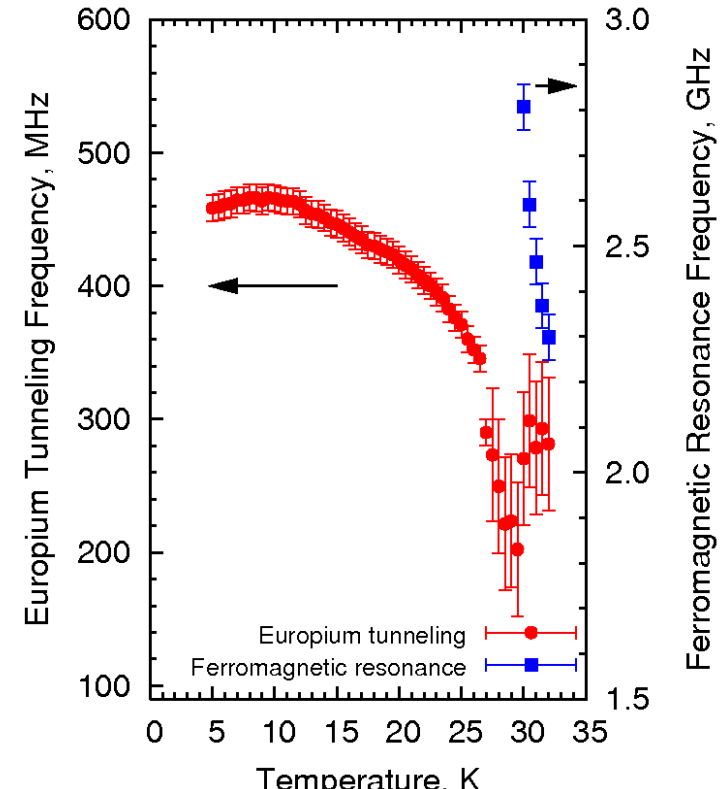
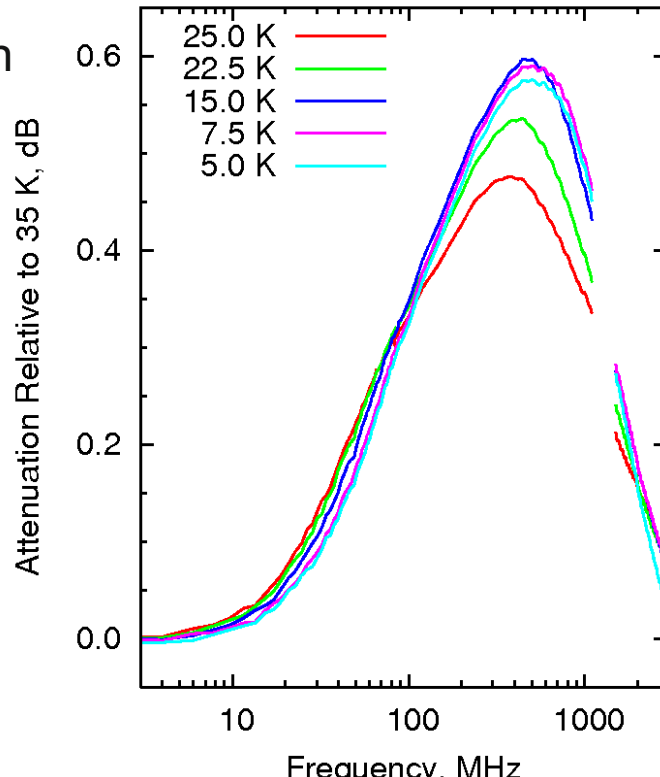
R. P. Hermann, V. Keppens, P. Bonville, G. S. Nolas, F. Grandjean, Gary J. Long, H. M. Christen, B. C. Chakoumakos, B. C. Sales, and D. Mandrus, *Phys. Rev. Lett.* **97**, 017401 (2006).

Tunneling dynamics

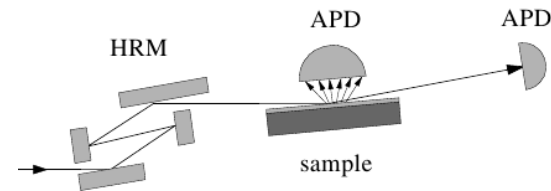


R. P. Hermann, V. Keppens, P. Bonville, G. S. Nolas, F. Grandjean, Gary J. Long, H. M. Christen, B. C. Chakoumakos, B. C. Sales, and D. Mandrus, *Phys. Rev. Lett.* **97**, 017401 (2006).

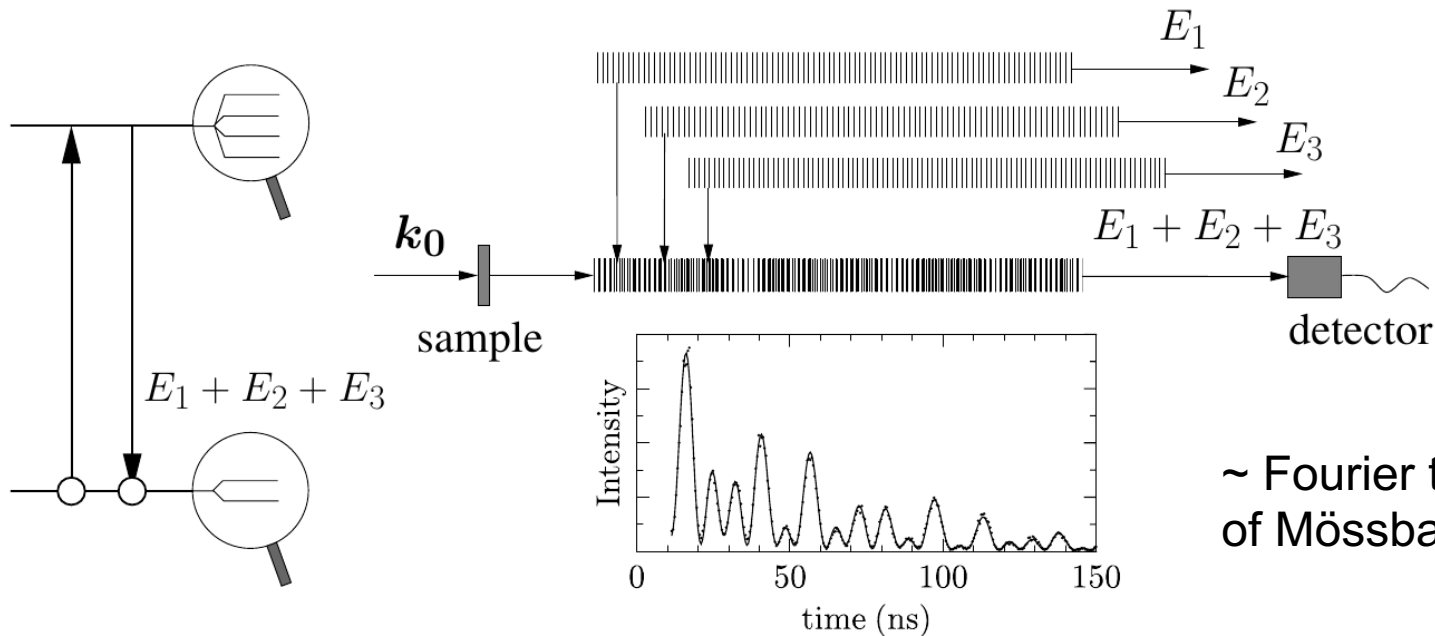
Microwave absorption



Nuclear forward scattering



Hyperfine splitting → Quantum beats



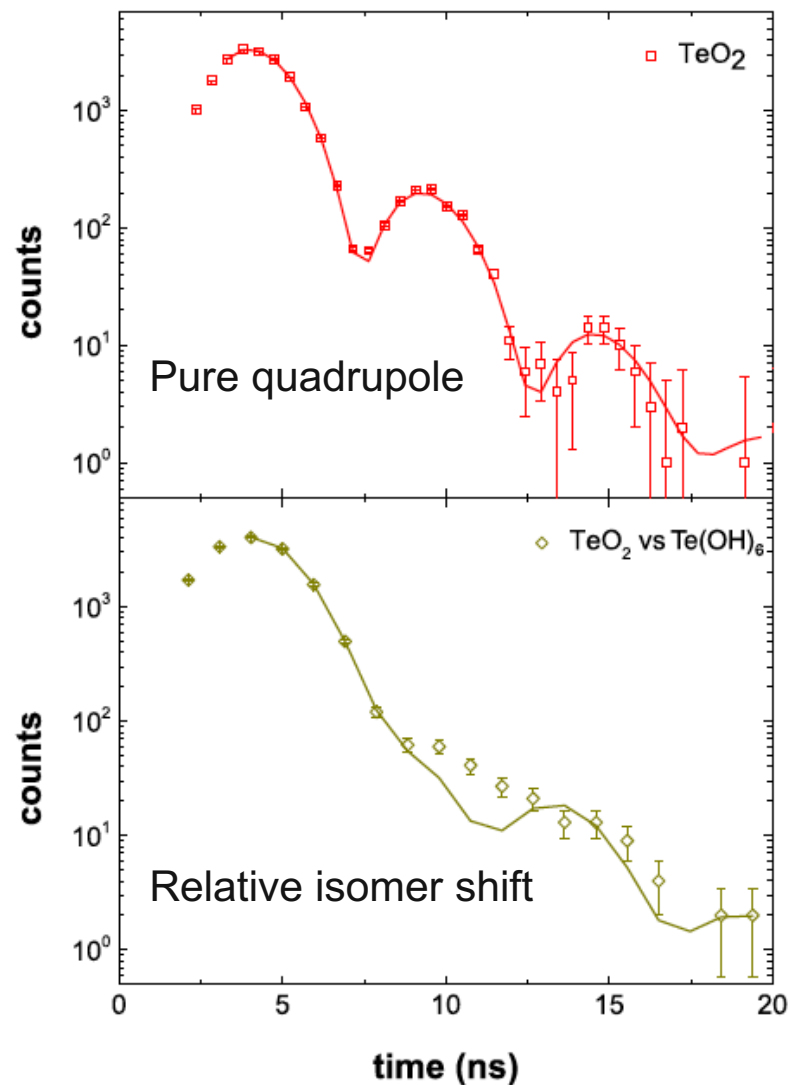
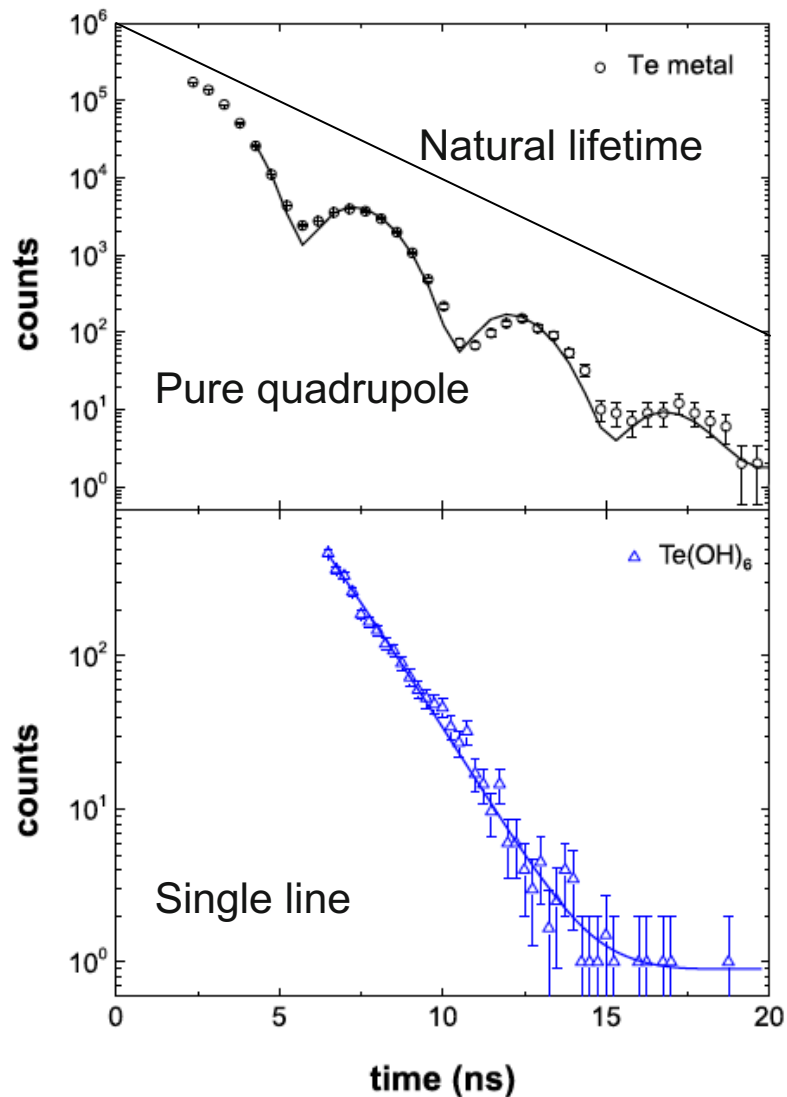
~ Fourier transform of Mössbauer spectrum

Multiple scattering → Dynamical beats

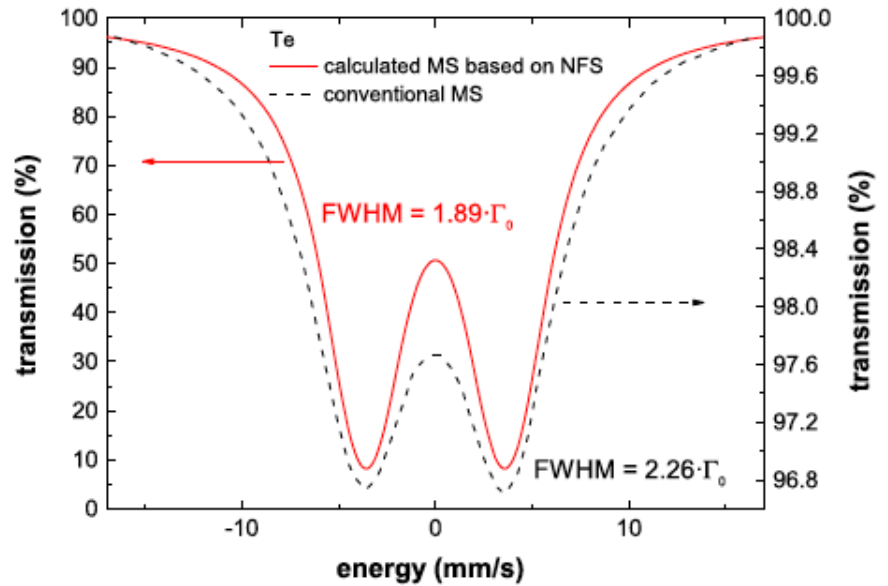
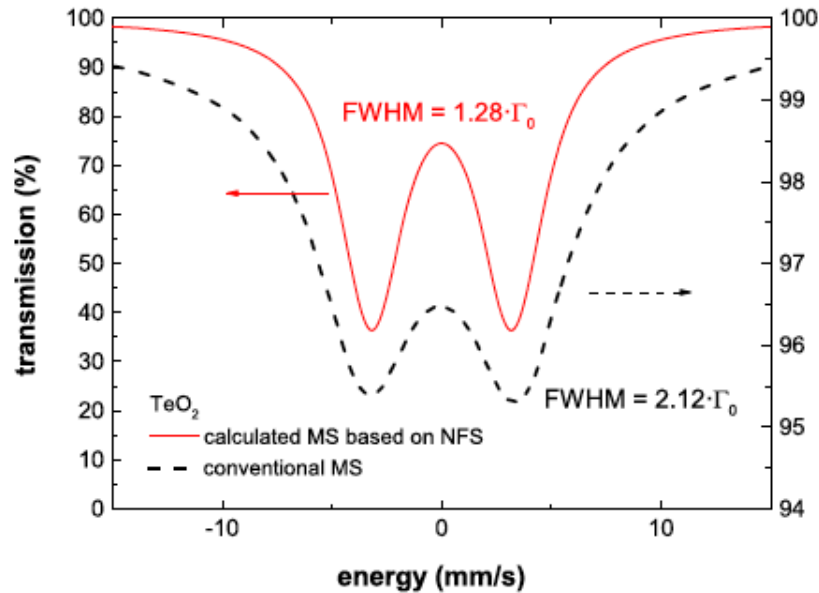
$$A(t) = \delta(t) - \gamma e^{-t/2\tau_0} \frac{J_1(2\sqrt{\gamma t})}{\sqrt{\gamma t}} \quad \text{with} \quad \gamma = \frac{k_0 d f_0}{\tau_0}$$

... except for thickness broadening

^{125}Te nuclear forward scattering



^{125}Te – NFS vs. Mössbauer spectroscopy



Intrinsic natural linewidth

Due to $^{125\text{m}}\text{Te}$ source broadening
NFS is the more elegant solution for
 ^{125}Te Mössbauer spectroscopy

At ORNL:

Opportunity for ^{125}Te or ^{129}I MS by activating
 ^{124}Te or ^{128}Te in Mg_3TeO_6 or $\text{Ba}_2\text{MgTeO}_6$
at HFIR

New kids on the block

^{187}Os @ 9.78 keV

Bessas *et al.*, PRB (2015)

^{125}Te @ 35.4 keV

Wille *et al.*, Europhys Lett (2010)

^{121}Sb @ 37.1 keV

Wille *et al.*, Europhys Lett (2006)

^{129}Xe @ 39.9 keV

Klobes *et al.*, Europhys Lett (2013)

^{61}Ni @ 67.4 keV

Sergueev *et al.*, PRL (2007)

^{73}Ge @ 68.7 keV

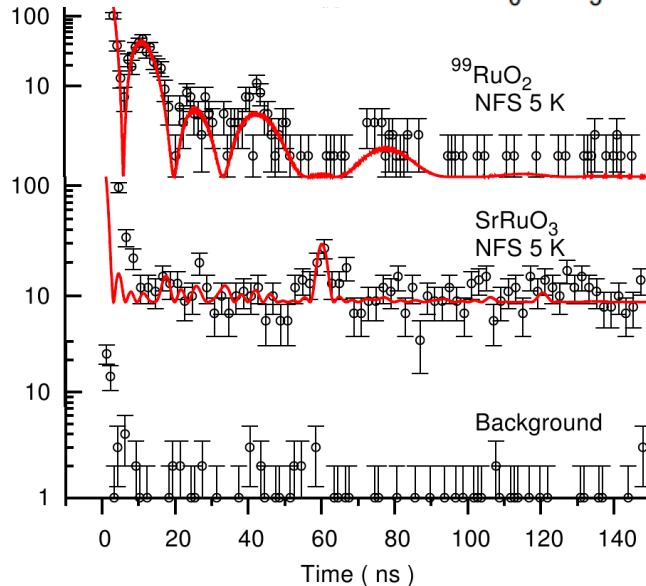
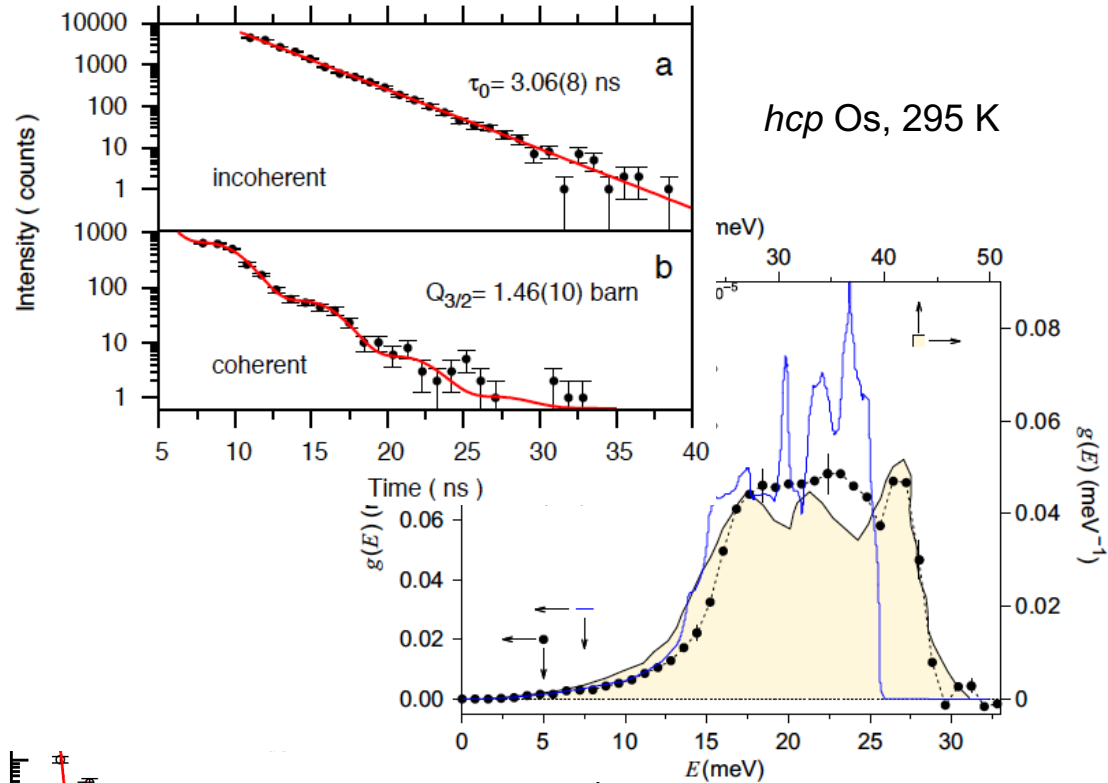
Simon *et al.*, Europhys Lett (2013)

^{174}Yb @ 76.5 keV

Masuda *et al.*, APL (2014)

^{99}Ru @ 89 keV

Bessas *et al.*, PRL (2014)



Acknowledgments

Manuel Angst, Forschungszentrum Jülich GmbH, Germany

Benedikt Klobes, Dimitrios Bessas, Abdelfattah Mahmoud, Vasilii Potapkin

Gary J. Long, Fernande Grandjean, U. Liege and Missouri U. Science & Technology

Ilya Sergueev, DESY, Germany

G. Nolas, U South Florida

P. Bonville, CEA Saclay

B. C. Sales, M. McGuire, B. Chakoumakos, H. Christen, ORNL

D. Mandrus, V. Keppens, UT Knoxville

J. M. Tarascon, E. McCalla, Coll. De France Paris, U. Amiens and ALISTORE

M. T. Sougrati, L. Stievano, U Montpellier

E. Brück, K. H. J. Buschow, U Amsterdam / U. Delft

R. Dronskowski, X. Liu, RWTH Aachen

R. Ruffer and A. Chumakov, E.S.R.F.

The European Synchrotron Radiation Facility, for provision of beam time.
Helmholtz Association of Research Centers / The University of Tennessee / U. Liège .